K-19-68-6 • 30 AUGUST 1968

FINAL REPORT

PROPELLANT SELECTION FOR SPACECRAFT PROPULSION SYSTEMS

CONTRACT NASw-1644

VOLUME III
THERMODYNAMICS AND PROPULSION

PREPARED FOR
NATIONAL AERONAUTICS AND SPACE ADMINISTRATION
OFFICE OF ADVANCED RESEARCH AND TECHNOLOGY
WASHINGTON, D.C.

GPO PRICE $ _____

CSFTI PRICE(S) $ _____

Hard copy (HC) 3.00

Microfiche (MF) .65

ff 653 July 65

K-19-68-6 • 30 AUGUST 1968

FINAL REPORT

PROPELLANT SELECTION FOR SPACECRAFT PROPULSION SYSTEMS

CONTRACT NASw-1644

VOLUME III
THERMODYNAMICS AND PROPULSION

PREPARED FOR
NATIONAL AERONAUTICS AND SPACE ADMINISTRATION
OFFICE OF ADVANCED RESEARCH AND TECHNOLOGY
WASHINGTON, D.C.

FOREWORD

This report was prepared by the Lockheed Missiles & Space Company, Sunnyvale, California, and contains the results of a study performed for the National Aeronuatics and Space Administration, Office of Advanced Research and Technology, under Contract NASw-1644, Propellant Selection for Spacecraft Propulsion Systems. The report is printed in three volumes:

Volume I Summary, Results, Conclusions, and Recommendations
Volume II Missions and Vehicles
Volume III Thermodynamics and Propulsion

CONTENTS

PRECEDING PAGE BLANK NOT FILMED.

ILLUSTRATIONS

TABLES

INTRODUCTION

This volume presents technical details of the thermodynamic analyses and the propulsion system analyses performed during the Propellant Selection Study.

Thermodynamic analyses were conducted to determine spacecraft thermal control and pressurization requirements for the Mars Orbiter and Mars Excursion Module (MEM) missions. The scope and depth of the thermal studies were sufficient to provide valid performance between candidate propellants. The analyses involved the computation of heat transfer to and/or from the propellant, such as heat from the external environment, other parts of the spacecraft, or from the pressurizing gas injected into the tanks. Because of the interaction between the pressurization system and system thermal behavior, pressurization and thermal analyses could not be conducted independent of one another, and were therefore integrated. The tank operating pressure levels and insulation requirements that were established were based upon the heat transfer and resulting propellant response.

The thermodynamic analyses conducted in Task I assisted in selecting representative missions and propellants for detailed investigation in Task II. The Task I analyses were based on simplified spacecraft thermal models for which tank external surface temperatures and resulting propellant heat rates were computed. During Task II, detailed analyses were conducted to evaluate propellant heating effects, determine pressurization system requirements, and optimize the thermodynamic parameters involved.

Mars Orbiter pump- and pressure-fed system analyses were conducted for the following baseline conditions:

- Propellant tanks oriented toward the sun
- Most favorable surface finish properties
- Nominal values for multilayer insulation conductivity

In addition to analysis of the baseline systems, Mars Orbiter pump-fed systems were analyzed for a range of conditions to assess the sensitivity of various parameter values relative to the baseline system, and to determine the optimum set of parameter values.

Sensitivity analyses have shown that the preferred vehicle orientation for cryogenic and space-storable propellants is sun-on-capsule (sunshielded). These analyses have shown that even if the most pessimistic performance values are used in the sensitivity analyses, nonvented tanks are still feasible.

The cryogenic and space-storable propellant operating pressures, insulation requirements and resultant total weights all increase with increasing absorptivity/emissivity (α/ϵ) ratio, mission length, and insulation thermal conductivity. Changing the vehicle orientation, so that no direct solar energy impinges on the tank, and subcooling the propellant decreases the operating pressure, insulation requirements, and system weight. The earth-storable propellants are relatively insensitive to many of these variations and can be accommodated with no weight penalty by selection of sun-on-tank orientation with specific surface finishes for each mission or operating condition.

Mars Orbiter pressure-fed systems were analyzed for a range of conditions similar to those for the pump-fed orbiter. A more detailed pressurization system analysis was performed because pressurization system weights became more important. Optimum conditions were obtained with a tradeoff between pressurant weights and insulation, vapor, and tank weights. When the environment caused propellant cooling, the optimum pressurant inlet temperature was higher than for a heated propellant. Pressure-fed system weights were greater than pump-fed system weights because the higher operating pressure resulted in greater tank and pressurant weights.

Only pump-fed systems were considered in the analyses for the Mars Excursion Module (MEM). The environment included a 30-day Mars stay, which was a factor in the system analysis. Vacuum jacketed cryogenic and space-storable propellant

tanks with multilayer insulation were required. Multilayer insulation was also assumed for NH_3 and earth-storable tanks, but vacuum jacketing was not required. As a result, cryogenics were continually heated, but earth storables stabilized near ambient temperatures.

The two sets of tankage for each stage were analyzed as pressure and volume connected, but thermally isolated. The inner tank for the MEM ascent second stage tended to optimize with a tradeoff between vapor weight and insulation weight, whereas the first stage (outer) tanks tended to optimize with tradeoffs between insulation weight and pressurant and tank weights.

Numerous supporting analyses were conducted on specific problem areas such as insulation venting, ascent heating, prelaunch conditioning, engine burn and heat soakback, penetration heat leaks, propellant tank thermal equilibrium, and differential boiloff. Sensitivity analyses were also conducted to evaluate the effects of α/ϵ variations, mission length, insulation conductivity variations, trans-Mars vehicle orientation, and variations in penetration heat leak rates. The effects of venting, subcooling, and providing 50 percent slush hydrogen also were studied.

Ascent heating effects are not important because insulation will vent rapidly. Therefore, prelaunch thermal studies were conducted to assess ground cooling requirements, propellant subcooling, and venting and propellant make-up requirements while on the launch pad. A helium purge is required for the H_2, and a dry air or nitrogen purge is required for the space-storable propellants. Spacecraft prelaunch requirements are adequate for the earth-storable propellants. All fluorinated oxidizers and B_2H_6 require prelaunch closed-loop vent systems due to their reactive characteristics.

Propulsion system analyses were conducted to such a level that comparisons between various propellant system requirements could be assessed in some detail. Data were gathered from the engine companies on propellant and propulsion system characteristics. Both basic engine data and engine design sensitivity data were

gathered. These data were evaluated and incorporated into the vehicle system optimizations activities, from which the study conclusions could be developed.

Propulsion system activities were divided into several areas. The first activity consisted of the gathering of parametric propulsion and propellant data. These data were evaluated and then used in the mission analysis in order to make a preliminary assessment of propulsion systems for a broad range of missions using representative cryogenic, space-storable, and earth-storable propellants. Subsequent to the mission analysis, two propulsion stages were selected. These were an 8,000-lb-thrust Mars Orbiter and a 30,000-lb-thrust Mars Excursion Module ascent stage. Further requests were made to the engine companies to solicit specific design and operational data for these engines when utilizing the propellants selected for Task II analysis.

In addition to synthesizing complete propulsion vehicle systems, engine sensitivity analyses were conducted. Requests were made to supporting engine companies for engine weight data and specific impulse data for a range of engine chamber pressures, expansion ratios, and mixture ratios utilizing the 8,000-lb-thrust engine. These data were then utilized to determine overall system weights and sensitivities for the Mars Orbiter Vehicle.

Section 1
THERMODYNAMIC ANALYTICAL APPROACH

A preliminary screening of missions and spacecraft was accomplished in Task I using results of past studies, parametric analysis, scaling laws, and NASA-supplied standard models. Five typical propellant combinations were considered, representing cryogenic, space-storable, and earth-storable propellants:

O_2/H_2	Cryogenic
F_2/H_2	Cryogenic
F_2/NH_3	Space storable
$FLOX/CH_4$	Space storable
N_2O_4/A-50	Earth storable

These propellant combinations were analyzed for numerous vehicles and missions representing earth and planetary orbit departure, orbital braking, planetary ascent, and space probes.

The measure of effectiveness assumed was the initial weight of the propulsive system as determined by the rocket equation. The minimum weight system was determined by a tradeoff of insulation and propellant boiloff weights. All propellant heating resulted in boiloff (groundrule for Task I only) at a constant pressure; therefore, propellant temperatures were constant. Propellant heating rates were based on the temperature difference between the propellant and the outermost insulation surface. These surface temperatures were averaged for (1) a random orientation in a planetary orbit and (2) during interplanetary transfer with sun-on-capsule orientation for cryogenics and space storables but sun-on-tank orientation for earth storables. Appropriate surface temperatures were thus obtained by selection of α/ϵ ratios and vehicle orientation. Diurnal heating variations in orbit or on a planet surface were time averaged.

This section describes the Task II analytical approach used to determine the thermal-pressurization parameters and to optimize thermal parameters, the radiation and conduction models used to synthesize the vehicles and the mission environment, the assumptions and general factors considered in the pressurization analysis, and the assumptions used in the optimization of systems.

The Epstein pressurant prediction correlation was adapted and a thermal-pressurization-optimization analysis made, incorporating real fluid properties correlations, collapse factors, and energy balances at each mission burn. These computational steps are shown on Fig. 1.

In addition to the propellants studied in Task I, the following additional propellant combinations were analyzed under Task II:

- OF_2/CH_4 Space storable
- OF_2/B_2H_6 Space storable (Mars Orbiter only)
- ClF_5/MHF-5 Earth storable

The propellant N_2O_4/A-50 was analyzed only for the Mars Orbiter Mission in Task II.

1.1 THERMAL MODEL DEVELOPMENT

Thermal models that describe physical elements of the spacecraft were developed to evaluate the effects of the external environment upon the propellant. The thermal models use an analogous electrical circuit consisting of conduction and radiation resistors and lumped node thermal capacitances which can be driven by either or both internal and external potentials (heat flux or temperature) on the computer.

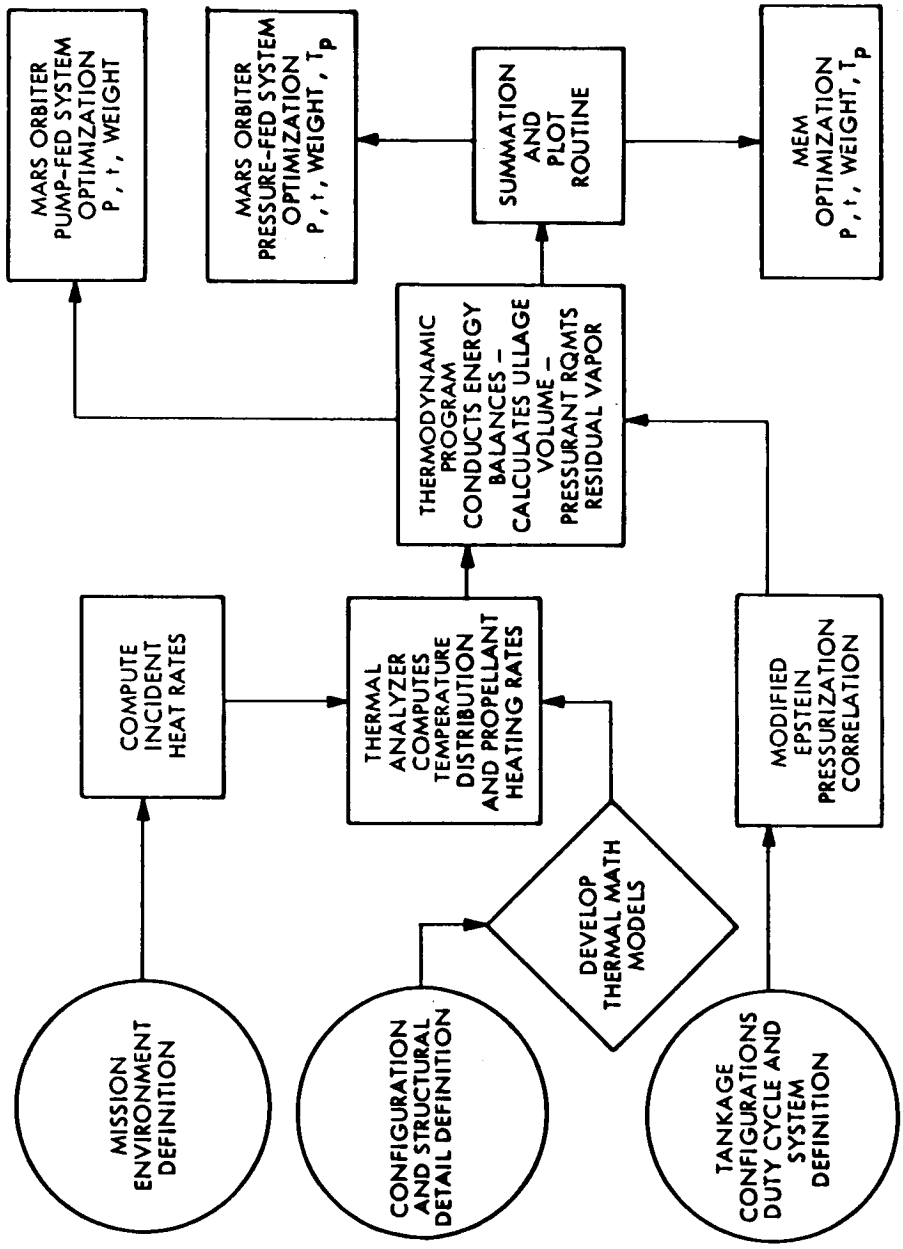

Fig. 1 Thermodynamic/Pressurization Optimization

The radiation network is developed by first obtaining detailed view factors between nodes (geometrical relationship) and then combining the view factors and external surface properties (emittances) to obtain the radiation network. The Heat Rate computer program (Ref. 1) is used to calculate (1) radiant view factors, (2) radiant interchange factors, and (3) direct incident or total absorbed solar, albedo, and planetary heat rates. The program can provide both card output and computer-generated plots, and can handle surfaces in the form of rectangles, trapezoids, discs, cylinders, cones, spheres, cubes, and paraboloids. Both view factors and radiation constants were determined with this program.

The conduction network accounts for conductive heat transfer through and around the vehicle structure, tank walls, propellant, and insulation. Conduction resistors were calculated between node centers; thermal capacities were lumped at each node center. Each node was considered to be isothermal; thus,the node division could affect the accuracy of the results. The total number of nodes and node locations were carefully selected to provide temperatures of sufficient accuracy to evaluate the propellants. The thermal models were adapted to each propellant system to account for propellant properties and tank size differences due to volume variations.

1.2 MISSION ENVIRONMENT

The environmental heating of the spacecraft was determined as a function of the mission sequence and trajectory. During the Mars transit phase, the primary energy source is the sun, and the heat sink is deep space at a temperature of absolute zero. The solar flux density varies inversely with the square of the distance from the sun and is computed as a function of time for specific transfer trajectories. When in earth or Mars orbit, the planet emission and reflected solar energy incident on the spacecraft are also computed. For Mars surface operations, convective heating from the atmosphere, planet albedo, and surface-heat emission are included.

1.3 PROPELLANT HEATING

The Thermal Analyzer computer program is used to calculate all thermal model nodal temperatures resulting from the space environment (i.e., solar, radiation to space, and onboard heat sources). The Thermal Analyzer program (Ref. 2) uses a finite difference solution technique to determine node temperatures resulting from an energy balance of the thermal model subjected to the environment. Steady-state temperatures were readily determined by setting all but the liquid propellant thermal capacities to zero. Heat transferred through the insulation and penetrations was then used to determine the propellant temperature rise. A typical physical system is shown on Fig. 2.

1.4 PRESSURIZATION

The pressurization system was synthesized for the various propellants with enough assumptions to assess the differences in system weights. In general, thermal equilibrium was assumed between the ullage volume and the propellant prior to each engine burn. This assumption implies propellant partial pressure equilibrium and no ullage temperature gradients. A special case was also studied for the H_2 tanks in which venting was considered. However, all other propellant combinations were nonvented. Developing pressurization systems for nonvented tanks results in a simple system and avoids the inherent problems of venting, such as contamination due to corrosive propellants, and the unknowns of the vent mechanism, such as ullage location and venting of pressurant or propellant vapor.

Helium pressurant was assumed for all the propellants except the pump-fed hydrogen, which was pressurized with hydrogen vapor. Previous applications and studies have shown that helium is generally optimum because it is light in weight, chemically inert, noncondensable and has good storage characteristics. This assumption also provides a common reference for performance comparisons between propellants.

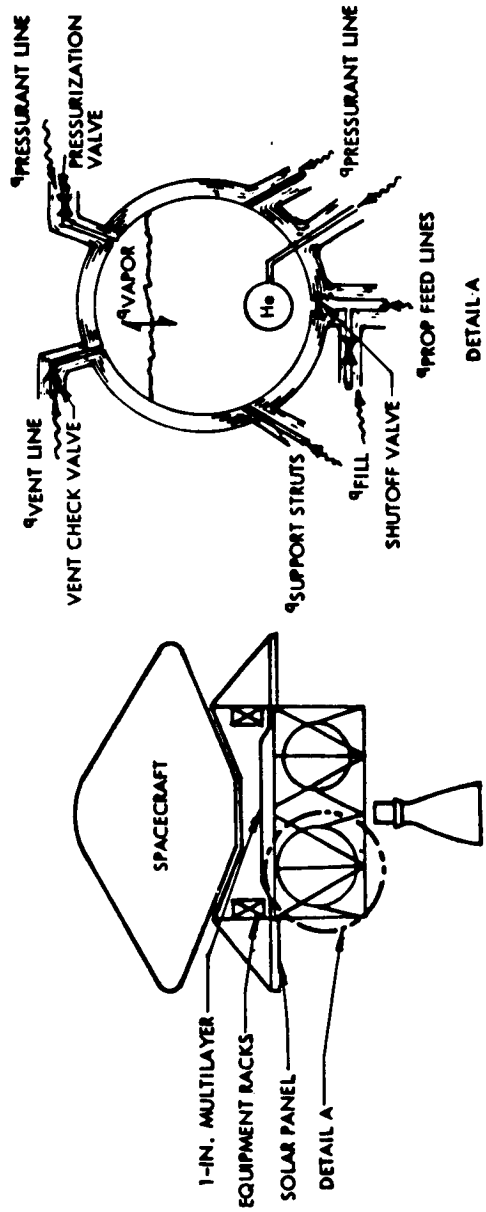

Fig. 2 Typical Propellant Tank Heat Inputs

The system considered in the pressurization analysis consists of the helium storage tank, associated plumbing, fill and shutoff valves, check valves, pressure regulators, and vent-relief valves. The high-pressure helium tanks were stored either within a propellant tank or within a tank insulation enclosure for all the propellants except the earth storables. In this case, helium tanks were assumed to be stored at 530° R. The helium was assumed to be stored within the colder propellant (fuel or oxidizer) at the warmest saturation temperature determined during the mission.

The pressure-fed hydrogen tanks must be pressurized by helium because no pump pressure head is available. The sum of the pressure drops through the feed lines and injector plus the chamber pressure of 100 psi was supplied by the pressurization system for all pressure-fed propellant systems.

Pressurant requirements were computed based on an adaption of the Epstein Correlation (Refs. 3 and 4) and energy balances within the ullage during an engine burn. The energy balance was computed for the liquid and ullage to establish the thermal equilibrium pressure and temperature resulting from the heated pressurant, environmental heating, and cooling due to propellant vaporization. Reduced temperature and pressure correlations were used for approximating real fluid properties.

1.5 SYSTEM OPTIMIZATION

The insulation thickness and operating pressure were optimized for each propellant by minimizing weights for a system consisting of the tank, vapor, pressurant, pressurant spheres, and insulation. The Thermal Analyzer program provided heating rates for all propellant tanks as a function of the specific design, orientation, and mission, for a span of insulation thicknesses. The Thermal-Pressurization analysis provided tank size, tank design pressure, vapor weight, pressurant and sphere weight, as a function of the heating rates obtained for each insulation thickness and for each pressurant inlet temperature, when considered as a variable. The Summation and Plot routines, required for determining the optimum values for the variables, also computed the propellant tank weights and the insulation weights for each propellant, insulation thickness, and pressurant inlet temperature, when applicable.

The tank weight was determined for various sizes of conical, spherical, and ellipsoidal geometries, each as a function of any operating pressure above that pressure corresponding to a minimum wall thickness of 0.040 inches. Insulation weight was determined as a function of tank area, insulation thickness, and insulation density. Insulation thickness was conservatively assumed constant over the surface of a tank. Some weight could be saved in a specific design by varying insulation thickness over the tank surface to tailor the thermal protection to the local need.

The system weights were obtained by summing the weights for each variable at each insulation thickness. Total system weights were plotted as a function of tank design pressure and insulation thickness with pressurant inlet temperature as a parameter. The optimum combination of parameters was then selected by examination of these plots.

Section 2
MARS ORBITER THERMODYNAMIC ANALYSIS

The Mars Orbiter spacecraft (Ref. 5) and its mission have been analyzed for all of the candidate propellants. The hydrogen propellant tanks were configured to an ellipsoidal geometry to maintain a reasonable spacecraft volume, with spherical oxidizer tanks. All other propellant combinations used a configuration of four spherical tanks with adjustments in diameter to accommodate the necessary propellant load. The study considered the nominal 195-day transfer trajectory to Mars with the orbit inject burn at Mars arrival and an orbit trim burn 10 days later at 205 days. Pump-fed and pressure-fed propulsion systems were optimized. The tank operating pressures for these two types of systems are significantly different; thus, the weights for the tank, vapor, pressurant, pressurant sphere, and insulation are significantly different. The sizes and numbers of tanks were varied, depending on the propellant combination and loading requirements shown in Table 1.

2.1 THERMAL MODELS

Two basic thermal models were required to describe (1) the large-ellipsoidal-fuel-tank/spherical-oxidizer-tank configuration for the O_2/H_2 and F_2/H_2 propellant combinations, and (2) the four-spherical-tank configuration for all the remaining propellant combinations. The two models are illustrated in Figs. 3 and 4. The external surface finish properties (α/ϵ) used for the analyses of each model along with the number of nodes and radiation and conduction resistors are also presented on Figs. 3 and 4 for each thermal model. The equipment section was assumed to be isothermal at 70° F throughout the entire mission.

The propellant feed line heat leaks were evaluated based upon nominal lengths between the tank and engine. A section of the line consisting of bellows was considered to increase the effective line length. The lines were considered to be well insulated so that

Table 1

MARS ORBITER TANK PROPELLANT LOADS SUN-ON-TANKS, PUMP-FED, 205-DAY MISSION

Propellant	No. of Tanks	Mass of Propellant Loaded per Tank (lb)
F_2	4	1,346
H_2	1	414
O_2	4	1,393
H_2	1	933
FLOX	2	2,834
CH_4	2	492
OF_2	2	2,775
CH_4	2	523
F_2	2	2,562
NH_3	2	775
N_2O_4	2	2,802
A-50	2	1,399
ClF_5	2	2,870
MHF-5	2	1,195

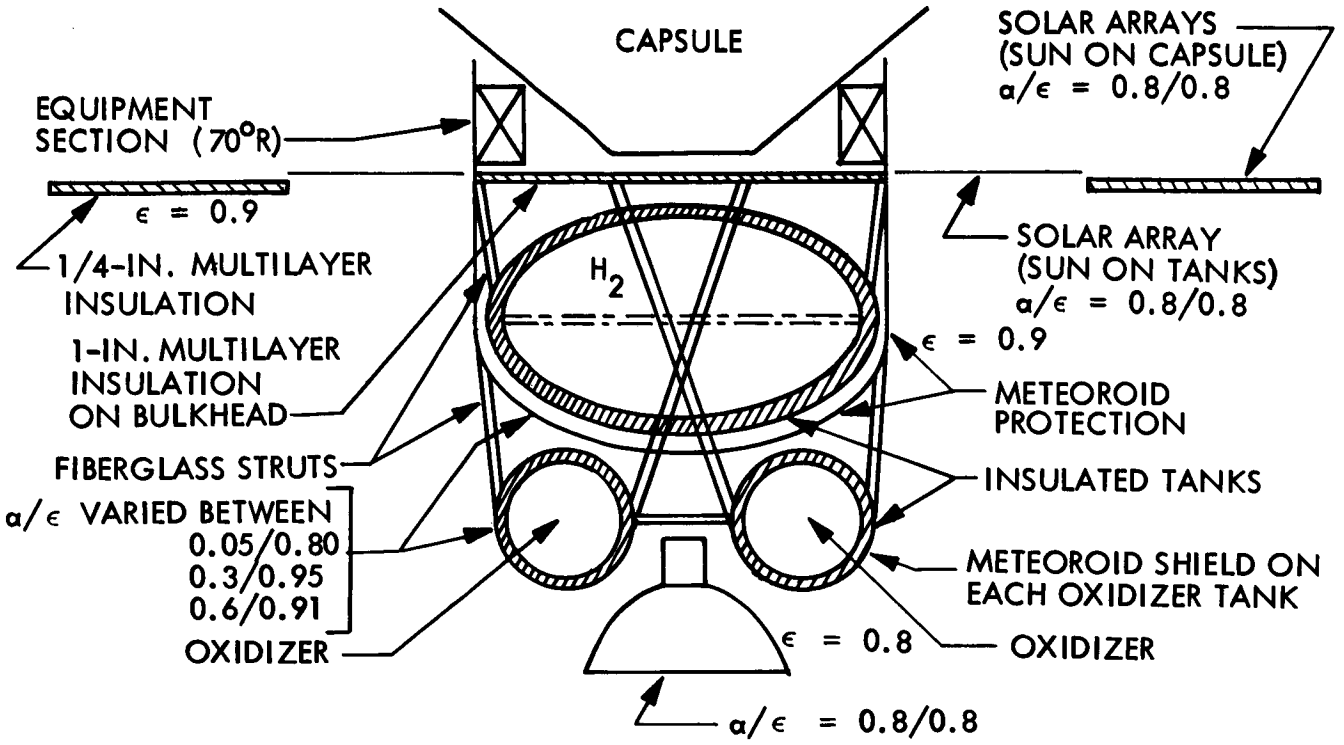

THERMAL MODEL — 39 NODES

RESISTORS:

H_2 TANK	EACH OXIDIZER TANK
70 RADIATION	26 RADIATION
22 CONDUCTION	9 CONDUCTION

ASSUMPTIONS:

1) STRUTS INSULATED
2) TEMPERATURE OF STRUT ENDS:
   TANK END = LIQUID TEMPERATURE
   OTHER END = TEMPERATURE OF OUTER INSULATION SURFACE, OXIDIZER'S OR 70°F (H_2)

Fig. 3 Mars Orbiter Thermal Model for Cryogenic Propellants

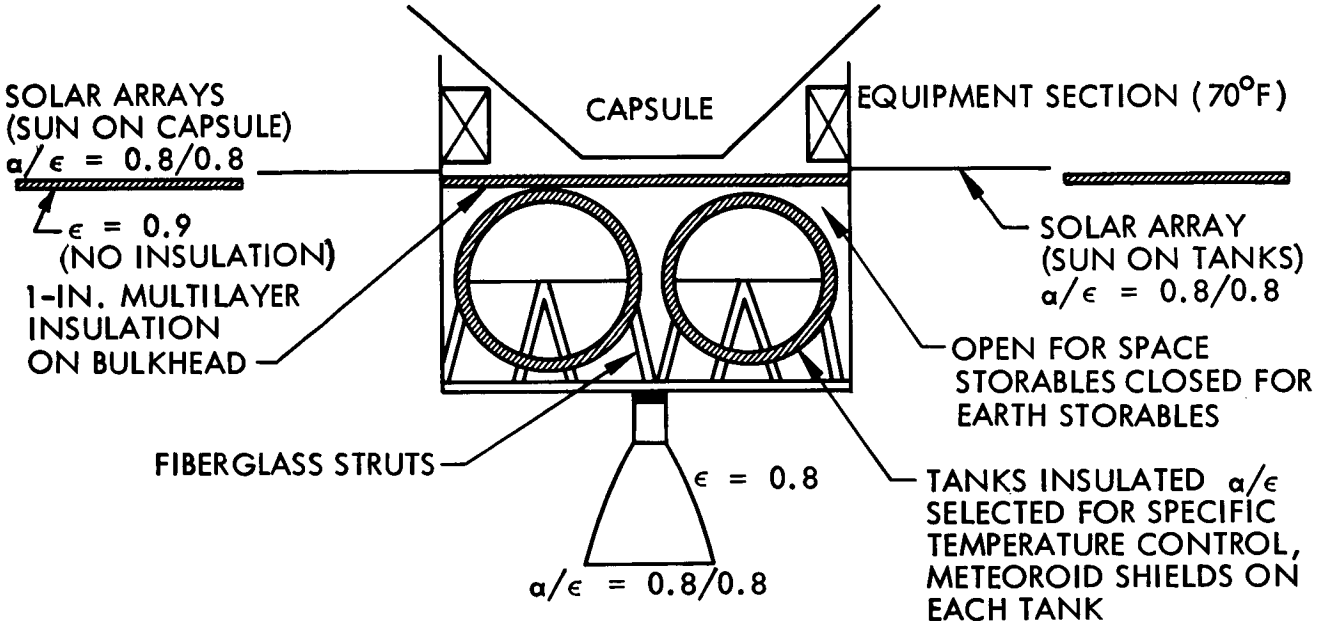

THERMAL MODEL

22 NODES
38 RADIATION RESISTORS PER TANK
9 CONDUCTION RESISTORS PER TANK

ASSUMPTIONS:

1) STRUTS INSULATED
2) TEMPERATURE OF STRUT ENDS:
   OTHER END = SAME TEMPERATURE AS OUTER INSULATION SURFACE
   TANK END = LIQUID TEMPERATURE

Fig. 4 Mars Orbiter Thermal Model for Earth- and Space-Storable Propellants

the total thermal resistance of the feed line was only through the feed line walls. The temperature differences through the insulation and between both ends of the propellant feed lines were assumed approximately equal to the temperature differences across the propellant tank insulation. Thus, the feed line produced another heat leak path, reducing the effectiveness of the insulation system, and more energy transfer resulted because of the propellant feed line penetration of the insulation.

The feed lines assumed were 0.010-in.-thick titanium, 3 in. in diameter for hydrogen and 2 in. in diameter for all other propellants. Where titanium compatibility with the propellant is a problem, stainless steel with 2.5 times the titanium conductivity would be used. An effective length of 5.5 ft was considered for the H_2 feed line, including a bellows, and a 3-ft length for all other propellants. The thermal conductivity of the 6Al-4V titanium walls was 1.3 Btu/hr-ft-°R for the hydrogen tank lines and 4.2 Btu/hr-ft-°R for the earth- and space-storable propellant lines.

The strut heat leaks were were handled in the same manner as the propellant feed lines; i.e., they were assumed to be insulated for their full length and only conduction heat transfer along the structure was computed. The insulation was assumed to be effective enough that no heat was lost or gained through the insulation. If the struts are shaded from external heat sources, some heat will actually be lost through the insulation; therefore, the computed heat leaks would be conservatively high. If the struts are exposed to direct solar incidence some heat will be gained through the insulation. In this case the computed heat leaks will be slightly low.

The multilayer insulation conductivity values used for the various propellants were selected from data presented in Ref. 6, and from results of laboratory tests of the insulation with one boundary at 525°R and other boundaries at 340° and 610°R. Other data are presented for warm boundary temperature ranging from 300°R to 500°R with the conductivity increasing with warmer boundary temperatures as shown by the data spread. These data are presented in Fig. 5 along with a data point from a typical flight-type installation obtained from an LMSC test of a 109-in.-diam. tank. The laboratory tests reported in Ref. 6 were conducted at the LMSC Thermophysics

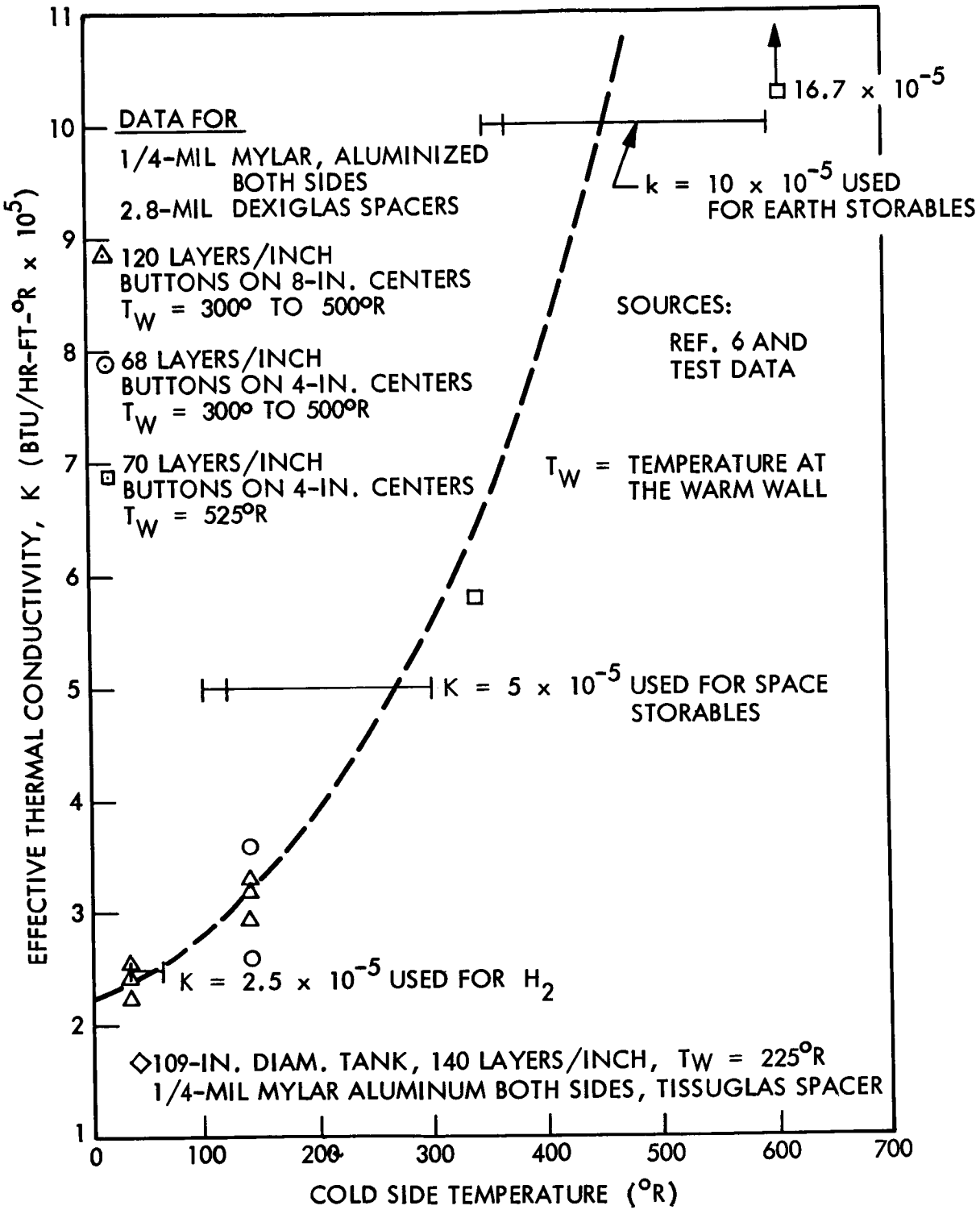

Fig. 5 Multilayer Insulation Thermal Conductivity

Laboratory using a double-guarded flat-plate calorimeter, as specified in ASTM C-177-45. Multilayer insulation conductivities were determined for several packing densities of aluminized Mylar radiation barriers and spacers. Reference 6 shows that the optimum packing density is around 70 layers per inch. Therefore, the design curve values shown on Fig. 5 for higher packing densities are somewhat conservative. The specific conductivity values assumed were 2.5×10^{-5} Btu-hr-ft° R for H_2 tanks; 5×10^{-5} for 0_2, F_2, and all other space storables; and 10×10^{-5} for the earth storables and for the thermal bulkhead. The use of discrete conductivity values for each propellant would result in slight differences in insulation requirements from the baseline values computed, but the system weight differences would be very small. Sensitivity analyses conducted using double these baseline conductivity values resulted in relatively small system weight increases (see section 3.6).

2.2 MISSION ENVIRONMENTS

The environment of the earth-to-Mars portion of the Mars Orbiter mission caused the most significant propellant heating. The response of the vehicles thermal model with a number of insulation thicknesses was determined as a function of this portion of the mission. The environments of other portions of the mission were then analyzed to determine their effect on the total mission.

The incident energy on the Mars Orbiter was primarily from the sun. The incident heat rates from the earth due to the earth's temperature and albedo were considered and found to be negligible because of the relatively short exposure time. The Mars Orbiter could be in a 100-nm earth orbit for 90 min. with both albedo and earth emission incident upon the spacecraft. However, the spacecraft would be in the earth's shadow almost half of the 90 min. The total energy incident on the spacecraft would be slightly less than with the vehicle in the sun full time without the earth heat inputs. The Mars heating effects can also be neglected due to the high altitude elliptical orbit of 1,000 km × 20,000 km, which results in a very short time spent near the planet. Also, the Mars surface heat fluxes due to its surface temperature and albedo are about half the earth heat fluxes. The vehicle solar heat rates were determined by calculating

the projected areas normal to the sun. The effect of specular reflections within the tankage configuration was approximated in the energy inputs, as a function of the reflectivity of the surface finishes.

The solar flux between Earth and Mars was determined as a function of time for the 195-day trajectory to Mars. A nominal solar constant at Mars of 213.4 Btu/hr-ft^2 was used for this study. A 290-day mission to Mars was also analyzed by extending the 195-day transit time to 290 days. A 650-day mission to Jupiter was also considered, utilizing the same spacecraft. The solar flux used as a function of time is shown on Fig. 6.

2.3 PROPELLANT HEATING

Propellant heating was computed for a number of insulation thicknesses using the Thermal Analyzer program for each propellant, orientation, and environment considered for each configuration. The propellant heating was obtained with steady-state temperatures computed from the thermal models subjected to the environment.

The ellipsoidal-tank model (Fig. 3) was used to analyze the O_2/H_2 and F_2/H_2 propellant combinations, and the four-spherical-tank model of Fig. 4 for all the other propellant combinations. The cases analyzed include surface finishes of α/ϵ = 0.05/0.80, 0.10/0.80, 0.3/0.95, and 0.6/0.91; orientations of sun-on-capsule and sun-on-tanks; and both 195- and 205-day missions. Subcooled and vented cases were considered for H_2 propellants. Propellant temperatures for both 195-day and 205-day missions were calculated to determine the effect of carrying approximately 5 percent of the total propellant load for the last 10 days of the mission.

The propellant heating calculation procedure was to first determine the steady-state temperatures and heat transfer rates at the initial point in the transfer orbit, using the liftoff propellant temperature. Then, the propellant temperature change over the first of five equal time increments was computed by assuming that the initial heat

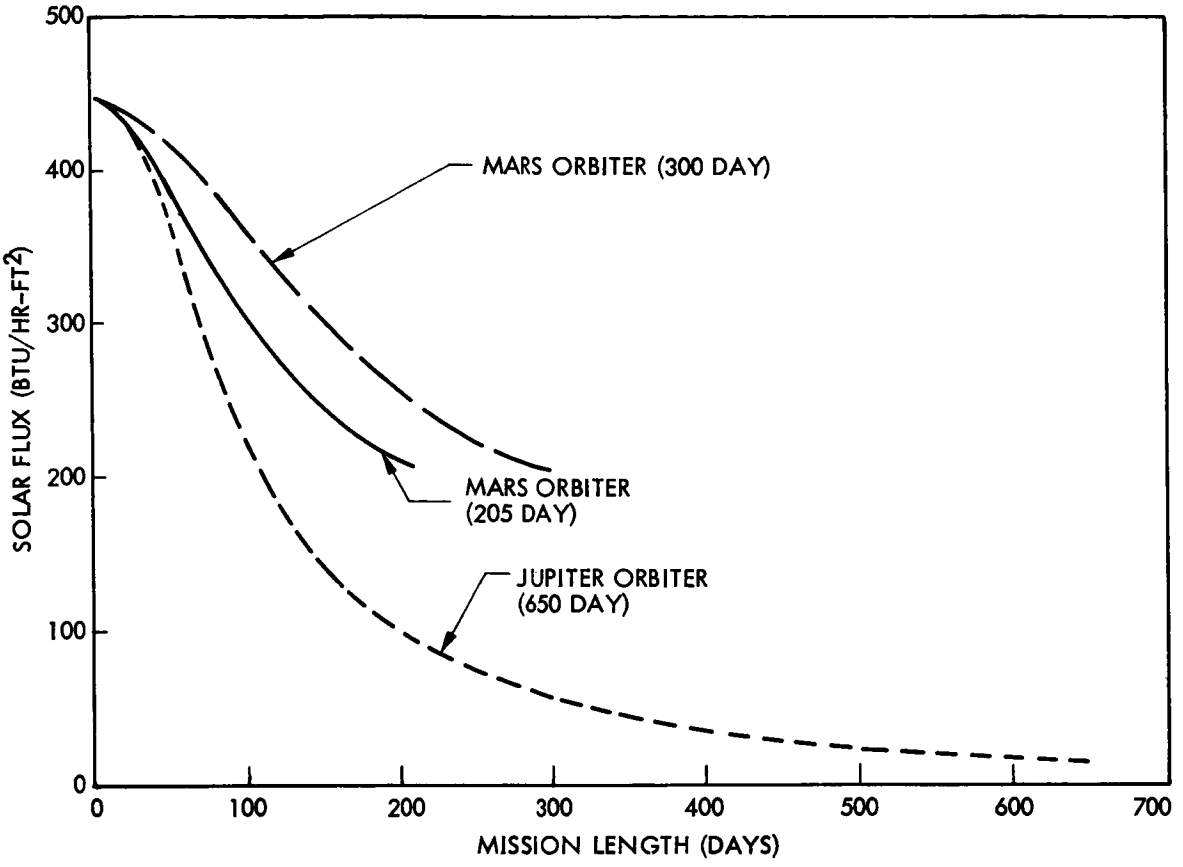

Fig. 6 Solar Flux Variation With Mission Duration

transfer rate to the propellant was constant over the entire time increment, as shown in an example on Fig. 7. At the next time point, the new propellant temperature was again held constant and the heat transfer to the propellant determined, etc. This procedure results in slightly higher surface temperatures because the solar heating decreases during the time interval and the propellant temperature could be increasing, thus decreasing the temperature difference and consequently the heating. A typical example is illustrated on Fig. 7 for the F_2 propellant. All propellants were assumed to be at their normal boiling point temperature at the start of the mission, with the exception of A-50 and MHF-5 which were assumed to liftoff at 530° R

The pressure-fed and pump Thermal Pressurization and Optimization analyses used the heat fluxes to or from the tank, computed in this manner, to account for the energy into both the propellant and ullage volume.

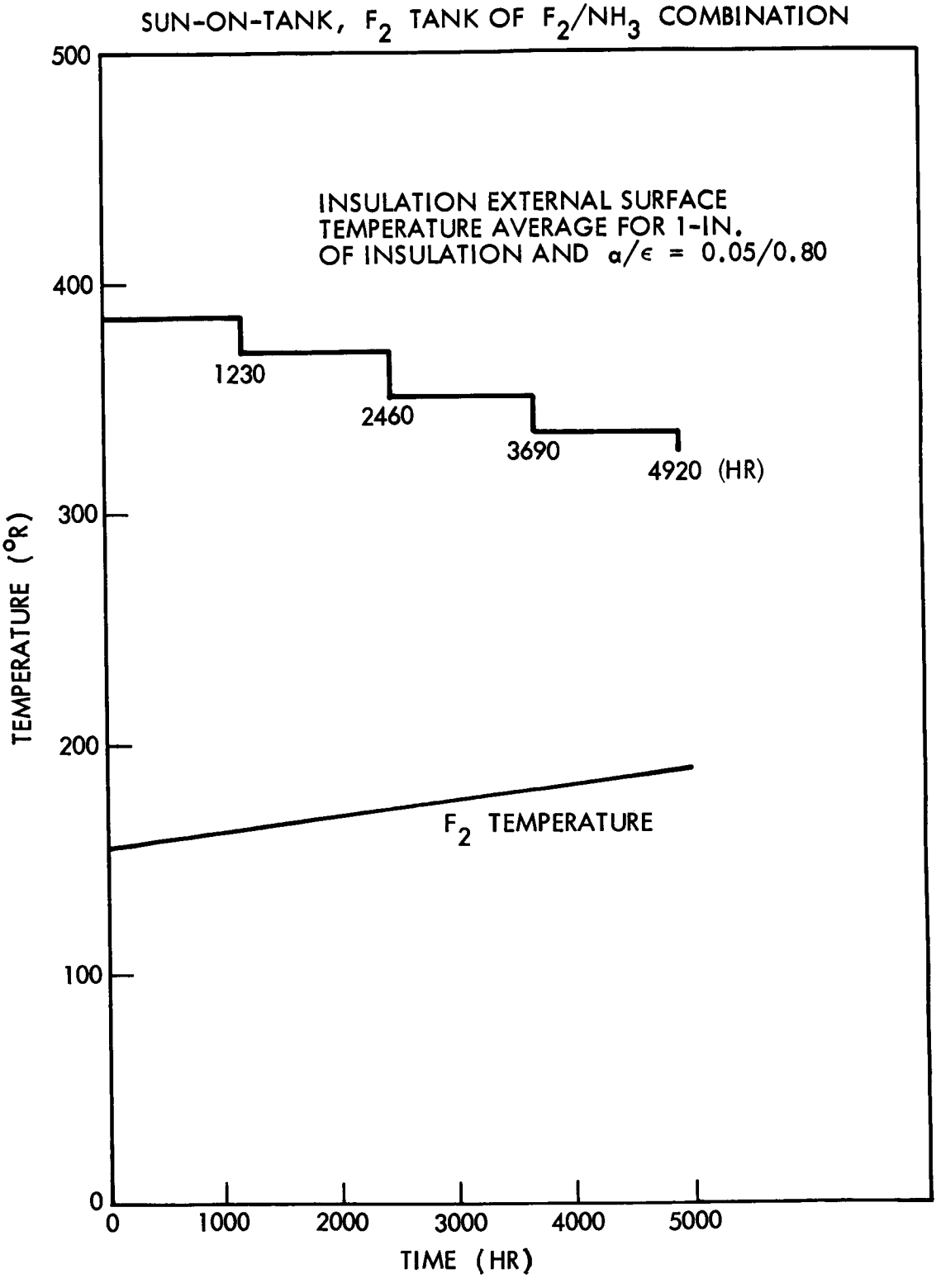

Fig. 7 Mars Orbiter Propellant and Surface Temperature Responses

2.4 PUMP-FED SYSTEMS ANALYSES

Analysis of the pressurization system, for which a schematic is shown on Fig. 8, was based on the following assumptions:

- Helium pressurization furnishes the net positive suction pressure (NPSP) of 4 psi above the propellant saturation pressure required for engine burn throughout expulsion.
- No propellant vaporization into the ullage occurs during expulsion.
- Ullage and liquid is at thermal equilibrium between burns so that the total tank pressure is the sum of partial pressures of the saturated propellant vapor and the partial pressure of the helium.
- Computation of the amount of helium required was based on an inlet temperature equal to propellant saturation temperature. This results in a conservatively high gas requirement but could cause a high tank pressure after burn due to the large partial pressure of helium after reaching thermal equilibrium. Heated helium, which collapses after burn to control tank pressure levels, would be used in most cases.

System operational considerations, that could affect overall weight but would be nearly equal for all propellants (and thus not affect the comparison between propellants), which were not considered, were:

- Preburn flow of propellant to thermally condition the engine
- Post flow of propellant to minimize engine heat soak back
- Any propellant containment or ullage orientation requirements

Since thermal equilibrium was assumed prior to the final burn, propellant vapor weights were determined using the ideal gas relations with propellant saturation temperature and pressure and the last burn ullage volume of 90 percent. Compressibility factors were applied for the oxygen, fluorine, and hydrogen propellants. An idle-mode start capability was assumed.

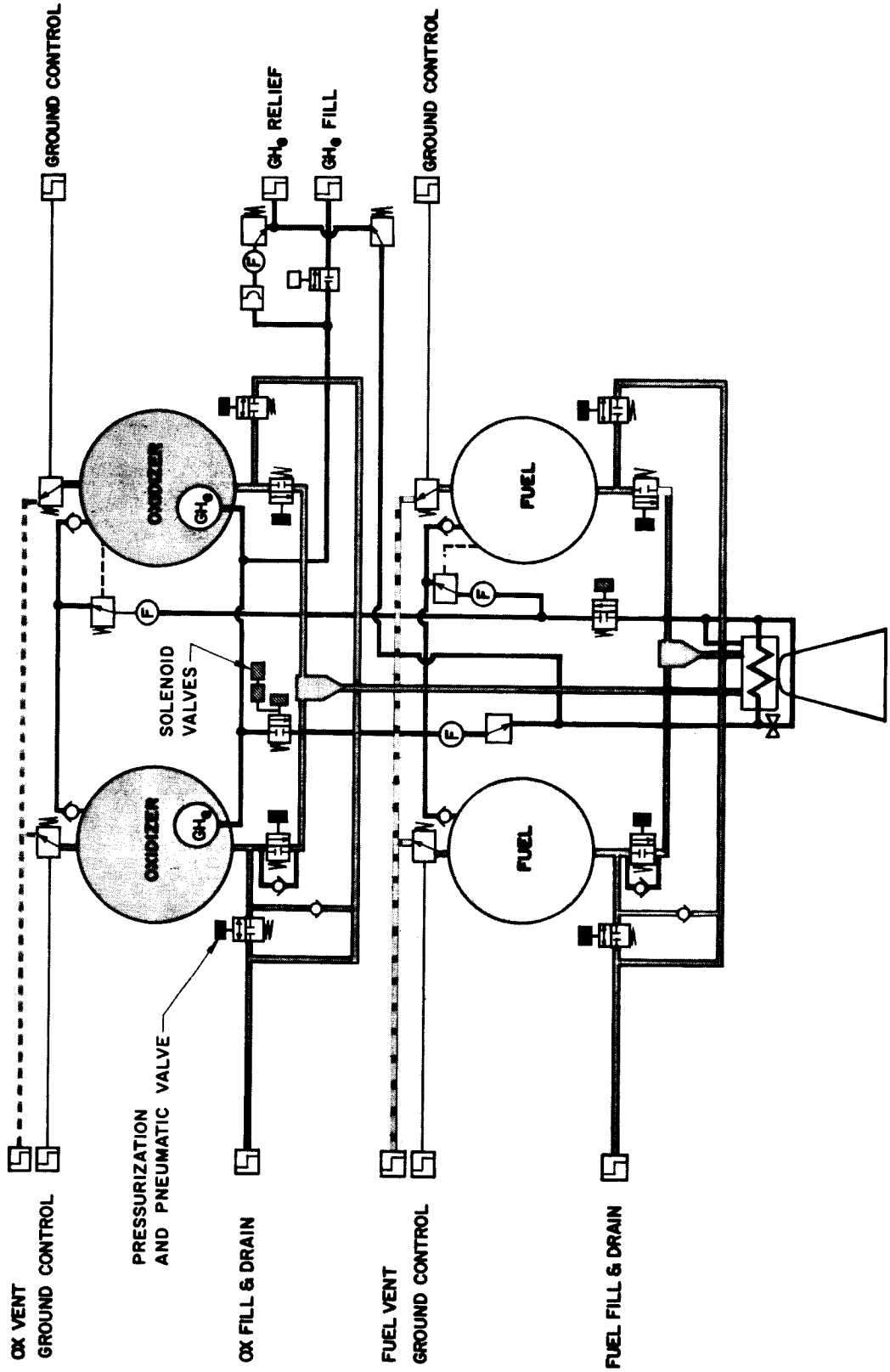

Fig. 8 Pump and Pressure Fed Mars Orbiter Plumbing Schematic

The heat transfer values through the struts, penetrations, and insulation accounted for in the computer models have been tabulated in Table 2 as typical individual heat leaks for O_2, H_2, FLOX, F_2, OF_2, and CH_4. The heat transfer rates are for the sun-on-tank cases with an $\alpha/\epsilon = 0.05/0.80$ surface finish taken at the midpoint of the transit to Mars.

The pump-fed pressurant weights computed ranged from 0.5 to 10 lb of helium, 50 to 70 lb of hydrogen, and total system weights of 27 to 117 lb, as listed on Table 3. Approximate mission pressure profiles are presented on Fig. 9, 10, and 11 for the A-50 propellant, F_2 propellant, and H_2 propellant, respectively. A typical optimization plot is shown on Fig. 12 for FLOX.

These reference system optimizations were for the condition with the sun-on-tank, nonvented, and a mission length of 205 days. Table 4 presents the propellant combinations with the reference optimum surface finishes, design pressures, and insulation thicknesses which are the reference conditions for the many sensitivity analyses conducted. The surface finish requirement for the earth storables was extrapolated to an α/ϵ ratio of 0.6/0.91 (degraded white Skyspar enamel or mosaic of black paint and aluminum). The design pressure for the earth storables was approximately the liftoff pressure since, over the mission, the tanks experience a net heat loss resulting in a subcooled propellant requiring minimum pressurization for burn. The analyses show that with the use of the proper surface finishes, the propellants will remain in liquid state throughout the mission; however, for conservatism to account for gradients, etc., a minimum of 1/4-in. of foam was specified.

The effect of the Mars planet heating on the Mars Orbiter for the 10 days prior to the last burn was assessed and verified to be negligible, as assumed in the analysis. An elliptical orbit of 1,000 km × 20,000 km was considered, with the spacecraft continuously in the sun. Due to the low Mars albedo of 0.15, the relatively low Mars surface temperature, and the highly elliptical orbit, which places the spacecraft near the planet for relatively short periods of time, the heating is very small and could result in an

Table 2

MARS ORBITER, COMPARISON OF STRUCTURAL AND INSULATION HEAT LEAKS
(BASELINE CONFIGURATION)

Propellant	Insulation Thickness (in.)	q_{total} (Btu/hr)	$q_{insulation}$ (Btu/Hr)	q_{strut} (Btu/hr)	$q_{penetration}$ (Btu/hr)
O_2	1	3.66	3.56	0.029	0.072
H_2	4	6.49	5.24	0.71	0.54
F_2	1	3.49	3.35	0.044	0.10
H_2	4	4.45	3.24	0.70	0.51
FLOX	1	6.11	5.41	0.58	0.12
CH_4	1	3.19	2.71	0.42	0.06
OF_2	1	3.49	3.06	0.36	0.07
CH_4	1	3.35	2.86	0.42	0.07
OF_2	1	3.37	2.91	0.36	0.10
B_2H_6	1	0.58	0.48	0.098	0.002
F_2	1	5.81	5.05	0.59	0.17
NH_3	1	-3.55	-3.87	0.22	0.10

NOTE: Sun-on-tank, α/ϵ = 0.05/0.80, and taken at midpoint in Earth-Mars trajectory.

*Insulation thickness at discrete points as read from computer output.

Table 3

MARS ORBITER PRESSURIZATION SYSTEM WEIGHTS

Propellant	Pump-Fed			Pressure-Fed			Lines, Fittings, Misc (lb)	Total Weights	
	He (lb)	He Storage Tank (lb)	Valves (lb)	He (lb)	He Storage Tank (lb)	Valves (lb)		Pump (lb)	Press. (lb)
O_2	6.8	9.8	22[a]	29.6	52	27	8	117[a]	465
H_2	70[a]	-		126	222				
F_2	4.6	8.2	21[a]	24.8	42.4	26	7	89	265
H_2	49[a]	-		59.5	105				
FLOX	10.4	35.4	19	24.0	80.4	19	5	88	174
CH_4	4.0	13.6		10.4	35.0				
OF_2	5.6	13.2	19	11.8	52.6	19	5	66	143
CH_4	6.6	16.8		16.0	38.4				
OF_2	-	-	19	11.4	48.2	19	5	-	125
B_2H_6	-	-		7.8	33.4				
F_2	6.2	19.2	19	19.2	59.6	19	5	52	132
NH_3	0.8	2		7.2	22.2				
N_2O_4	0.6	6	18	9.4	78.8	18	4	33	211
A-50	0.6			7.0	60.6				
ClF_5	0.5	4	18	8.0	68.0	18	4	27	180
MHF-5	0.5			5.6	48.6				

(a) GH_2 Pressurization.

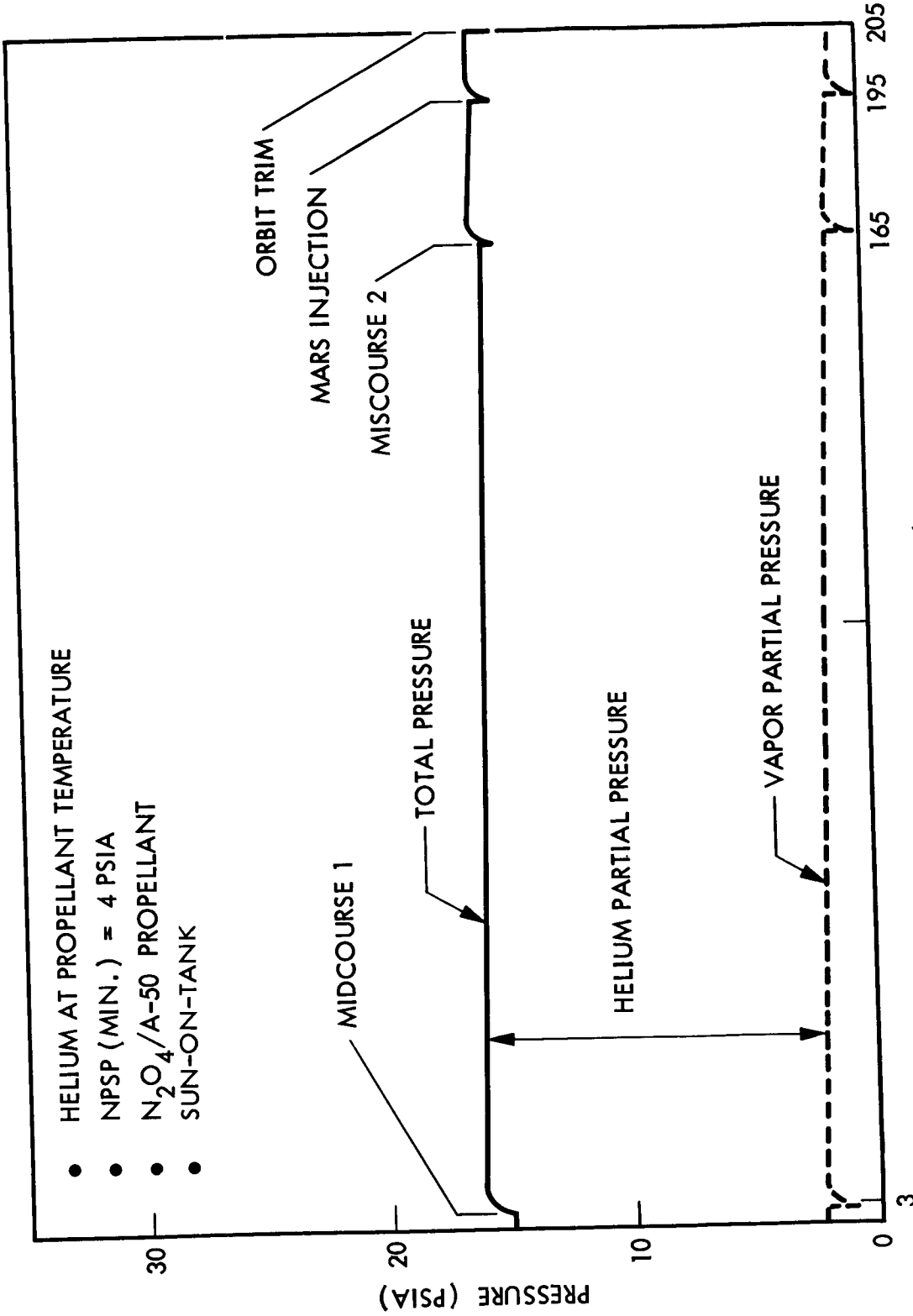

Fig. 9 Pump-Fed A-50 Tank Pressure Profile for Mars Orbiter

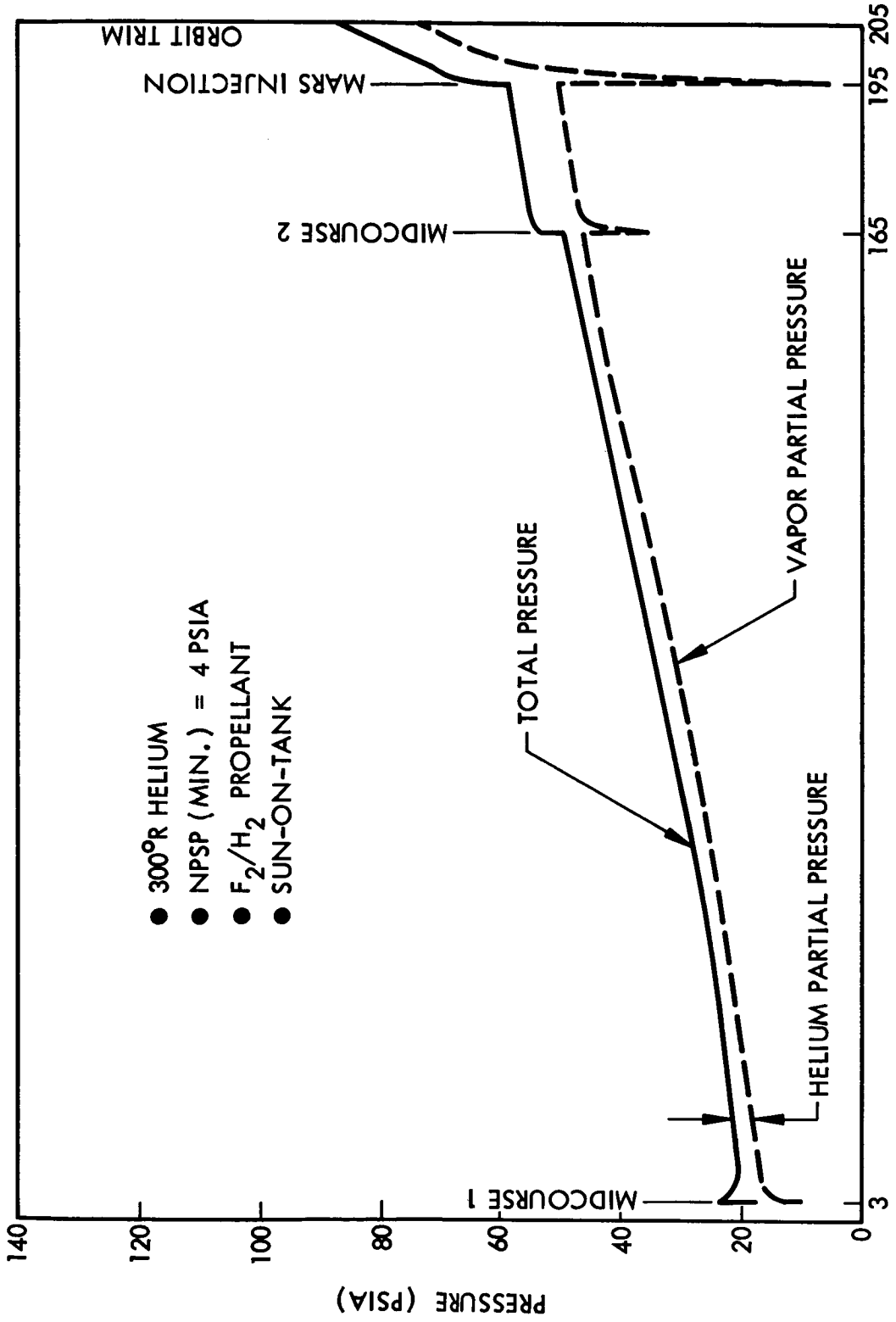

Fig. 10 Pump-Fed F_2 Tank Pressure Profile for Mars Orbiter

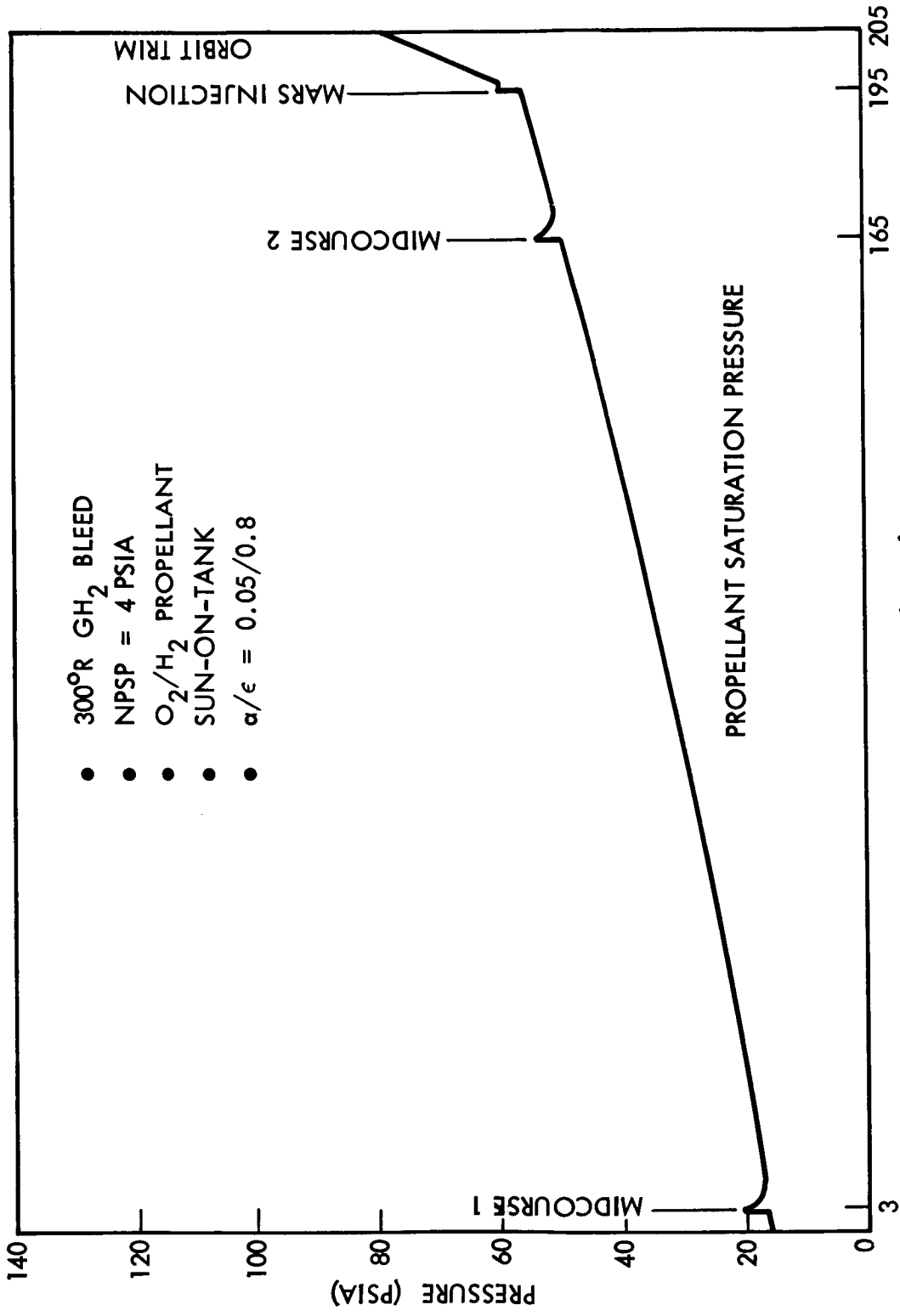

Fig. 11 Pump-Fed H_2 Tank Pressure Profile for Mars Orbiter

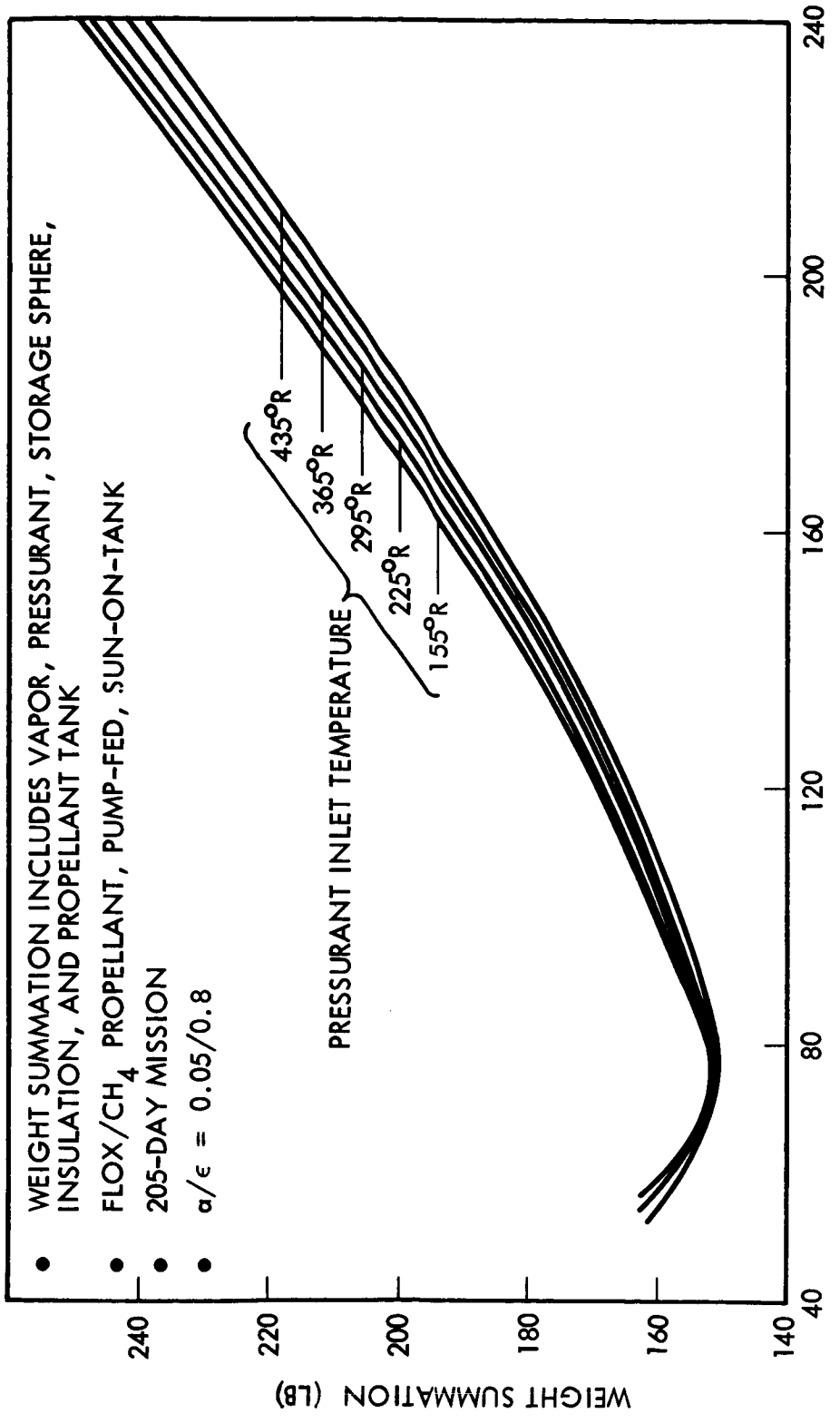

Fig. 12 Mars Orbiter FLOX Tank Optimization

Table 4

MARS ORBITER PROPELLANT SYSTEM OPTIMIZATIONS – PUMP-FED, SUN-ON-TANKS, NONVENTED, 205-DAY MISSION

Propellants	Surface Finish (α/ϵ ratio)		Design Pressure (psia)		Insulation Thickness (in.)	
	Oxidizer	Fuel	Oxidizer	Fuel	Oxidizer	Fuel
O_2/H_2 [a]	0.05/0.80	0.05/0.80	58	96	3/4	4-5/8
F_2/H_2 [a]	0.05/0.80	0.05/0.80	40	130	1-1/8	4-5/8
$FLOX/CH_4$	0.05/0.80	0.05/0.80	57	107	1-1/2	3/4
OF_2/CH_4	0.05/0.80	0.05/0.80	45	107	1-1/8	3/4
F_2/NH_3	0.05/0.80	0.60/0.91 [b]	59	15 [c]	1-3/8	Min. [d]
N_2O_4/A-50	0.60/0.91 [b]	0.60/0.91 [b]	15 [c]	15 [c]	Min. [d]	Min. [d]
ClF_5/MHF-5	0.60/0.91 [b]	0.60/0.91 [b]	15 [c]	15 [c]	Min. [d]	Min. [d]

(a) Elliptical tank configuration
(b) Extrapolated
(c) Maximum pressure at liftoff
(d) Minimum approximately 1/4-in. foam

average insulation temperature rise of approximately 6° F above that with no Mars heating. Several propellants were examined considering (1) the insulation thickness selected due to the optimization, (2) temperature rise of the propellant over the last 10 days, and (3) the temperature difference across the insulation. The H_2 propellant temperature rise due to the Mars heating would be 0.15° F, whereas the F_2, CH_4, and OF_2 propellants would be about 0.26° , and 0.35° , and 0.22° F, respectively, which are not significant temperature changes for this analysis.

2.5 PRESSURE-FED SYSTEMS

The mission, environment, and thermal models for the pressure-fed Mars Orbiter were the same as described in the preceeding sections. However, a more detailed Thermal-Pressurization analysis was required for the pressure-fed system than was conducted for the pump-fed system because of the significantly higher operating pressure. The more detailed analysis procedures developed for the pressure-fed system was then applied to subsequent analyses of the pump-fed systems.

2.5.1 Analysis

The pressurization system (Fig. 8) must supply the net positive suction pressure (N (NPSP) requirements, chamber pressure (P_c), and pressure drops through the feed system. The pressure-fed chamber pressure and pressure drops require higher operating pressures, more pressurant, and larger pressurant storage spheres than the pump-fed systems.

The minimum tank operating pressure is the sum of the system pressure drop (feed lines and injector) plus the 100-psi chamber pressure. Helium pressurant always supplies the 100-psi chamber pressure plus any portion of the system pressure drop not provided by the propellant vapor pressure. When the sum of the propellant saturation pressure (P_v) plus 100 psi is greater than the minimum operating pressure, the chamber pressure (P_c) is then greater than 100 psi. However, when P_v plus 100 psi

is less than the minimum operating pressure, additional helium is required (P_c is never less than 100 psi) to maintain the tank pressure at the minimum. The following system and analytical parameters were used to analyze the pressure-fed systems:

- System Parameters
  - Heated helium pressurant for all tanks
  - P_c = 100 psia
  - Idle mode start
  - Helium stored in lowest temperature propellant
  - Helium storage pressure = 4,500 psia
  - Helium residual pressure after isothermal blowdown = 350 psia
  - Nonvented tanks
- Analytical Parameters
  - Liquid and ullage in thermal equilibrium at start of each burn
  - Mixed ullage energy balances between propellant vapor and pressurant gas during pressurization and liquid expulsion
  - Heat-transfer collapse factor based on a modified Epstein correlation
  - System (liquid and ullage) energy balance computed for periods between burns
  - Ullage volume adjusted to account for liquid expansion due to heating
  - Temperature and pressure dependent properties

The analytical sequence used for the thermodynamic/pressurization optimization is illustrated on Fig. 1. The same basic methods were used for determining the thermal model, incident heat rates, thermal analyzer program, and optimization for both pump-fed and pressure-fed systems. The analysis incorporated the Epstein correlation and the Thermal-Pressurization optimization programs, which are discussed in the following sections.

2.5.2 Epstein Correlation

The Epstein pressurization correlation was used to compute the heat transfer collapse factors when heated pressurant is injected into the tanks (Refs. 3 and 4). Epstein

et al developed this analysis to predict pressurant requirements for complete tank drains with heat transfer and stratification of the pressurant gas. Pressurant requirements could be predicted for partial drains if the volume drained were large compared to the initial ullage volume. However, multiple-burn spacecraft pressurant predictions, with small volume change per burn, required additional analysis. Significant modifications were made to the correlation to allow application to multiburn systems.

The predominant factor in multiburn spacecraft not considered in the Epstein correlation was the relatively large, cold ullage which has a significant thermal inertia compared with the hot pressurization gas which cools and collapses the pressurant. The modification made to account for this collapse was a computation of a mixed ullage temperature using an energy balance, which was superimposed on the ullage heat transfer collapse factor from the Epstein correlation. For each burn, appropriate reference temperatures and characteristic diameters were selected to compute the Epstein correlation collapse factor. The mixed ullage temperatures for prepressurization or the slight volume changes for idle-mode start were computed assuming a constant volume process, and assuming a constant pressure process for expulsion.

2.5.3 Thermal Pressurization

The computation procedure of the Thermal Pressurization program had been developed for analyzing thermodynamic parameters affecting propellant tank storability and pressurization at each burn event of a multiburn mission. This program permits evaluation of the interaction of several parameters and makes possible the analysis of a relatively large number of conditions.

The following factors were considered as either input parameters or dependent variables in the Thermal Pressurization program:

- Gas inlet temperature for prepressurization or idle-mode start
- Expulsion gas temperatures
- Liftoff ullage volume

- Type of pressurant gas
- Propellant heating as a function of insulation thickness
- Propellant mass adjustment for residual vapor
- Tank volume adjustment for propellant mass, initial ullage, or internal pressurant storage changes
- Heated area as a function of volume changes
- Type of propellant
- Multiple burns for a complete mission
- NPSP or pressure requirements

Ullage volume was adjusted empirically and used as input to the program to minimize the high total tank pressures resulting from liquid expansion and high helium partial pressures. Nominal initial propellant loads are adjusted to account for propellant vapor residuals. Internally stored pressurant spheres, ullage volume, and vaporized propellant volume additions to the initial propellant tank volume significantly increased the tank size and thus the surface area and propellant heating.

The number of different propellants analyzed necessitated considerable search to obtain valid physical and thermodynamic property data. Particular problems were encountered in obtaining enthalpies or specific heats for the vapors. A reduced temperature and pressure correlation was used (Ref. 7) for changes in specific heat beyond the low (50 psia or less) pressure. Specific heat at constant volume was computed using ideal gas relations and the specific heat at constant pressure for each reduced temperature and pressure. Vapor compressibility factors were obtained using another reduced temperature and pressure correlation developed by Redlich-Kwong (Ref. 8 and 9). Liquid densities were obtained from various sources and curve fitted to equations having the form of:

$$\rho = CT + D$$

Where ρ is liquid density, T is absolute temperature, and C and D are constants. Saturation pressure-temperature relations were curve fitted to equations having the form of:

$$\ln P = A + B/T$$

Where P is absolute pressure, A and B are constants, and T is absolute temperature. Heats of vaporization at normal boiling point (NBP) were obtained from the literature and values at other pressures determined by applying Theisen's Correlation, as reported by Gambill (Ref. 10).

Only nonvent systems were considered in the analysis; therefore, the partial pressure of noncondensable pressurant sometimes exceeded NPSP. When this occurred, no pressurant was added until the partial pressure of noncondensable helium in the ullage was reduced by expulsion to the required NPSP. New ullage conditions were then calculated assuming an isentropic expansion, permitting computation of pressurant required to complete expulsion of the impulse propellant.

The fluid and pressurization system schematic considered for the pressure-fed system analyses are shown on Fig. 8 with the vent valves, fill and drain disconnects, pressurization system with regulators, etc. The helium was stored internally or externally within the insulation enclosure at the lowest propellant temperature for cryogenic and space-storable propellants to minimize the sphere size. Helium was stored outside the earth-storable propellant tanks, since no storage temperature advantage could be gained with internal storage.

Storage spheres of T2-6Al-4V-ELI titanium were assumed, at a storage pressure of 4,500 psia, a storage temperature equal to the highest temperature reached by the coldest of the two propellants (fuel or oxidizer), and an isothermal expansion to a residual pressure of 350 psia. Pressurant sphere size was limited to less than the 17.5-in.-diam. manhole of the spherical propellant tanks. Up to 22-in.-diam. spheres were assumed for the elliptical hydrogen tanks to minimize the number of pressurant

spheres required. These size limitations and the large pressurant mass requirements were the major factors in selecting a storage sphere pressure of 4,500 psia.

After the pressurant requirements for a burn were determined and the propellant expelled, the constituents of the tank were assumed to come to thermal equilibrium. An energy balance was then taken within the tank to determine the propellant saturation and total tank pressures for the burn. This energy balance considered the environment heating, the energy exchange between the pressurant, vapor, and liquid, and the mass transfer between the liquid and ullage.

Vaporization during expulsion was neglected due to the short expulsion time and low coefficients of diffusivity. Therefore, propellant partial pressures were very low after a large burn, requiring propellant vaporization to reach equilibrium. Heating from the injected pressurant and the external environment of a nearly full tank of liquid primarily raises the liquid temperature. However, with a nearly empty tank, heat inputs will tend to vaporize liquid at a constant or decreasing temperature. These factors are important in determining propellant temperature, pressure, and the residual vapor weight.

For any given mission, propellant, pressurization system, vehicle orientation, and initial ullage volume, the Thermal Pressurization program will provide as output tank radius, pressurant weight, pressurization system weight, and residual vapor weight as functions of tank operating pressure, insulation thickness, and pressurant inlet temperature. These parametric data from a matrix from which a set of optimum system parameters can be selected.

2.5.4 Optimization

The output of the Thermal Pressurization program was the input to a program that sums the various weights and then plots the matrices of data in several formats. The weight relationships for the propellant tank with pressure, and the insulation with

thickness, were computed as a function of the tank radius in the optimization program. Plots were made for each propellants vapor weight, pressurant and storage sphere weight, tank weight, and insulation weight, as a function of the total tank pressure, with various pressurant inlet temperatures as parameters. Summations of these individual weights were also plotted as a function of both the total tank pressure and the insulation thickness, for the five pressurant inlet temperatures. Typical optimization plots for both a pump-fed and a pressure-fed system for FLOX are presented on Figs. 12 and 13 for comparison. The individual plots of vapor, pressurant, and tank pressure and insulation thickness, were prepared for each propellant to develop Tables 3 and 5, but were too numerous to present here. With the optimization plots, optimum thermal-pressurization parameters were selected as the point where system weight was a minimum. Thus, the optimum combination of pressurant inlet temperature, insulation thickness, and operating pressure was determined, as well as the weight sensitivity of the individual parameters. The effects of liquid expansion with temperature rise were included in the analysis.

2.5.5 Results

The vertical portion of the pressure-fed FLOX weight plot (at 195 psia) on Fig. 13 results from insulation thicknesses greater than the optimum value. The optimum system weight occurs at the point where all of the propellant thermal inertia is utilized. Therefore, helium pressurant must supply at least 100 psi chamber pressure, and the minimum system weight occurred when the propellant vapor pressure was just sufficient to overcome the line and injector pressure drops. Additional insulation results in lower propellant vapor pressure and greater system weight because additional pressurant is required for the line and injector pressure drops. Less than the optimum amount of insulation causes an increased system weight due to the higher than minimum operating pressure requiring a heavier propellant tank and increased residual vapor weight.

Pressure-fed optimization plots (Fig. 13) were not as flat near the optimum as those for pump-fed systems (Fig. 12). The pump-fed optimization for FLOX (Fig. 12) shows that

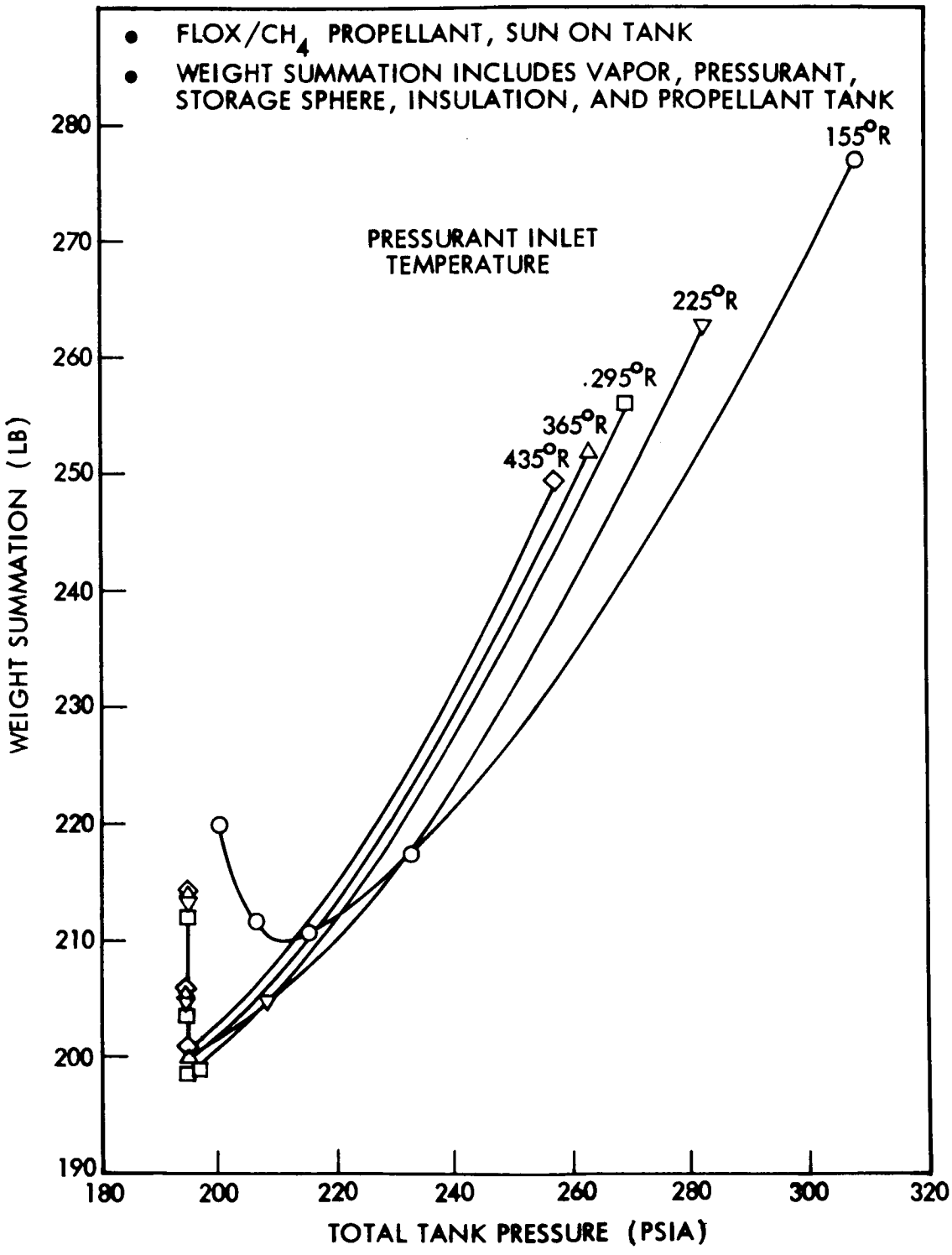

Fig. 13 Mars Orbiter Pressure-Fed FLOX Tank Optimization

Table 5

MARS ORBITER OPTIMIZATION RESULTS – 205-DAY MISSION

Propellant	Pump-Fed System			Pressure-Fed System			
	P[a] (psia)	T[b] (in.)	α/ϵ Ratio	P[a] (psia)	T[b] (in.)	Pressure[c] Drop (psi)	α/ϵ Ratio
F_2	40	1-1/8	0.05/0.80	190	1-1/4	90	0.05/0.80
H_2	130	4-5/8	0.05/0.80	198	4	90	0.05/0.80
O_2	58	3/4	0.05/0.80	195	1-1/4	70	0.05/0.80
H_2	96	4-5/8	0.05/0.80	175	3	70	0.05/0.80
FLOX	57	1-1/2	0.05/0.80	195	1-1/2	95	0.05/0.80
CH_4	107	3/4	0.05/0.80	224	1-1/8	95	0.05/0.80
OF_2	45	1-1/8	0.05/0.80	198	1	95	0.05/0.80
CH_4	107	3/4	0.05/0.80	233	1	95	0.05/0.80
OF_2	-	-	-	178	1	60	0.05/0.80
B_2H_6	-	-	-	201	1/2	60	0.05/0.80
F_2	59	1-3/8	0.05/0.80	195	1-1/2	95	0.05/0.80
NH_3	16	1/4	0.3/0.95	198	1/4	95	0.3/0.95
N_2O_4	<15	1/4	0.6/0.91	165	1/4	65	0.6/0.91
A-50	<15	1/4	0.6/0.91	165	1/4	65	0.6/0.91
ClF_5	<15	1/4	0.6/0.91	165	1/4	65	0.6/0.91
MHF-5	<15	1/4	0.6/0.91	165	1/4	65	0.6/0.91

(a) P = tank maximum operating pressure
(b) T = insulation thickness
(c) Feed line and injector pressure losses include regeneratively cooled passages, where applicable.

a 20-psi change in operating pressure results in only a 5-lb difference in system weight. This was due to the minimum tank gauge allowing relatively high operating pressures, so the optimum was primarily a tradeoff between insulation and vapor weight. When the operating pressure started affecting tank weight, as in a hydrogen tank, the optimum point was better defined.

The results of the Mars orbiter optimizations for the sun-on-tank pressure-fed systems are presented in Table 5, along with the pump-fed system optimizations. Although the insulation requirements were similar for the pressure- and pump-fed system, the weights of the tank, insulation, pressurant, pressurant sphere, and vapor system were significantly higher for the pressure-fed vehicle due to the much higher operating pressures. Table 3 contains sun-on-tank Mars orbiter pressurization system weights for both the pressure-fed and pump-fed vehicles and illustrates the greater weights for the pressure-fed system. The tank weight was greater for the pressure-fed systems due to the higher operating pressures.

Approximate mission pressure profiles are shown for the pressure-fed systems for the H_2 tank, CH_4 tank, and NH_3 tank on Figs. 14, 15, and 16, respectively. The total tank pressure, as well as the vapor partial pressures, are presented to show the behavior of each during the engine burns and the effect of heating between burns.

The expulsion process was assumed to occur without propellant vaporization while the operating pressure was maintained with either helium pressurant or a blowdown process, if sufficient tank pressure existed prior to burn. Thermal equilibrium between burns drops the helium partial pressure due to cooling of the hot pressurant gas. Thermal equilibrium also causes the propellant partial pressure to increase from a low value at the end of burn to the liquid saturation pressure. Total tank pressure would rise with propellant heating since the cooled helium partial pressure remains constant, except when compressed by liquid expansion. The vertical lines at each event on Fig. 14, 15, and 16 indicate the pressure span from preburn operating pressure to the post-burn pressure drop resulting from helium pressurant cooling.

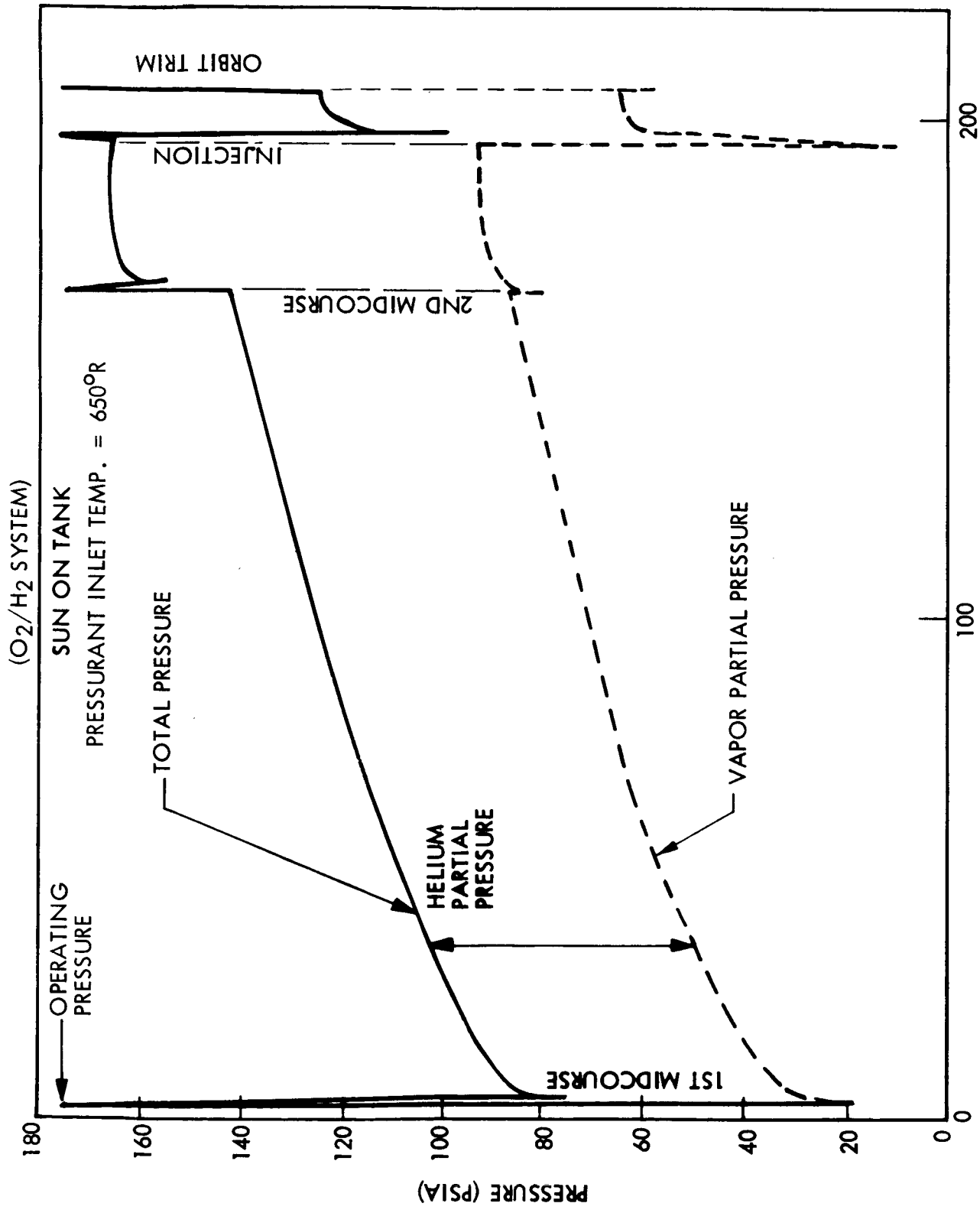

Fig. 14 Pressure-Fed H_2 Tank Pressure Profile for Mars Orbiter

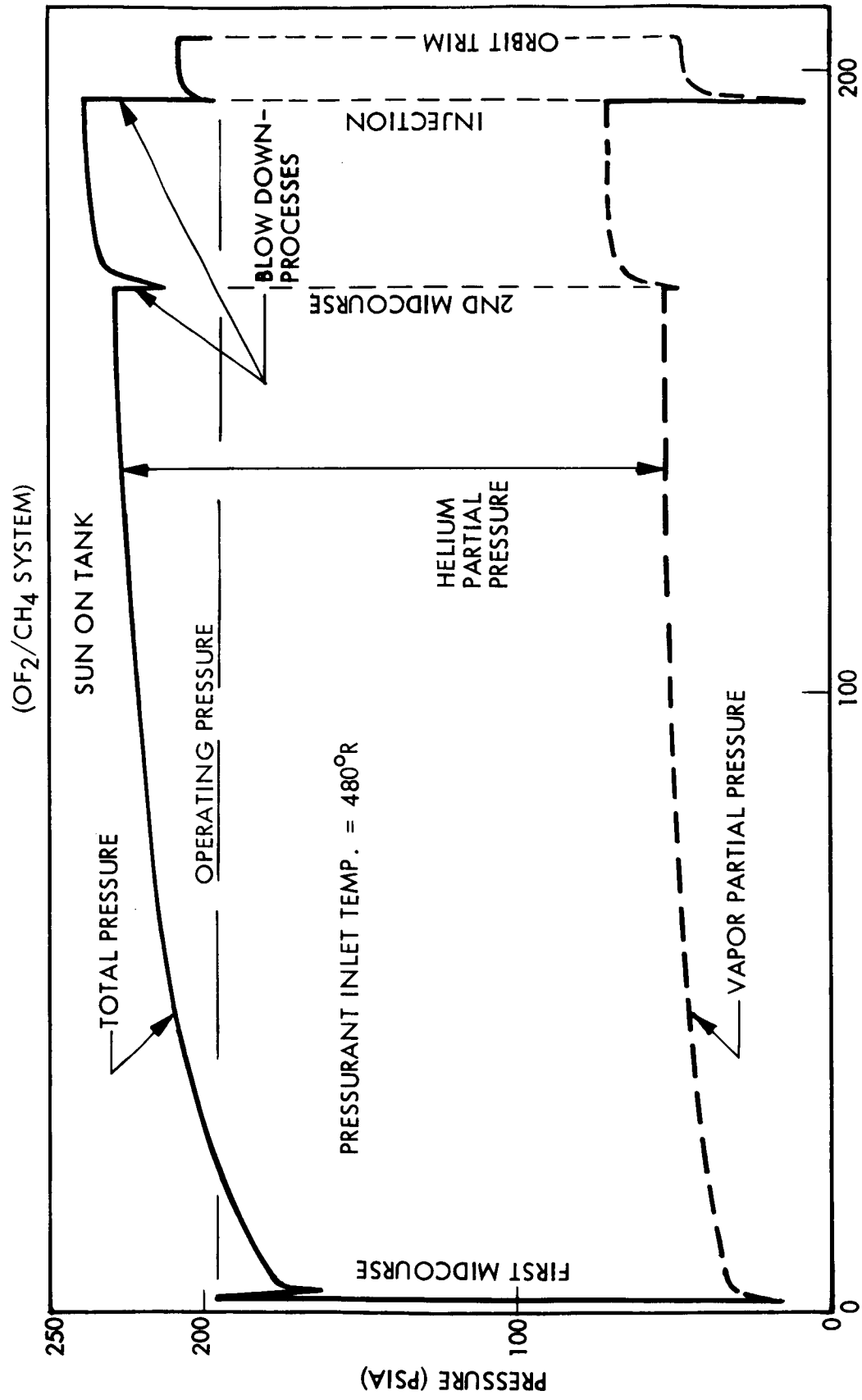

Fig. 15 Pressure-Fed CH_4 Tank Pressure Profile for Mars Orbiter

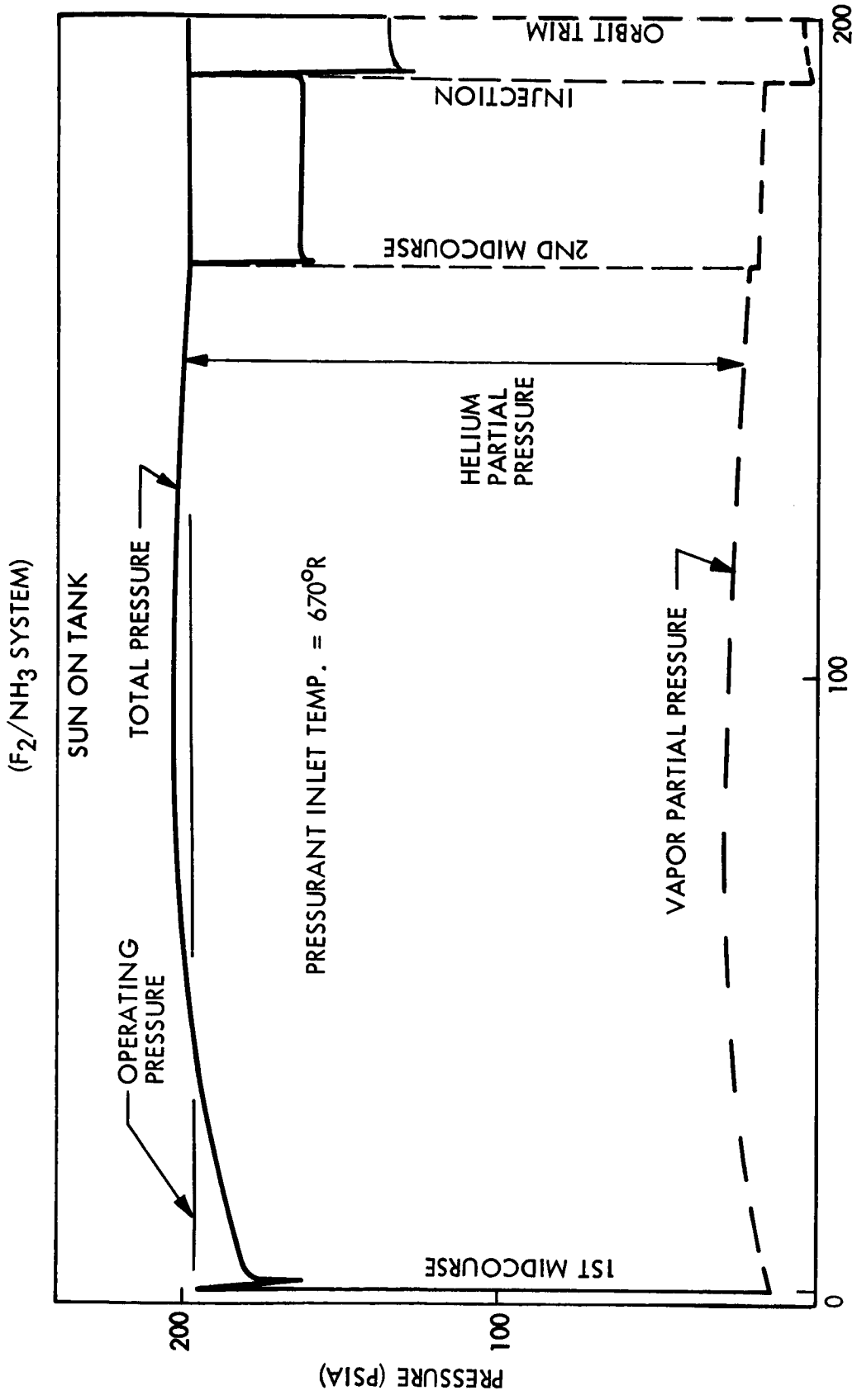

Fig. 16 Pressure-Fed NH_3 Tank Pressure Profile for Mars Orbiter

The subsequent slow pressure rise is the result of propellant vaporization to partial pressure equilibrium after burn, propellant heating causing a saturation pressure rise, and ullage compression by liquid expansion. These pressure relations were computed only at each event and the relative time-relations deduced.

Several of the maximum or tank design pressures listed in the summaries of Table 5 were different for each of the propellant pairs. A transient mixture ratio variation could result from these unequal tank pressures since the mixture ratio of a pressure-fed engine is fixed by the supply pressures. A mixture ratio control may therefore be required. The pressures listed on Table 5 are maximum or tank design pressures which occur prior to the burn at either Midcourse-2 or Orbit Injection. The operating pressure is generally at the nominal level required for the pressure drop plus the chamber pressure. A tank pressure greater than operating pressure results where liquid expansion and propellant vaporization for thermal equilibrium have more effect on the tank pressure than the cooling of the hot helium pressurant. This occurs with small ullage volumes and relatively large heat inputs, and is quite dependent on the initial ullage volume. However, an isentropic expansion or blowdown of the ullage volume was assumed in the analysis for reducing the tank design pressure to the operating pressure during the burn. The volume changes computed for these isentropic expansions totaled less than 3 percent of the total propellant load for all but the OF_2/CH_4 propellant combination, which had a 5-percent blowdown for the CH_4. These peak pressure blowdowns could cause a transient fuel-rich mixture ratio for the space storables and an oxidizer-rich mixture ratio for the O_2/H_2.

The effects of these transients on the total mission are assumed to be small, although a more detailed study should be made on the potential start-up problems and the effect on ΔV of short duration nonoptimum mixture ratios.

2.6 MARS ORBITER PUMP-FED SENSITIVITY ANALYSIS

Many analyses were conducted to assess the effect of various thermal control surface finishes, vehicle orientation, mission length, and insulation conductivity on the

thermal and pressurization parameters that influence performance. Also, as a part of the sensitivity study, venting and subcooling conditions for the hydrogen propellant were analyzed. These analyses are compared to the results for the baseline pump-fed Mars Orbiter, which are presented in Tables 4 and 5.

2.6.1 Surface Finish Characteristics

The tank surface finishes analyzed with the propellant tanks oriented towards the sun were:

- LMSC Optical Solar Reflector (OSR) with an α/ϵ of 0.05/0.8 (second surface mirror with silver-coated fused silica)
- LMSC OSR with an α/ϵ of 0./0.8 (aluminum coated)
- White Thermatrol paint with a degraded α/ϵ of 0.3/0.95

The OSR surfaces have been tested at the LMSC Thermophysics Research Laboratory and found to be extremely stable when exposed to both ultraviolet and electromagnetic radiation. OSR surfaces have been flow on several Air Force programs. OSR is presently manufactured in small squares (1.5 in. by 1.5 in.) and applied to the surface by use of adhesives, which results in about twice the weight of a painted surface and increased material and application cost. The air drying White Thermatrol paint on the tank was studied because several propellants require higher α/ϵ surfaces, and also because it was necessary to determine the penalties if the surface finishes were constrained to paints.

The results of the analyses are presented in Table 6 for α/ϵ = 0.05/0.8, 0.1/0.8, and 0.3/0.95 surface finishes, with the sun on the tank for the 205-day mission. The effect of increasing the α/ϵ ratio for the cryogenic and space-storable propellants is to increase the optimum operating pressure, insulation requirements, and total weight (tank, vapor, and insulation). The effect of using white paint, instead of an OSR surface, is an increase in tank, vapor, and insulation weight. The earth-storable propellants require higher α/ϵ surfaces to prevent freezing and/or to maintain the

Table 6

MARS ORBITER SENSITIVITY TO TANK SURFACE FINISH – PUMP-FED, 205-DAY MISSION
SUN-ON-TANK, NONVENTED

Propellant	α/ϵ = 0.05/0.8[a]			α/ϵ = 0.1/0.8[b]			α/ϵ = 0.3/0.95[c]		
	P (psia)	t (in.)	Wt (lb)[d]	P (psia)	t (in.)	Wt (lb)[d]	P (psia)	t (in.)	Wt (lb)[d]
O_2	58	3/4	107				85	1	121
H_2	96	4-5/8	725				115	4-3/4	735
F_2	40	1-1/8	116				75	2	147
H_2	130	4-5/8	495				150	4-3/4	505
FLOX	57	1-1/2	137	65	1-5/8	143	70	2	153
CH_4	107	3/4	87	110	7/8	92	160	1-1/8	97
OF_2	45	1-1/8	114	52	1-1/4	118	58	1-1/2	131
CH_4	107	3/4	87	110	7/8	92	160	1-1/8	97
F_2	59	1-3/8	119	68	1-1/2	133	70	2	165
NH_3	<15	Min.[g]	70	<15	Min.[g]	70	16	1/4 Min.[g]	68
N_2O_4	<15	1[e]	102	<15	3/4[e]	97	<15	1/2[e]	92
A-50	<15	1-3/8[f]	92	<15	1-1/4[e]	90	<15	3/4[f]	82
ClF_5	<15	Min.[g]	77	<15	Min.[g]	77	<15	Min.[g]	77
MHF-5	<15	3/8[e]	74	<15	1/4[e]	72	<15	Min.[g]	72

(a) LMSC OSR (silver), second surface mirror.
(b) LMSC OSR (aluminum), second surface mirror.
(c) Degraded white thermatrol paint.
(d) Weight of tank, vapor, and insulation (per tank).
(e) Insulation to prevent freezing.
(f) Insulation to maintain T_{min} = 35° F.
(g) Minimum insulation: 1/4-in. multilayer earth storable, 1/2-in. for space storables.

temperature above a minimum allowable limit. The maximum tank pressure for the earth storables is the liftoff pressure because the propellants experience a net heat loss over the mission. As the α/ϵ increased, the insulation requirements drop off to a minimum for the optimum α/ϵ surface (propellant in equilibrium with environment) and increase as the α/ϵ ratio increases beyond the optimum. Thus, the baseline optimizations for the earth-storable propellants specify an α/ϵ ratio of 0.6/0.91 with minimum insulation thickness. Table 4 presents the baseline surface finish α/ϵ, design pressure, and insulation thickness for each propellant. Minimum insulation of 0.25 in. of foam (ρ = 2.5 lb/ft^3) was specified for the earth storables since the analysis shows that no insulation was required with the proper α/ϵ surface. A quarter inch of multilayer could be used instead of the 0.25 in. of foam, since the present technology of multilayer insulation has proven the ease of application and manufacture.

2.6.2 Vehicle Orientation

Two vehicle orientations were analyzed: 1) propellant tanks toward the sun (considered as the Mars Orbiter reference or baseline), and 2) capsule toward the sun. This latter orientation requires that the solar array be extended out further from the equipment section. The weight penalty for extending the solar arrays was 90 lb.

Table 7 presents results of the optimizations for both vehicle orientations with optimum surface finishes for the 205-day mission. The surface finish combinations (on the tank, back of the solar arrays, and equipment section) were adjusted to provide a minimum heating environment for the cryogenic and space-storable propellants, and adjusted to provide a nominal environment for the earth-storable propellants. Operating pressures, insulation requirements, and the weight of tank, vapor, and insulation for the cryogenic and space-storable propellants were lowest with the capsule oriented toward the sun. However, with this orientation, the earth-storable propellants require more insulation to prevent freezing, thus the weight increases. Significant weight savings could be realized with sun-on-capsule orientation for the cryogenic propellants, whereas the

Table 7

MARS ORBITER SENSITIVITY TO VEHICLE ORIENTATION – PUMP-FED, 205 DAY MISSION, NONVENTED, SUN-ON-TANK

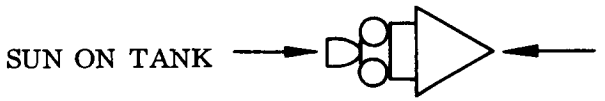

Propellant	Sun-on-Tank (α/ϵ = 0.05/0.8)			Sun-on-Capsule			Weight, ΔW (lb) (All Tanks)	
	P (psia)	t (in.)	Wt (lb)[c] (One Tank)	P (psia)	t (in.)	Wt (lb)[c] (One Tank)		
O_2	58	3/4	107	< 15	1/2 Min.	86	84	404
H_2	96	4-5/8	725	72	1-3/4	405	320	
F_2	40	1-1/8	116	< 15	1/2 Min.	82	68	301
H_2	130	4-5/8	495	80	1-3/4	262	233	
FLOX	57	1-1/2	137	32	1/2 Min.	102	70	104
CH_4	107	3/4	87	< 15	Min.	70	34	
OF_2	45	1-1/8	114	< 15	Min.	79	70	104
CH_4	107	3/4	87	< 15	Min.	70	34	
F_2	59	1-3/8	119	28	1/2	97	44	26
NH_3[a]	16	1/4 Min.	68	< 15	3/4[d]	77	-18	
N_2O_4[b]	< 15	1/4 Min.	86	< 15	2[d]	121	-70	-126
A-50[b]	< 15	1/4 Min.	73	< 15	2[e]	101	-56	
ClF_5[b]	< 15	1/4 Min.	75	< 15	3/8[d]	77	- 4	- 26
MHF-5[b]	< 15	1/4 Min.	71	< 15	5/8[d]	82	-22	

(a) α/ϵ = 0.3/0.95 degraded white thermatrol.
(b) α/ϵ = 0.6/0.91 degraded white skyspar.
(c) Weight includes insulation, vapor and tank.
(d) Insulation to prevent freezing.
(e) Insulation to maintain above T_{min} = 35° F.

ΔW = sum of tank weight for sun-on-tank minus sum of tank weight for sun-on-capsule.

weight savings were small for the space-storable propellants when offset by the 90 lb penalty for extending the solar arrays. The weight savings indicated may not be fully realized when energy gains during the midcourse burns, the orbit injection burn, and orbit trim burn, when the tanks would be exposed to some incident solar energy, are considered. In summary, sun-shielding can result in significant weight savings for the propellant combinations O_2/H_2 and F_2/H_2, marginal (if any) weight savings for the space-storable propellants, and a weight penalty for the earth-storable propellants.

2.6.3 Mission Duration

Environments consisting of several different mission lengths were analyzed to assess the sensitivity to the baseline optimizations. A 195-day mission was analyzed wherein the orbit inject burn was the final burn for the primary propulsion system, and a secondary propulsion system was used for the orbit trim burn. The 290-day mission followed the same trajectory as the 195-day mission except that the transit time was stretched out. This mission required a secondary propulsion system. The 650-day mission was a flight to Jupiter (out to 5.2 AU) and assumed a ΔV burn at arrival equivelant to the Mars Orbiter injection burn, with no subsequent orbit trim maneuver. Table 8 presents the results of the optimizations for the 195-day, 290-day, and 650-day missions.

The longer flight time of the 290-day mission over the 195-day mission results in increased heat transfer to the propellant, and this heat increase shifts the system weight optimization to higher pressures and insulation thicknesses for the cryogenic and space-storable propellants. If surface finish were not changed for the longer mission, the earth-storable propellants would require slightly more insulation than the baseline to prevent freezing, since these propellants experience a heat loss during the mission. Tank surface finishes with higher α/ϵ ratios can be used to compensate for mission length increases; thus, with optimum surface finishes, no weight differences would occur. With higher α/ϵ, higher tank pressures would occur during the initial mission phase, but no weight increase results due to staying within the tank minimum gage.

Table 8

MARS ORBITER SENSITIVITY TO MISSION DURATION WITH NO ORBIT TRIM BURN – PUMP-FED, NONVENTED, SUN-ON-TANK, α/ϵ = 0.05/0.8

Propellant	195-Day Mission[a]			290-Day Mission[b]			650-Day Mission[c] (to Jupiter)		
	P (psia)	t (in.)	Wt (lb)[f]	P (psia)	t (in.)	Wt (lb)[f]	P (psia)	t (in.)	Wt (lb)[f]
O_2	100	1/2 Min[e]	89	160	1/2	90	168	1/2	90
H_2	86	3-3/4	630	106	4-1/4	750	174	4-1/2	870
F_2	80	1/2 Min.[e]	87	100	5/8	89	110	1/2	88
H_2	120	4-1/4	455	140	5-1/4	550	190	5-3/4	610
FLOX	150	5/8	93	175	5/8	96	175	3/4	98
CH_4	164	1/2 Min.	75	180	5/8	79	210	1/2	75
OF_2	85	1/2	85	123	1/2	89	133	1/2 Min.	84
CH_4	164	1/2 Min.	75	180	5/8	79	210	1/2	75
F_2	74	1/2	87	183	5/8	94	183	3/4	95
NH_3[d][e]	<15	1/4 Min.	68	<20	1/4 Min.	68	<30	1/4 Min.	68
N_2O_4[d][e]	<15	1/4 Min.	86	<20	1/4 Min.	86	<30	1/4 Min.	86
A-50[d][e]	<15	1/4 Min.	73	<20	1/4 Min.	73	<30	1/4 Min.	73
ClF_5[d][e]	<15	1/4 Min.	75	<20	1/4 Min.	75	<30	1/4 Min.	75
MHF-5[d][e]	<15	1/4 Min.	71	<20	1/4 Min.	71	<30	1/4 Min.	71

(a) 195-day mission with orbit inject burn only
(b) Stretched out 195-day mission with orbit inject burn only } Requires secondary propulsion system for orbit trim
(c) Jupiter mission with orbit inject burn only
(d) Surface finish optimum for each mission
(e) Minimum insulation: 1/2 in. multilayer (space storables), 1/4-in foam (earth storables)
(f) Weight includes insulation, vapor, and tank (per tank)

The 650-day mission to Jupiter (5.2 AU), where the solar flux is 16.4 Btu/hr-ft^2, presents a much colder environment than the Mars mission where the solar flux is about 200 Btu/hr-ft^2. With the longer mission, but a colder environment, the cryogenics are affected slightly toward higher operating pressures, small insulation increases, and small weight changes. For the space-storable propellants, the outer insulation temperature approaches or was below the propellant temperature, resulting in a near equilibrium condition or a slight heat loss. The mission environment results in a heat gain for the initial phase, but a net heat loss for the total mission for all but the H_2 propellant. Thus, the design pressure and insulation requirements were determined based upon the maximum propellant temperature during the mission. The outer insulation temperature is always above the hydrogen propellant temperature and results in a heat gain over a longer time span. Also, the effect of the H_2 tank strut connected to the 70° F equipment section causes a near constant rate of heat gain during the longer mission, and increases pressure, insulation, and weight requirements. For the earth-storable propellants, either a higher α/ϵ ratio of more insulation would be required to prevent freezing.

Table 9 presents the results of a 300-day mission which, like the 205-day mission, considers performing the orbit inject burn with the primary propulsion system. The optimum operating pressures, insulation requirements, and the total weight will all increase with the longer mission duration. The hydrogen tank optimizes at pressures about 20-psi higher, with around 1-in. more insulation, and with a total weight increase of about 100 lb. The space-storable tank, vapor, and insulation system weight increases are on the order of 10 percent or less. The earth-storable propellants system weight changes can be minimized by surface finish changes.

2.6.4 Insulation Conductivity

The effect of degraded insulation (increased conductivity) upon the optimizations was evaluated for the sun-on-tank orientation. The degraded insulation analysis considered that the conductivity (k) was twice the baseline values: for H_2, $k = 2.5 \times 10^{-5}$

Table 9

MARS ORBITER SENSITIVITY TO MISSION DURATION WITH ORBIT TRIM BURN – PUMP-FED, NONVENTED, SUN-ON-TANK, α/ϵ = 0.05/0.8

Propellant	205-Day Mission (Baseline)			300-Day Mission[a]		
	p (psia)	t (in.)	Weight (lb)[b]	p (psia)	t (in.)	Weight (lb)[b]
O_2	58	3/4	107	80	1	119
H_2	96	4-5/8	725	114	5-1/4	855
F_2	40	1-1/8	116	50	1-1/4	122
H_2	130	4-5/8	495	150	5-3/4	595
FLOX	57	1-1/2	137	75	1-5/8	146
CH_4	107	3/4	87	140	1	95
OF_2	45	1-1/8	114	56	1-1/4	126
CH_4	107	3/4	87	140	1	95
F_2	59	1-3/8	119	74	1-5/8	142
NH_3	<15	1/4 Min.	68	20	1/4 Min.	68
N_2O_4	<15	1/4 Min.	86	<20	1/4 Min.	86
A-50	<15	1/4 Min.	73	<20	1/4 Min.	73
ClF_5	<15	1/4 Min.	75	<20	1/4 Min.	75
MHF-5	<15	1/4 Min.	71	<20	1/4 Min.	71

(a) Stretched out 205-day mission, including orbit trim burn.
(b) Weight of tank, vapor, and insulation (per tank).
(c) Surface finish optimum for each mission, 1/4 in. min. foam (ρ = 2.5 lb/ft^3).

Btu/hr-ft-°R degrades to 5.0×10^{-5}; for space storables, $k = 5.0 \times 10^{-5}$ degrades to 10.0×10^{-5}; and for the earth storables $k = 10.0 \times 10^{-5}$ degrades to 20.0×10^{-5}. The effect of degrading the insulation conductivity was to increase the insulation weight at each pressure; thus, the optimums were at higher operating pressures, thicker insulation, and greater total weights (Table 10). The cryogens and space storables were affected quite significantly. The optimum insulation thicknesses increased between 25 and 100 percent, and the operating pressures increased between 12 and 54 percent, resulting in increased total weights. The earth-storable propellants were not affected significantly since, with the optimum α/ϵ ratio, the environment temperatures were very near the propellant temperature.

2.6.5 Venting

Venting was considered only for the liquid hydrogen propellant. The propellant boiloff weight was determined as a function of insulation thickness and tank operating pressure. The boiloff and insulation weights were summed for each operating pressure considering the difference in penalties associated with a fixed weight and one where boiloff was dumped overboard. The minimum total weight of insulation and boiloff thus was determined as a function of the operating pressure and summed with the tank and vapor weights to determine the optimum operating pressure.

Table 11(A) presents the results of the vented H_2 tank analysis with the nonvented 205-day baseline for comparison. The oxidizer tanks (O_2 and F_2) were assumed to be cooled by the vented hydrogen vapor with a resultant decrease in operating pressure, insulation, and total weight. The oxidizer tanks reached a maximum pressure which dropped off once venting started; however, the tank weight remained constant because the maximum pressure was less than the pressure for the minimum tank gage. The total system weight differences do not reflect the increased tank weight due to the additional hydrogen that was vented during the mission. This weight increase would be in the order of 6 to 10 percent for the H_2 tanks, or 12 lb for the O_2/H_2 combination and 14 lb for the F_2/H_2 combination. The weight of the vapor vented during the mission

Table 10

MARS ORBITER SENSITIVITY TO INSULATION CONDUCTIVITY – PUMP-FED, NONVENTED, 205-DAY MISSION, SUN-ON-TANK, α/ϵ = 0.05/0.8

Propellant	Baseline Insulation			Degraded Insulation			Insulation Conductivity (Btu/hr-ft-°R)	
	p (psia)	t (in.)	Weight (lb)[a]	p (psia)	t (in.)	Weight (lb)[a]	$K_{baseline}$	$K_{degraded}$
O_2	58	3/4	107	65	1-1/2	142	5.0×10^{-5}	10.0×10^{-5}
H_2	96	4-5/8	725	140	6-3/8	920	2.5×10^{-5}	5.0×10^{-5}
F_2	40	1-1/8	116	58	1-3/4	134	5.0×10^{-5}	10.0×10^{-5}
H_2	130	4-5/8	495	187	6-1/4	640	2.5×10^{-5}	5.0×10^{-5}
FLOX	57	1-1/2	137	83	2-3/8	162	5.0×10^{-5}	10.0×10^{-5}
CH_4	107	3/4	87	165	1-1/4	101	5.0×10^{-5}	10.0×10^{-5}
OF_2	45	1-1/8	114	69	1-1/2	136	5.0×10^{-5}	10.0×10^{-5}
CH_4	107	3/4	87	165	1-1/4	101	5.0×10^{-5}	10.0×10^{-5}
F_2	59	1-3/8	119	78	2-1/2	155	5.0×10^{-5}	10.0×10^{-5}
NH_3[b]	16	1/4 Min.[c]	68	~ 18	1/4 Min.[c]	68	10.0×10^{-5}	20.0×10^{-5}

(a) Weight of tank, vapor, and insulation (per tank)
(b) α/ϵ = 0.3/0.95 baseline
(c) Minimum 1/4-in. multilayer

Table 11

MARS ORBITER SENSITIVITY TO VENTING AND SUBCOOLING – PUMP-FED, 205-DAY MISSION, SUN-ON-TANK, α/ϵ = 0.05/0.8

(A) VENTING HYDROGEN

Propellant	Nonvented			Vented H_2 – Oxidizer Tanks Cooled by H_2 Vapor				ΔWeight[b] Nonvented Minus Vented (lb)
	p (psia)	t (in.)	Weight (lb)[a]	p (psia)	t (in.)	Weight (lb)[a]	Vented Vapor (lb)	
O_2	58	3/4	107	15	1/2	86	140	254
H_2	96	4-5/8	725	66	2-1/4	510		
F_2	40	1-1/8	116	15	1/2	82	125	161
H_2	130	4-5/8	495	70	2	363		

(B) SUBCOOL HYDROGEN

Propellant	$T_{initial} = T_{NBP}$ (36.8°R)			H_2 Initial Temperature Triple-Point (24.9°R)			H_2 Initial Condition 50 Percent Slush		
	p (psia)	t (in.)	Weight (lb)[a]	p (psia)	t (in.)	Weight (lb)[a]	p (psia)	t (in.)	Weight (lb)[a]
O_2	58	3/4	107	58	3/4	107	58	3/4	107
H_2	96	4-5/8	725	66	3-3/4	525	66	3	460
F_2	40	1-1/8	116	40	1-1/8	116	40	1-1/8	116
H_2	130	4-5/8	495	95	3-3/4	386	82	3-1/2	346

(a) Weight includes insulation, vapor, and tank (per tank)
(b) Δ Weight based on summation for all tanks.

was 140 and 125 lb, respectively, for the O_2/H_2 and F_2/H_2 combinations. To obtain a spacecraft weight penalty, vented vapor weights were multiplied by a tradeoff factor of 0.69. The weight savings for the vented system of around 245 and 161 lb, respectively, for the O_2/H_2 and F_2/H_2 combinations, must be reduced by the weight increase for the larger tank to a net propellant system (without propellant) weight saving of 242 and 152 lb total, respectively. The final effect on the total spacecraft stage weight is a net weight reduction of 466 and 340 lb respectively.

Venting of space-storable propellants was not considered, since no significant weight savings could be attained. All the space-storable optimizations were on the flat or minimum gage portion of the tank weight curve, and the insulation thicknesses were around 1 in. Venting would reduce the insulation requirements to around 0.5 in., and would reduce the operating pressure and the vapor weight; however, the vapor to be vented must be carried on board the spacraft and requires a larger tank, resulting in additional system weight. It appears that space-storable propellants should not be vented because the potential weight gain is small and venting is complex.

Venting of earth-storable propellants was not considered since these propellants optimize with minimum insulation and pressures. Therefore, with proper selection of surface finish, these propellants can be maintained within reasonable temperature bounds and no weight savings could be achieved by venting.

2.6.6 Subcooling

The effect of subcooling propellants prior to liftoff is to increase thermal capacity. Prelaunch subcooling of H_2 propellant to its triple point (24.9° R) and below to 50 percent slush were analyzed. The effect of subcooling was to decrease both operating pressure and insulation requirements, and to reduce stage weight by 1.3 percent for F_2/H_2 and 3 percent for O_2/H_2 for triple-point H_2, and by 2.3 percent for F_2/H_2 and 4 percent for O_2/H_2 for 50 percent slush H_2. Subcooling of the space-storable propellants was not analyzed since the weight gains that could be realized were very small (on the order of 20 lb) due to operating pressures of the tank being less than minimum tank gage limits.

Table 11 (B) presents the results of the optimization for subcooling hydrogen to the triple point and to 50 percent slush. The normal boiling point initial condition results are presented for comparison.

2.7 SHADOW-SHIELD EVALUATION

The effect of shielding the propellant tanks from the sun was briefly evaluated by using data available from the sun-on-capsule and sun-on-tank analyses. It was assumed that the sun-on-capsule condition represented a case of total propulsion system shading. This 100-percent effective shield gives the lowest possible total heat input to the hydrogen propellant, and actually results in cooling of the other propellants analyzed. Maximum heating of all propellants for any surface finish occurred with the sun on the tanks; thus, both maximum and minimum heating (or in some cases cooling) limits were established. A sun-on-tank orientation with a shield to shade the propellant tanks was assumed to result in a heat input between these limits. However, because sun-on-capsule orientations caused cooling for all but the hydrogen, judgement was required to interpolate along the locus of heat-input-dependent weight/pressure curves. The shadow shield assumed consisted of one or more circular radiation shields mounted aft of the propellant tanks with the engine protruding through the center. This condition differs from the sun-on-capsule orientation because exposure of the engine to the sun results in higher engine temperature and, therefore, a higher engine feed line heat leak. The shield also reduces the view factor between propellant tanks and space, and tank insulation surface temperatures, therefore, tend to be slightly higher than for the sun-on-capsule condition.

2.7.1 Pump-Fed Mars Orbiter

Optimum system weights for the sun-on-tank and sun-on-capsule, from the analyses of O_2, F_2, FLOX, OF_2, and CH_4 propellants, are plotted as a function of tank pressure in Fig. 17. Data points were included for the three different surface finishes analyzed for the sun-on-tank orientation. Heating variations due to different surface finishes for

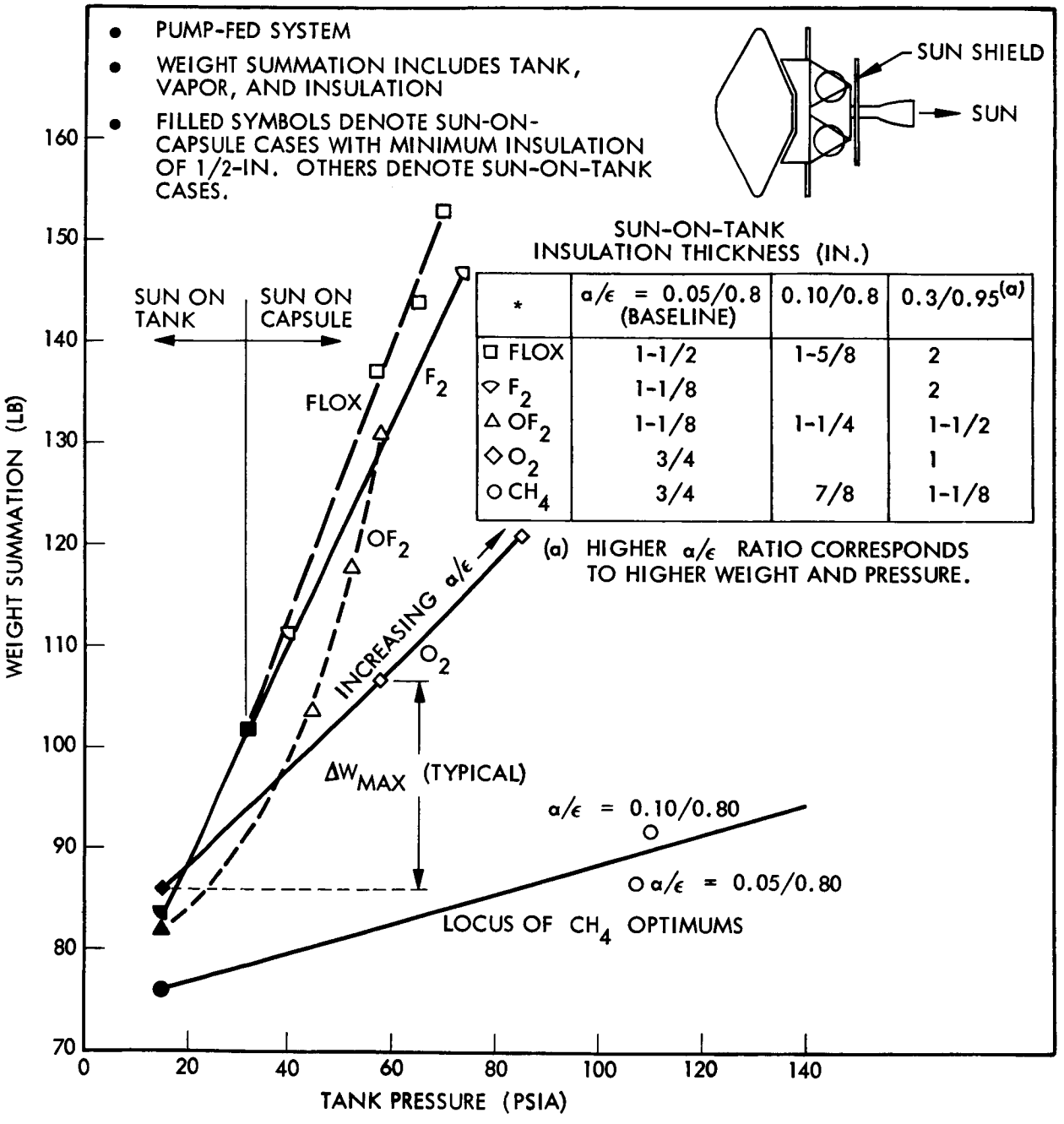

Fig. 17 Mars Orbiter Pump-Fed Sun-Shield Evaluation

sun-on-capsule orientation were slight. Tank pressure was a direct function of heat input; therefore, the curves on Fig. 17 represent system weights as a function of heat input and are assumed to be the locus of the optimum points of system weight vs. pressure curves.

Estimates of optimum insulation thickness, tank pressure, and the corresponding tank, vapor, and pressurant weights could be made for the sun shield case by determining what percentage additional heating occurs relative to the lower (sun-on-capsule) limit. However, for all propellants (except for hydrogen) a net cooling occurred for the sun-on-capsule orientation. The heating which occurs with a sun shield is a point which lies between these two limits (sun-on-capsule, and sun-on-tank with $\alpha/\epsilon = 0.05/0.8$). If the net heating with the sun shield were zero, or if cooling occurred, the sun-on-capsule weight/pressure optimum point could be attained, together with the maximum possible weight reduction. Operating pressures for these cooled propellants were estimated using the maximum possible system weight reduction with a minimum 0.5-in. insulation thickness for points with an $\alpha/\epsilon = 0.05/0.8$ surface finish and sun-on-tank orientation. This assumes the sun shield would be at least effective enough to reduce the heating, and thus saturation pressure and vapor weight, so that only the minimum 0.5-in. insulation would be required. The system weight would thus be reduced by the amount of the insulation weight reduction.

Since the operating pressure ranges were well below the maximum for the minimum tank gage, tank weight would be unaffected. The vapor weight would be much less than for the unshielded sun-on-tank case but slightly more than for the sun-on-capsule case. An approximation of the vapor weight reduction (2.5 to 7 lb) was made using the minimum operation pressure. The weight reductions per tank obtainable with sun shields ranged from 6 to 11 lb for CH_4 up to 25.9 to 35 lb for FLOX, as shown in Table 12. The additional inert weight required for a sun shield was not included.

The optimum hydrogen system weights plotted as a function of pressure on Fig. 18 differ from the other propellants because of differences in hydrogen properties and

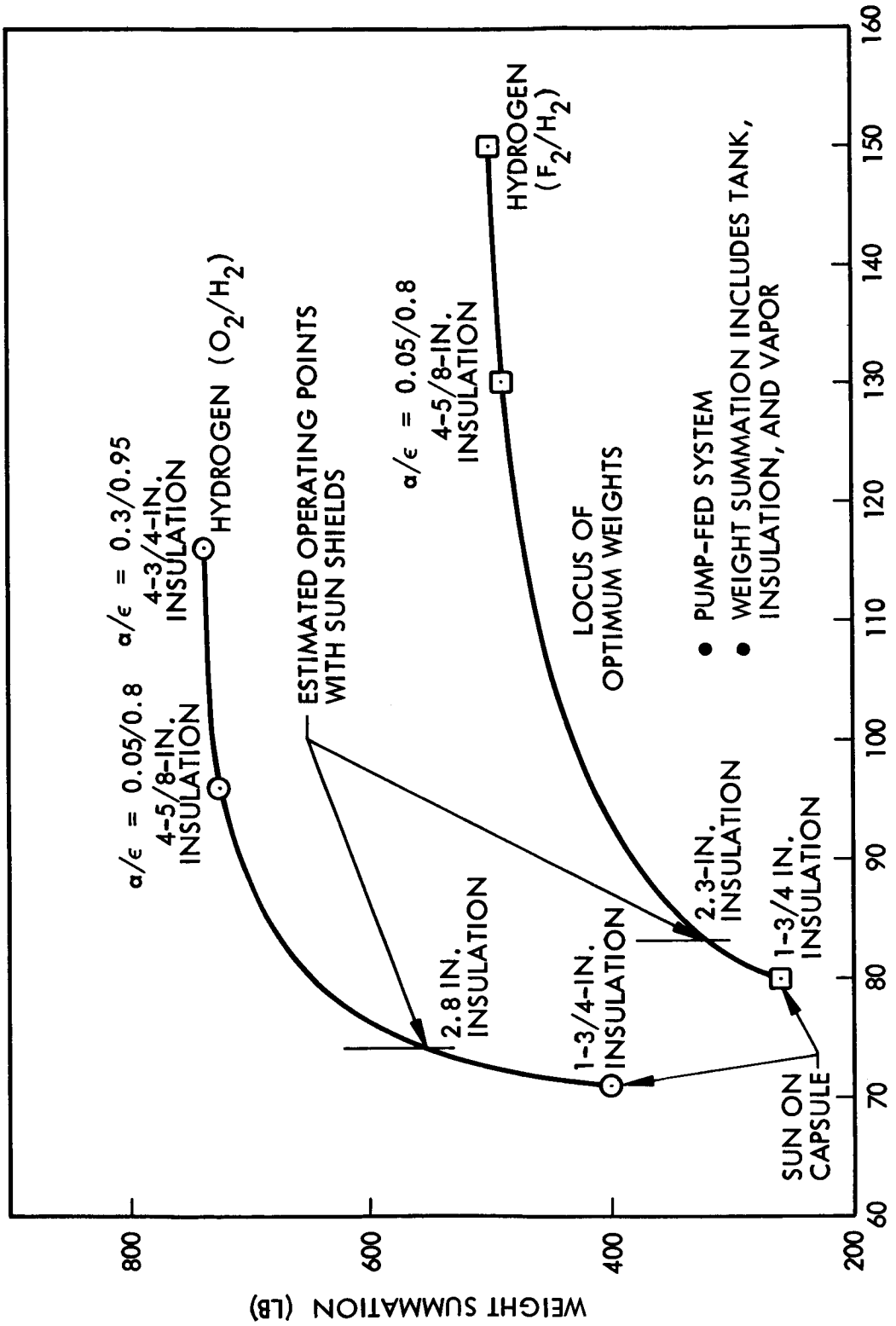

Fig. 18 Mars Orbiter Pump-Fed H_2 Tanks Sun-Shield Evaluation

Table 12

WEIGHT REDUCTIONS POSSIBLE BY SUN SHIELDING – PUMP-FED MARS ORBITER

Propellant	Potential Weight Reduction Range (lb/tank)	
	Minimum	Maximum
FLOX	25.9	35.0
F_2	16.1	29.5
OF_2	17.2	21.5
O_2	8.0	21.0
CH_4	6.0	11.0

because heating occurred for both orientations. The locus of optimum H_2 weight-pressures shows a large weight savings potential by using a sun shield (over 300 lb). This difference in weight for the shielded and unshielded configurations results primarily from two factors: The tank weight is a strong function of pressure, and the insulation weights are significantly different. With the shielded configuration it was estimated that the propellant temperature increase during the mission was 4 percent greater than for the sun-on-capsule oriented H_2/O_2 and H_2/F_2 systems. This would cause a 4 and 3 psi rise in H_2 saturation pressures respectively, giving total H_2 tank pressures of 64 and 93 psia. The weights and insulation thicknesses for these pressures are 500 lb and 2.8 in. for the O_2/H_2 tanks, and 293 lb and 2.3 in. for the F_2/H_2 tanks. The insulation thickness was estimated by finding the tank and vapor weights at the new H_2 operating pressure (74 and 93 psia) and subtracting these from total system weight. The difference is their insulation weight, which gives the new insulation thickness.

It appears that significant weight savings (nearly half the insulation requirement) could be realized by sun shielding the pump-fed hydrogen systems. More detailed analysis of sun shields is recommended to better define the requirements. To illustrate the potential of shadow shields, Table 13 presents the estimated weights, per tank, of

Table 13

MARS ORBITER SHADOW SHIELD COMPARISON

Propellant	Sun-on-Capsule		Shadow Shield		Sun-on-Tank α/ϵ = 0.05/0.8	
	Total Weight (lb)[a]	t (in.)[b]	Total Weight (lb)[a]	t (in.)[b]	Total Weight (lb)[a]	t (in.)[b]
O_2	90[c]					
	86	1/2	99	1/2	107	3/4
H_2	405	1-3/4	500	2.8	725	4-5/8
	581		599		832	
F_2	90[c]					
	82	1/2	96	1/2	112	1-1/8
H_2	262	1-3/4	293	2.3	495	4-5/8
	434		389		607	
FLOX	90[c]					
	102	1/2	111	1/2	137	1-1/2
CH_4	76	1/2	81	1/2	87	3/4
	268		192		224	
OF_2	90[c]					
	82	1/2	87	1/2	104	1-1/8
CH_4	76	1/2	81	1/2	87	3/4
	248		168		191	

(a) Weights of insulation, tank, vapor and pressurant (per tank).
(b) Insulation thickness.
(c) Weight penalty for reorienting solar panels.

insulation, tank, vapor, and pressurant for the shadow shield case as compared with the sun-on-capsule and sun-on-tank cases. Weight of the shadow shield has not been estimated, but would be small.

2.7.2 Mars Orbiter Pressure-Fed System

For the pressure-fed systems, sun shields could be used to reduce system weight by reducing insulation requirements. The system operating pressure would not change from the sun-on-tank case since, in most cases, it was dictated by the total of the line and injector pressure drops plus the chamber pressure. Thus, no reduction in tank weight could be realized. The optimum system weight occurred at the point where all the propellant thermal inertia was utilized. Helium pressurant was always required to supply the 100-psi chamber pressure; thus, the minimum system weight occurred when the propellant vapor pressure was just sufficient to overcome the line and injector pressure drops.

With the use of a sun shield, the optimum propellant temperature and corresponding vapor pressure can be attained with less insulation since the propellant heating rate would be reduced. Thus, tank and pressurant weights remain nearly constant (affected slightly by lower ullage volume requirements), but the total system weight would be reduced. If the sun shielding were effective enough to cause a net heat loss during the mission, system weights would be a minimum, since both vapor and insulation weights would be a minimum. However, the pressurant requirements could be slightly increased due to the reduced vapor partial pressure.

For reduced heating conditions, the ullage volume requirements are less, which reduces overall system weights. The ullage volume requirements would be insignificant for most propellants with the exception of hydrogen and methane. For example, the sun-on-tank pressure-fed hydrogen system tanks require about 20 percent ullage volume. This large ullage volume requirement and corresponding tank weight could be decreased significantly with sun shields.

2.8 MARS ORBITER WORST-ON-WORST ANALYSIS

An analysis was made of the Mars Orbiter vehicle considering that the nominal insulation conductivity and penetration heat leaks were doubled, that only white paint surfaces could be used, and the helium pressurant storage spheres were to be man-rated. This combination of adverse design conditions was entitled the worst-on-worst design.

2.8.1 Assumptions

In order to evaluate the Mars Orbiter worst-on-worst requirements, the following conditions were assumed:

- Vehicle orientation
  - Sun-on-capsule for all propellants except the earth storables
  - Sun-on-tanks for N_2O_4/A-50 and ClF_5/MHF-5, using $\alpha/\epsilon = 0.6/0.91$ and $\alpha/\epsilon = 0.3/0.95$
  - Sun-on-tanks and capsule for F_2/NH_3, using an $\alpha/\epsilon = 0.3/0.95$
- Insulation conductivities (two times the baseline values)
  - $k = 5.0 \times 10^{-5}$ Btu/hr-ft-°R for H_2
  - $k = 10.0 \times 10^{-5}$ Btu/hr-ft-°R for O_2, F_2, FLOX, CH_4, OF_2, and B_2H_6
  - $k = 20.0 \times 10^{-5}$ Btu/hr-ft-°R for NH_3, N_2O_4, A-50, ClF_5, and MHF-5
- Penetration heat leaks (twice baseline values)
  - Half the baseline thermal resistance for the propellant feed and pressurant line penetrations
  - Half the baseline support strut thermal resistances

Both the pump-fed and pressure-fed systems were analyzed. The F_2/NH_3 propellant combination was analyzed for both the sun-on-capsule condition and the sun-on-tanks with α/ϵ of 0.3/0.95 (white paint), to determine the optimum orientation. Also, the sun-on-tank earth storable cases were analyzed with $\alpha/\epsilon = 0.3/0.95$ and $\alpha/\epsilon = 0.6/0.91$ to determine the optimum surface finish.

The sun on the capsule results in the minimum system weight for the F_2/NH_3 propellant combination and, therefore, was the only one presented. This occurred even through 2.5-in. of insulation were required to prevent freezing the NH_3 because with the sun on the tanks, the F_2 required over 3 in. of insulation and the F_2 tank is slightly larger than the NH_3 tank. The N_2O_4/A-50 propellant combination results in minimum system weight with α/ϵ = 0.6/0.91, while the ClF_2/MHF-5 combination optimizes with the α/ϵ of 0.3/0.95 due to the lower freezing points.

Many of the propellants experienced a net heat loss during the mission, resulting in minimum insulation thicknesses. The results presented on Table 14 for both the pump-fed and pressure-fed systems include the operating pressure, insulation thickness, the percent ullage volumes, pressurant inlet temperature (° R), and the system weight for a single tank.

2.8.2 Heating Rates

The computed worst-on-worst heat transfer rates between the propellants and the environment are presented for the optimum insulation values, preferred vehicle orientation, and surface finish, at a point midway between Earth and Mars. The results are tabulated on Table 15 with the rates of total heat transfer, heating through the struts, and heating through penetrations. The propellant temperatures as well as the average insulation temperatures are also presented for reference. Several of the propellants experience a net heat loss during the mission. The major heat leak generally was through the insulation, but strut and penetration heat leaks were important to the tanks for hydrogen, FLOX, CH_4, and the F_2 of the F_2/NH_3 combination.

2.8.3 Pressurant Requirements

Pressurant requirements for the worst-on-worst analysis were determined for the optimum set of insulation thickness, tank size, ullage volume, and vapor weight. However, variations in conductivity and propellant heating could require more pressurant than specified at the worst-on-worst optimum, so such additional pressurant

Table 14

WORST-ON-WORST ANALYSIS RESULTS – MARS ORBITER

Propellant	Orientation	Pump-Fed System					Pressure-Fed System				
		Ullage (%)	Pressurant Inlet Temperature (° R)	Operating Pressurant (psia)	Insulation Thickness (in.)	Tank(a) System Weights (lb)	Ullage (%)	Pressurant Inlet Temperature (° R)	Operating Pressurant (psia)	Insulation Thickness (in.)	Tank(a) System Weights (lb)
O_2	Sun-on-Capsule	5	165	18	1/2	79	5	408	175	1/2	102
H_2		17	408	52	2	439	21	498	175	2	1,153
F_2	Sun-on-Capsule	5	155	18	1/2	91	5	345	190	1/2	93
H_2		21	345	59	2	290	21	498	190	2	721
FLOX	Sun-on-Capsule	5	279	52	1/2	119	5	403	195	1/2	177
CH_4		5	200	22	1/2	80	5	650	195	1/2	106
OF_2	Sun-on-Capsule	5	230	19	1/2	91	5	545	195	1/2	144
CH_4		5	312	22	1/2	82	5	650	195	1/2	117
OF_2	Sun-on-Capsule						5	545	160	1/2	130
B_2H_6							5	650	160	1/2	112
F_2	Sun-on-Capsule	5	155	52	1/2	103	5	525	195	5/8	161
NH_3		3	650	18	2-1/2	106	5	650	195	2-1/2	123
N_2O_4	Sun-on-Tank	3	650	25	5/8	99	3	650	165	1/2	169
A-50	$\frac{\alpha}{\epsilon} = \frac{0.6}{0.91}$	3	650	15	5/8	87	3	650	165	5/8	145
ClF_5	Sun-on-Tank	3	410	20	3/8	86	3	650	165	1/2	151
MHF-5	$\frac{\alpha}{\epsilon} = \frac{0.3}{0.95}$	3	410	15	3/8	75	3	650	165	1/2	123

(a) Weights included are vapor, pressurant including sphere insulation, and tank.

Table 15

MARS ORBITER PROPELLANT HEATING RATES – WORST-ON-WORST

Propellant	Orientation	T_{NBP} or $T_{liftoff}$ (° R)	At Analysis Point $T_{propellant}$ (° R)	Average $T_{insulation}$ (° R)	$t_{insulation}$ (in.)	q_{total} (Btu/hr)	$q_{insulation}$ (Btu/hr)	q_{struts} (Btu/hr)	$q_{penetrations}$ (Btu/hr)
O_2	Sun-on-Capsule	162.7	148.4	115.1	1/2	- 4.94	- 4.72	0.10	0.12
H_2		36.8	44.6	115.2	2	6.76	4.76	1.41	0.59
F_2	Sun-on-Capsule	153.4	142.4	113.6	1/2	- 3.70	- 3.51	-0.08	-0.11
H_2		36.8	47.2	115.4	2	4.84	2.86	1.40	0.58
FLOX	Sun-on-Capsule	155.0	167.0	181.4	1/2	2.65	1.83	0.56	0.26
CH_4		201.4	204.0	191.0	1/2	- 0.63	- 1.15	0.35	0.17
OF_2	Sun-on-Capsule	230.0	224.3	197.1	1/2	- 2.81	- 3.14	0.22	0.11
CH_4		201.4	203.8	191.0	1/2	- 0.65	- 1.17	0.35	0.17
OF_2	Sun-on-Capsule	230.0	224.0	196.7	1/2	- 2.68	- 3.01	0.22	0.11
B_2H_6		325.5	273.7	206.6	1/2	- 6.86	- 6.74	-0.10	-0.02
F_2	Sun-on-Capsule	153.4	165.7	181.2	1/2	2.64	1.80	0.57	0.27
NH_3		431.9	407.9	208.3	2-1/2	- 8.11	- 6.79	-0.88	-0.44
N_2O_4	Sun-on-Tanks	530.0	536.2	505.2	5/8	- 5.94	- 6.10	0.33	-0.17
A-50	$\frac{\alpha}{\epsilon} = \frac{0.60}{0.91}$	530.0	535.8	505.1	5/8	- 5.02	- 5.18	0.33	-0.17
ClF_5	Sun-on-Tanks	466.8	470.9	441.0	3/8	- 7.87	- 8.10	0.15	-0.08
MHF-5	$\frac{\alpha}{\epsilon} = \frac{0.30}{0.95}$	530.0	496.7	441.2	3/8	-12.78	-12.61	-0.01	-0.16

NOTE: All values taken at midpoint of Earth-Mars trajectory
NBP = normal boiling point.

requirements must be estimated. If less than the optimum pressurant were required due to potential propellant heating changes, the pressurant supply would be adequate and of less concern.

Table 15 lists the net heating or cooling at one point in the mission for all propellants analyzed for worst-on-worst conditions. The heat leaks were small only for the CH_4 system, so heating or cooling trends would vary directly with any insulation conductivity change assumed.

If the pressurant system were sized for high propellant heat rates, obtaining an optimistic conductivity value would reduce propellant heating and cause an increase in pressurant requirements. Additional pressurant would be required because the pressure regulator assumed would require additional pressurant to compensate for the reduced propellant vapor pressure in the ullage. The additional pressurant and pressurant sphere weights required for a pressure-fed propellant heated less than predicted by the worst-on-worst analysis would be only about 3 lb, or a 10 percent increase. Additional H_2 pressurant weights would be about 36 lb, which is also about 10 percent of the nominal. Pump-fed system pressurant weights were less than 25 lb total, and the additional pressurant weights for low heat leaks would be less than 3 lb.

Section 3
MEM THERMODYNAMICS ANALYSIS

Analyses of the MEM ascent stage were performed for pump-fed propulsion systems only. The Mars Excursion Module (MEM) spacecraft configuration and nominal mission as defined in the North American Rockwell (NAR) study (Refs. 11 and 12) have been analyzed. The inner tank configuration was fixed as ellipsoidal, with the O_2/H_2 propellant combination requiring an additional cylindrical section for the hydrogen. The outer tanks were all spherical, again except for the O_2/H_2 combination for which conical hydrogen tanks were assumed in order to maximize the propellant capacity. The sizes and number of outer tanks were varied dependent upon the propellant combination and the loading requirements (Table 16).

3.1 MEM THERMAL MODEL

The MEM thermal model used to compute heat leaks through the tank insulation and supports is shown in Fig. 19. During earth orbit and transit to Mars, the MEM ascent stage is enclosed within the Aerobraker. The model includes both the effects of conduction and radiation while in the Aerobraker and convection while on the Mars surface. The propellant combinations analyzed were loaded in the inner and outer tanks. The inner tanks were sized to carry a maximum propellant load within a fixed maximum diameter. The numbers and sizes of outer tanks were determined as required to contain the remaining propellant and all ullage. The conical tank configuration of the O_2/H_2 propellants was simulated with two spheres having an equivalent volume and surface area. Tank surface areas and strut sizes were computed for each propellant system.

Effective conductances were computed for various types of penetrations to estimate the propellant feed and pressurization line heat leaks. Propellant lines connecting the inner

Table 16

MEM PROPELLANT TANK LOADS

Propellant	Outer Tanks		Innter Tanks (One Each)		
	No. of Tanks	Mass Per Tank (lb)	Mass Per Tank (lb)	Second Burn Mass (lb)	Percent of Full Tank (Second Burn)
O_2	2	7,670	2,700	1,089	40.3
H_2	4	640	450	181	40.2
F_2	2	5,070	4,360	1,124	25.8
H_2	3	260	335	86	25.7
FLOX	2	4,635	6,400	1,003	15.7
CH_4	1	1,630	1,124	187	16.6
OF_2	2	4,435	6,710	1,155	17.2
CH_4	1	1,680	1,265	215	17.0
F_2	2	4,085	6,625	1,085	16.4
NH_3	1	2,480	2,010	325	16.2
ClF_5	2	5,065	8,470	1,200	14.2
MHF-5	1	4,220	3,530	500	14.2

and outer tanks were assumed to be filled with propellant. Half of the heat input through the line insulation was assumed to go into each of the two connected tanks. Engine feed lines were assumed empty and effective conductance was computed from the point of penetration to the outer insulation surface, accounting for the axial temperature gradient along the pipe, as well as the radial gradient through the insulation. Pressurization lines were assumed empty (check valve near tank) because stagnant helium in the line was found to have little effect on heat transfer. Insulation and pipe wall thicknesses were assumed for various diameter pressurization and propellant lines. The lines were assumed to be stainless steel with an average thermal

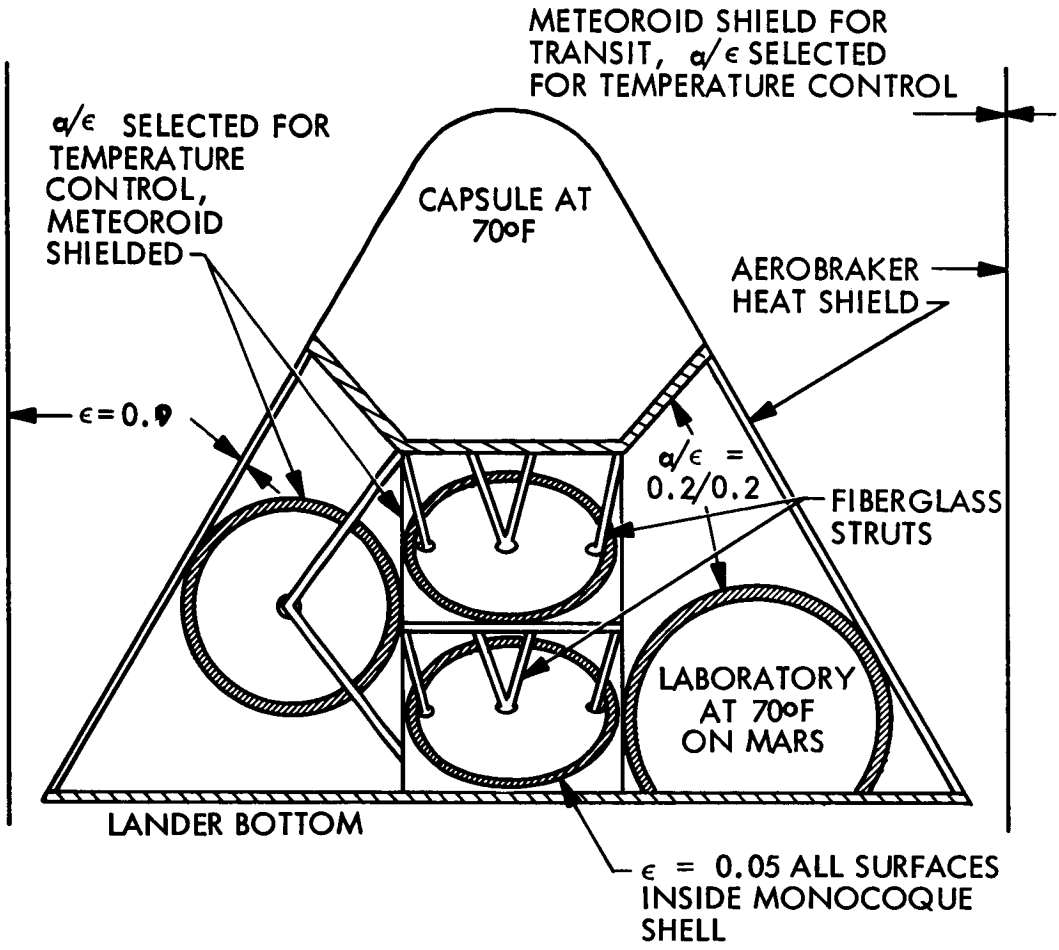

BASIC THERMAL CONFIGURATION

THERMAL MODELS

Inner Tanks

2 Tanks, 2 Nodes per tank

Outer Tanks

2 Tanks, 4 Nodes per tank

38 Nodes, 51 Conduction Resistors, and 146 Radiation Resistors

Assumptions

Struts insulated
Capsule and laboratory are wrapped with 1 in. of multilayer insulation
The "Lander Bottom" is thermally isolated by 1 in. of multilayer insulation
Mars atmosphere temperature = 495°R, wind velocity 200 ft/sec

Fig. 19 MEM Thermal Model

conductivity of 7.0 Btu/hr-ft-°R. As an alternate, titanium lines with an average thermal conductivity of 1.8 Btu/hr-ft-°R also were considered for the H_2 tank.

3.2 MEM ENVIRONMENT

The MEM mission consists of the following three phases:

- 30-day earth orbit stay
- 160-day Earth-Mars transit time
- 30-day Mars surface stay

During earth orbit and transit, the MEM is located within the Aerobraker whose temperature-time history, taken from Ref. 11, was used as a boundary condition for the MEM propellants. The external and internal Aerobraker surface finishes were adjusted to provide a favorable environment to the propellants. The manned capsule portion of the MEM was assumed to be held at a constant 70°R and to have 1 in. of multilayer insulation surrounding the capsule. The laboratory portion was also assumed to be wrapped with 1 in. of multilayer insulation, and was assumed to be at 70°F for the Mars stay.

The earth orbit was assumed to have an altitude of 270 nm and an orbit-solar incidence angle (β) of 52 deg with the vehicle horizontal. A β-angle of 52 deg results in the shortest time in the Earth's shadow and the maximum heating condition for a launch from ETR. For the transit phase, the vehicle was assumed to be rotating end-over-end in a plane containing the solar vector. An α/ϵ ratio of 0.06 on the Aerobraker was assumed for all propellants except MHF-5 and ClF_5; a ratio of 1.07 was used for these. The nominal α/ϵ of 0.25 from the NAR study was also analyzed for all the propellants.

Aerobraker temperatures were computed independent of the interior energy balance or heat transfer. The Aerobraker was then held at these temperatures, at shown in Fig. 20, for the interior energy balance for the earth orbit and Mars transit phases.

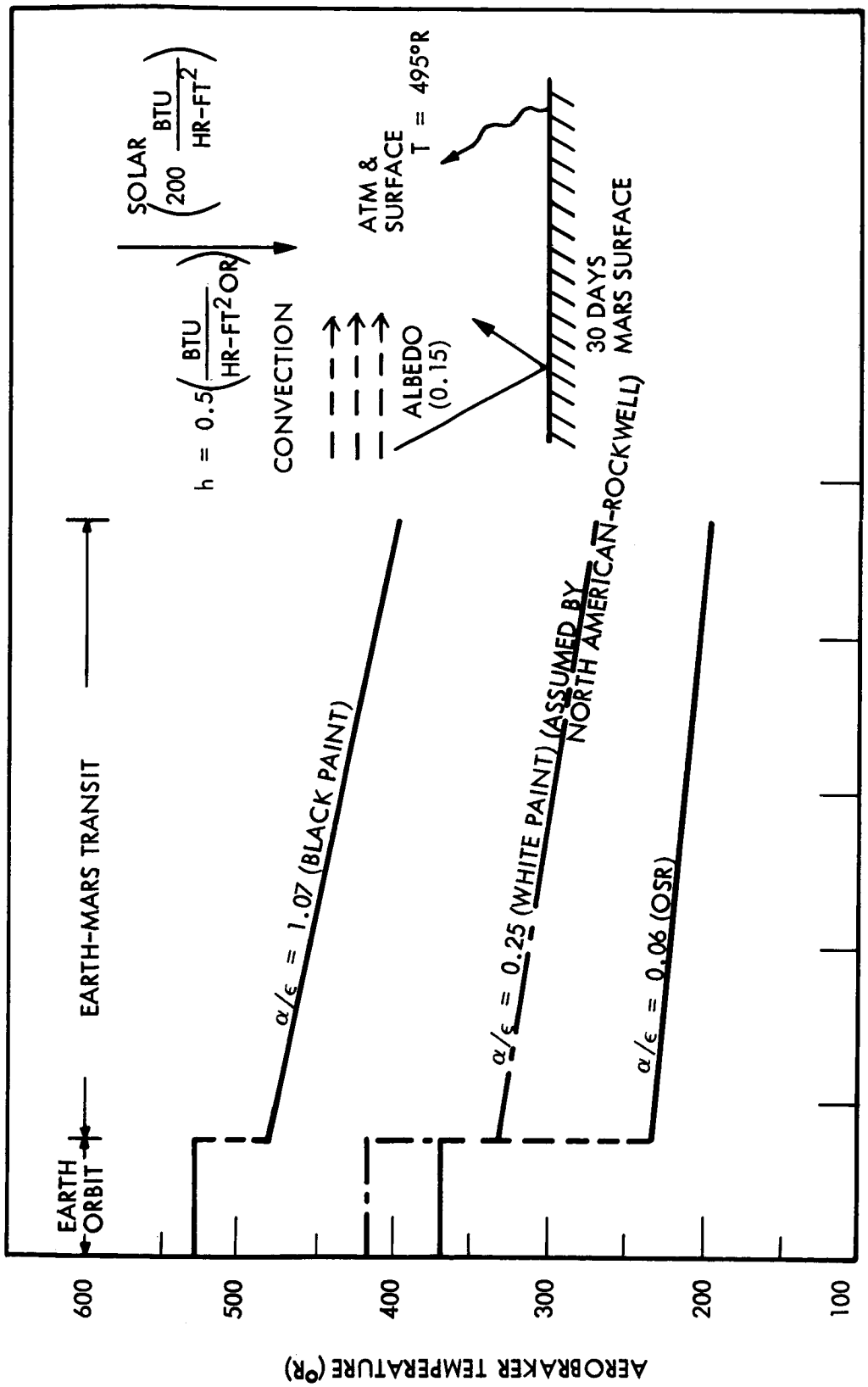

Fig. 20 MEM Mission Environment

While on the surface of Mars, the heat shield is removed, exposing the outer propellant tanks to the atmosphere. The thermal environment of the MEM on the Mars surface was based on the JPL Mars Atmosphere VM-7. Accordingly, a constant temperature of 495° R for the planet and atmosphere was used for the 30-day stay, and diurnal variations were neglected. Average daily solar heat rates to the landed vehicle were computed by an orbital heating program wherein the local planet surface was modeled, as well as the vehicle, and the sun was assumed to pass directly overhead. The local planet surface was assumed to be flat and to have a reflectivity (albedo) of 0.15 for solar energy. The following α/ϵ ratios were used for the propellant tanks: 0.93/0.88 for MHF-5 and ClF_5, 0.2/0.9 for NH_3, and 0.5/0.80 for all others. For the monocoque shell and the lander bottom, an α/ϵ of 0.93/0.88 was used for MHF-5 and ClF_5, and a value of 0.05/0.80 was used for all the other propellants.

3.3 MEM PROPELLANT HEATING

The thermal models were subjected to the mission environment using the Thermal Analyzer program to compute the propellant heating rates for each phase of the mission. Constant propellant heating rates were computed from quasi-steady-state energy balances during each of the three mission phases using time-averaged environmental conditions during each phase. This approach was justified because of the small effect propellant temperature changes had on propellant tank heating rates during any given phase. The detailed application of the thermal analyzer program to the computation of MEM heating rates is described below.

Convection from the Mars atmosphere was applied to the thermal model with a coefficient computed by conventional methods of 0.5 Btu/hr-ft^2-° R, based on characteristic lengths of 2 to 6 ft for all vehicle surfaces. This high convection coefficient primarily was caused by the continuous surface wind speed of 220 ft/sec, as specified in VM-7. A wind velocity of 50 ft/sec would yield a coefficient of about 0.2. Approximately 4 to 20 percent of the total propellant heating in the MEM mission was due to convection on the Martian surface.

Degradation of multilayer insulation conductivity due to the Martian atmosphere was considered. At atmospheric pressure of 5 mb, as specified in VM-7, will cause the conductivity to increase by a factor of approximately 200 relative to an evacuated condition. The increased heat leak would be sufficient to heat any of the cryogenic or space-storable propellants from the triple-point to critical-point temperature in 6 to 20 days with 5 in. of insulation. Therefore, it can be concluded that these propellants will require vacuum-jacketed tank insulation. The earth-storables and NH_3 do not require vacuum jackets because they are in no danger of freezing or overheating on the Martian surface.

Table 17 presents the itemized heat inputs per tank for each propellant. Four types of heat leaks are listed: (1) wall-insulation, (2) struts, (3) inter-tank lines (full or liquid), and (4) all other penetrations (empty). The latter category includes fill lines, feed lines, vent lines, and pressurization lines.

3.4 MEM SYSTEM OPTIMIZATION

The analytical procedure used for the MEM pump-fed system is basically that used for the orbiter systems. The primary difference is in the NPSP requirements and the method of handling the interconnected first- and second-stage tanks. During the first burn (Mars ascent), all of the outer tank propellant, as well as from 61 to 86 percent of the inner tank propellant, is consumed. The propellant loadings and the propellant remaining after the ascent burn were presented in Table 16. Since the tanks are plumbed in series, the propellants remaining in the inner tanks at the end of the first burn are assumed to be at the propellant conditions in the outer tank just before the burn. The system and analytical parameters used to analyze the MEM system are as follows:

- System Parameters
  - Helium (except heated vapor over H_2 for expulsion) pressurant
  - NPSP = 4 psia minimum
  - Helium stored in lowest temperature propellant of second-stage tank

Table 17

MEM TOTAL HEAT INPUT PER TANK

Tank	Q_{total} (Btu)	$Q_{insulation}$		Q_{struts}		$Q_{penetrations}$ (Stainless Steel)		$Q_{inter-tank}$	
		(Btu)	(%)	(Btu)	(%)	(Btu)	(%)	(Btu)	(%)
O_2 Inner	30,970	24,490	79.1	3,210	10.4	2,800	9.0	470	1.5
Outer	90,120	84,030	93.2	5,050	5.6	840	0.9	200	0.2
H_2 Inner	17,580	11,450	65.1	1,490	8.5	4,300	24.5/14.2[a]	340	1.9
Outer	21,640	17,050	78.8	2,840	13.1	1,670	7.7	80	0.4
F_2 Inner	36,610	28,950	79.1	4,180	11.4	2,980	8.1	500	1.4
Outer	42,860	38,820	90.6	2,900	6.8	920	2.1	220	0.5
H_2 Inner	16,580	10,840	65.4	1,340	8.1	4,240	25.6/16.7[a]	160	1.0
Outer	12,020	8,720	72.5	1,690	14.1	1,560	13.0	50	0.4
FLOX Inner	41,450	35,140	84.8	2,410	5.8	3,420	8.3	480	1.2
Outer	44,950	38,300	85.2	5,500	12.2	930	2.1	220	0.5
CH_4 Inner	27,800	23,870	85.9	1,550	5.6	1,960	7.1	420	1.5
Outer	41,850	40,100	95.8	1,000	2.4	620	1.5	130	0.3
OF_2 Inner	35,330	32,400	91.7	1,130	3.2	1,580	4.5	220	0.6
Outer	12,650	11,260	89.0	1,140	9.0	200	1.6	50	0.4
CH_4 Inner	30,500	26,420	86.6	1,670	5.5	1,980	6.5	430	1.4
Outer	43,720	41,960	96.0	1,000	2.3	630	1.4	130	0.3
F_2[b] Inner	47,550	40,290	84.7	2,790	5.9	3,920	8.2	550	1.2
Outer	41,050	34,410	83.8	5,300	12.9	1,080	2.6	260	0.6

(a) Titanium lines.
(b) F_2/NH_3 Propellant.

  - Helium inlet temperature ≥ saturated liquid temperature
  - First- and second-stage tanks pressure-connected but thermally isolated
- Analysis
  - Liquid and ullage in thermal equilibrium before pressurization
  - Energy balance between propellant vapor and pressurant gas during pressurization and expulsion
  - Heat-transfer collapse factor based on Epstein correlation computation
  - System (liquid and ullage) energy balance computed for the period between burns
  - Ullage volume adjusted to account for liquid expansion due to heating
  - Outer volume adjusted to account for liquid expansion from inner tanks

The propellant plumbing and pressurization system considered for the MEM analyses is presented in Fig. 21. Flight hardware details shown include squib-operated valves to disconnect and separate the outer propellant tanks after first burn.

The optimization plots are presented in Figs. 22 and 23 for FLOX for both the inner and outer propellant tanks. The summations of the tank, pressurization, insulation, and vapor weights are presented as a function of the total tank pressure for various pres surant inlet temperatures. The optimum operating pressure and insulation thickness generally are different for the inner and outer tanks. However, identical insulation thicknesses were assumed while computing the propellant mass exchange from the inner to outer tanks resulting from propellant expansion following heating of the fixed volume inner tank propellant. The total system optimum is therefore not exact; the difference, which is slight, is in propellant transferred by expansion for different insulation thicknesses and the resultant change in outer tank size and ullage.

The outer cryogenic and space-storable tanks tend to optimize at high pressurant inlet temperatures, while the inner tank generally requires lower pressurant inlet temperatures because of the pressurant enthalpy absorbed by the liquid. Optimum pressurant inlet temperatures were determined for both inner and outer tanks, although a dual temperature heat exchanger may not be practical.

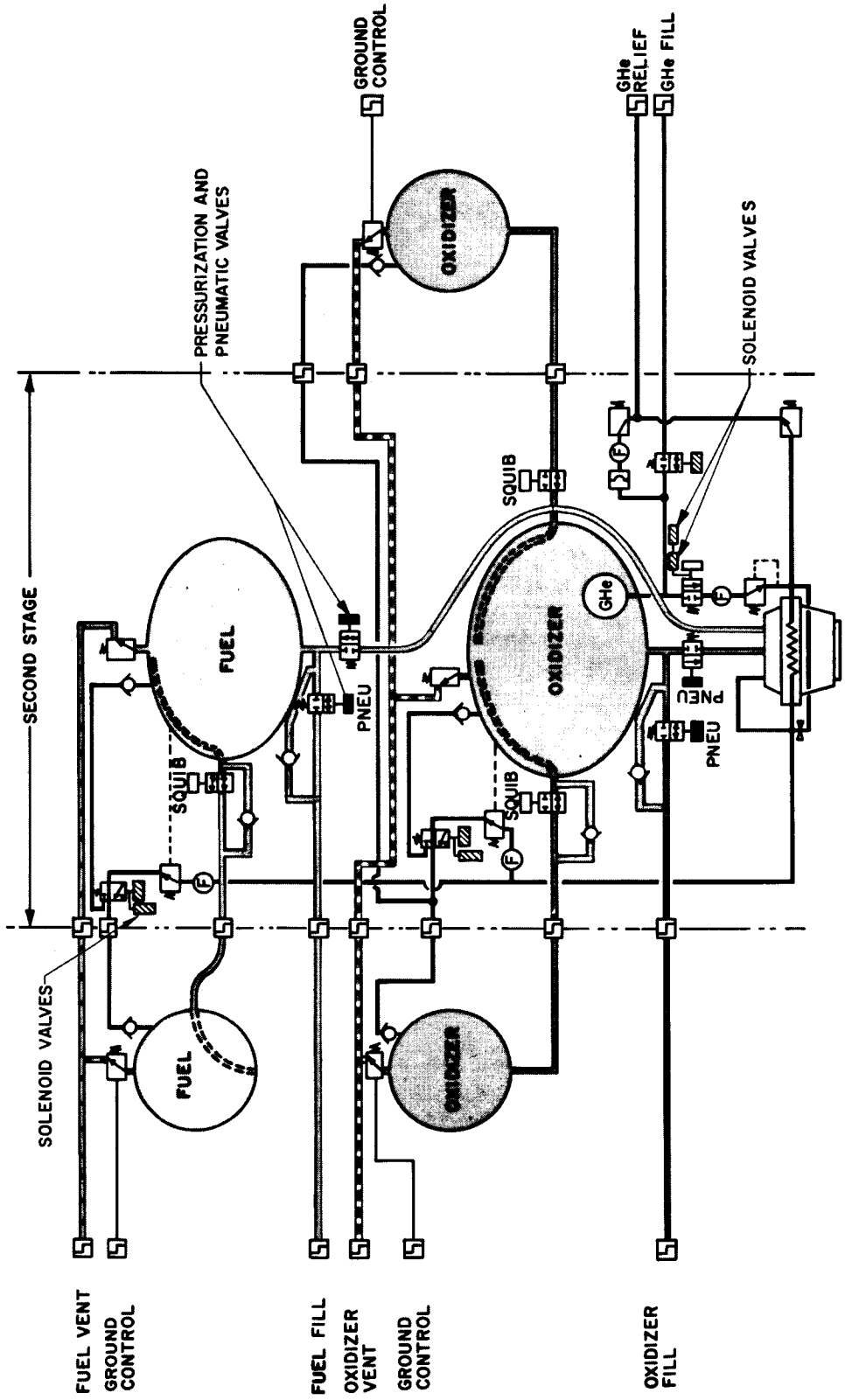

Fig. 21 Space-Storable Plumbing System for MEM

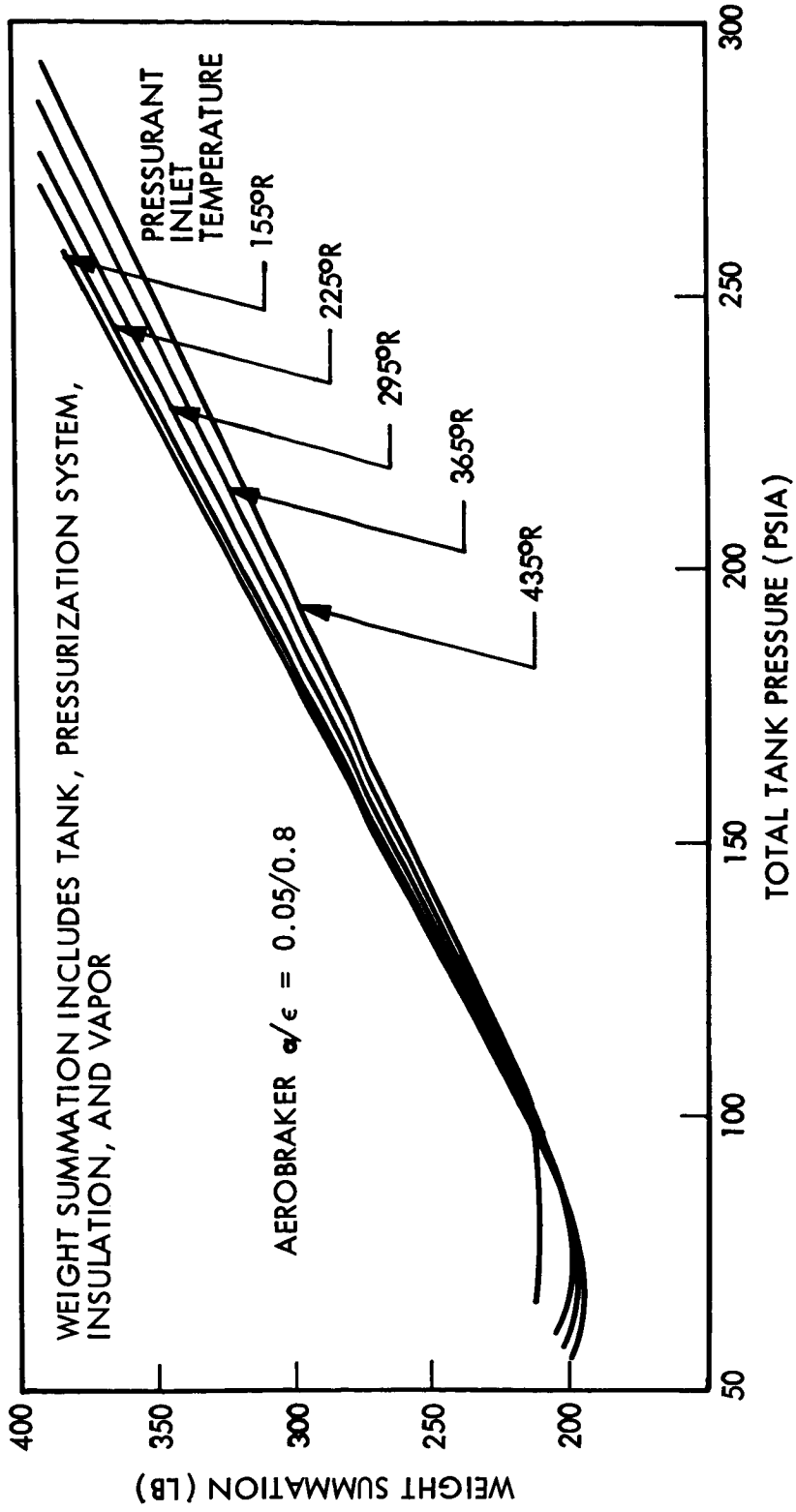

Fig. 22 MEM Pump-Fed Optimization – Inner FLOX Tank

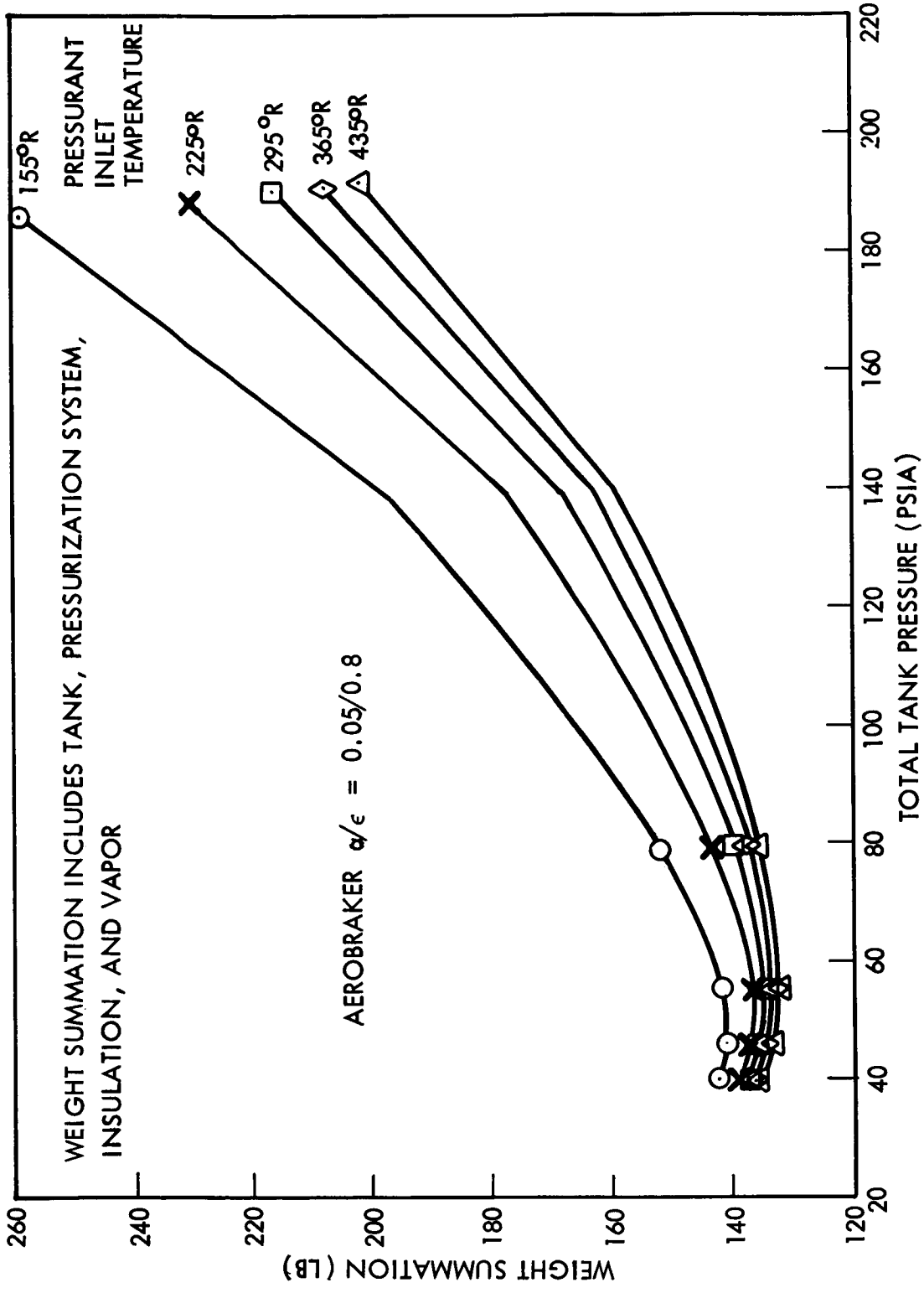

Fig. 23 MEM Pump-Fed Optimization -- Outer FLOX Tank

The results of the MEM optimization are presented in Table 18, which includes the ullage volume requirements, tank pressures, insulation requirements, and surface finish.

The MEM pressurization system weights are presented in Table 19. The individual pressurant, storage, valves, lines, and fitting weights are presented for both the inner and outer tanks, along with the total system weights. The approximate MEM mission pressure response for the H_2, F_2, and NH_3 tanks are presented in Figs. 24, 25, and 26.

The propellant temperature response for the MEM mission, including the period of earth orbit and transit to Mars while enclosed by the Aerobraker and the period while exposed to the Martian surface environment, is shown in Fig. 27 for hydrogen, fluorine, and ammonia. Nominal insulation thicknesses are considered for these temperature responses. The mars orbiter propellant temperature response is also presented for comparison. Because of the direct incident solar energy on the orbiter, the propellants are exposed to a higher energy environment and, consequently, experience a greater temperature rise for the same insulation thickness. The sharp temperature change near the end of the orbiter mission occurs because about 95 percent of the propellant is expelled with no change in the environment. The MEM propellants experience increased heating while on the Mars surface because of exposure to the Martian atmosphere with the heat shield removed.

An analysis was conducted to determine the effect of using a white paint ($\alpha/\epsilon = 0.25$) instead of OSR ($\alpha/\epsilon = 0.06$) on the Aerobraker. The insulation thicknesses and operating pressures increased for all cryogenic and space-storable propellants but the earth storables were not affected (Table 18). The major effect on system weight was the increase in insulation weight caused by optimum thicknesses increasing by as much as 1 in. The hydrogen tank weights also increased because the minimum gage pressure was exceeded. None of the weight increases exceed 20 percent of the sum of vapor, pressurant, insulation, and tank weights.

Table 18

MEM THERMODYNAMIC OPTIMIZATION AND AEROBRAKER SURFACE-FINISH SENSITIVITY

Propellant	α/ϵ of Tank	α/ϵ of Nominal Aerobraker	α/ϵ of White-Painted Aerobraker	Total Pressure (psia)				Insulation Thickness (in.)				Initial Ullage (%)	
				Aerobraker With Nominal α/ϵ		Aerobraker With White Paint		Aerobraker With Nominal α/ϵ		Aerobraker With White Paint		Aerobraker With Nominal α/ϵ	Aerobraker With Nominal α/ϵ
				Outer	Inner	Outer	Inner	Outer	Inner	Outer	Inner		
O_2	0.05/0.8	0.05/0.8	0.3/0.95	61	61	51	54	1/2	1	1	1-1/2	10	10
H_2	0.05/0.8	0.05/0.8	0.3/0.95	79	79	77	77	4	4	5	5	16	16
F_2	0.05/0.8	0.05/0.8	0.3/0.95	46	60	56	82	3/4	1	1	1	9	12
H_2	0.05/0.8	0.05/0.8	0.3/0.95	102	102	112	112	4	3-1/2	5	5	23	23
FLOX	0.05/0.8	0.05/0.8	0.3/0.95	56	67	65	68	3/4	1	1	1-1/2	8	10
CH_4	0.05/0.8	0.05/0.8	0.3/0.95	50	54	49	70	1/2	3/4	1	1	17	17
OF_2	0.05/0.8	0.05/0.8	0.3/0.95	37	54	43	64	1/2	1/2	1	1	9	9
CH_4	0.05/0.8	0.05/0.8	0.3/0.95	49	53	48	60	1/2	3/4	1	1-1/4	12	17
F_2	0.05/0.8	0.05/0.8	0.3/0.95	52	70	50	71	7/8	1	1-1/2	1-1/2	9	10
NH_3	0.2/0.9	0.05/0.8	0.3/0.95	42	64	42	64	1/2	1/2	min	min	5	5
ClF_5	0.93/0.88	0.93/0.88	0.3/0.95	27	34	27	34	min	min	min	min	3	3
MHF-5	0.93/0.88	0.93/0.88	0.3/0.95	<15	<15	<15	<15	min	min	min	min	3	3

Table 19

MEM PRESSURIZATION SYSTEM WEIGHTS

Propellant	He (lb)		Storage Tank (lb)		Valves (lb)		Lines and Fittings (lb)		Totals (lb)	
	Outer[b]	Inner[b]	Outer	Inner	Outer	Inner	Outer	Inner	Outer	Inner
O_2	22	4	38	8	30	46	16	16	198	82
H_2	92[c]	8[c]	–	–						
F_2	10	2	16	4	23	43	14	90	90	65
H_2	27[c]	2[c]	–	–						
FLOX	12	4	36	13	14	36	10	10	92	70
CH_4	5	2	15	5						
OF_2	8	4	16	8	14	36	10	10	72	67
CH_4	7	3	17	6						
F_2	8	4	28	13	14	36	10	10	68	68
NH_3	2	1	6	4						
ClF_5	2	1	14	10	13	36	8	8	42	62
MHF-5	1	1	4	6						

(a) Refers to outer propellant tanks.
(b) Refers to inner propellant tanks.
(c) GH_2 pressurant.

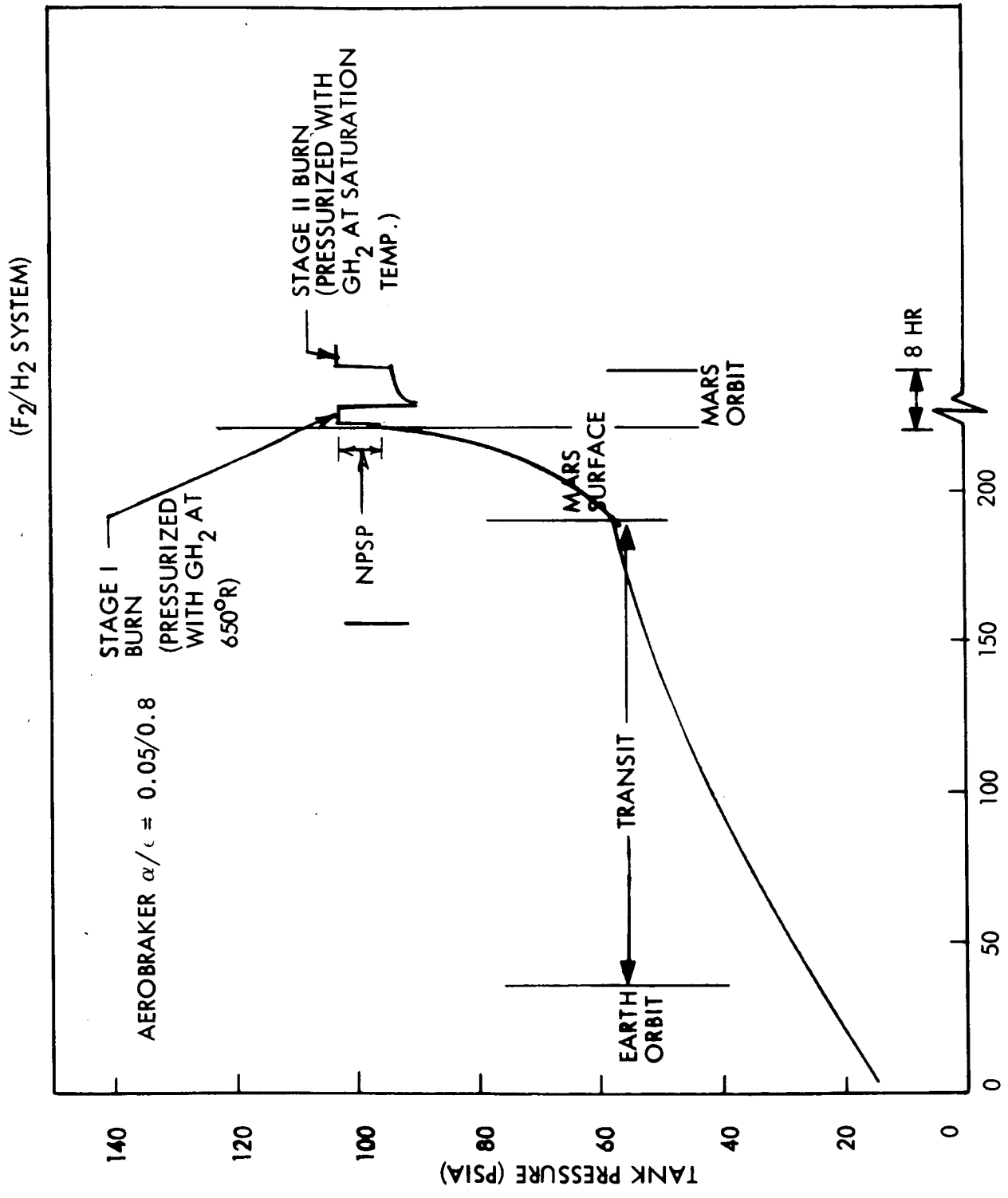

Fig. 24 MEM H_2 Tank Pressure Profile

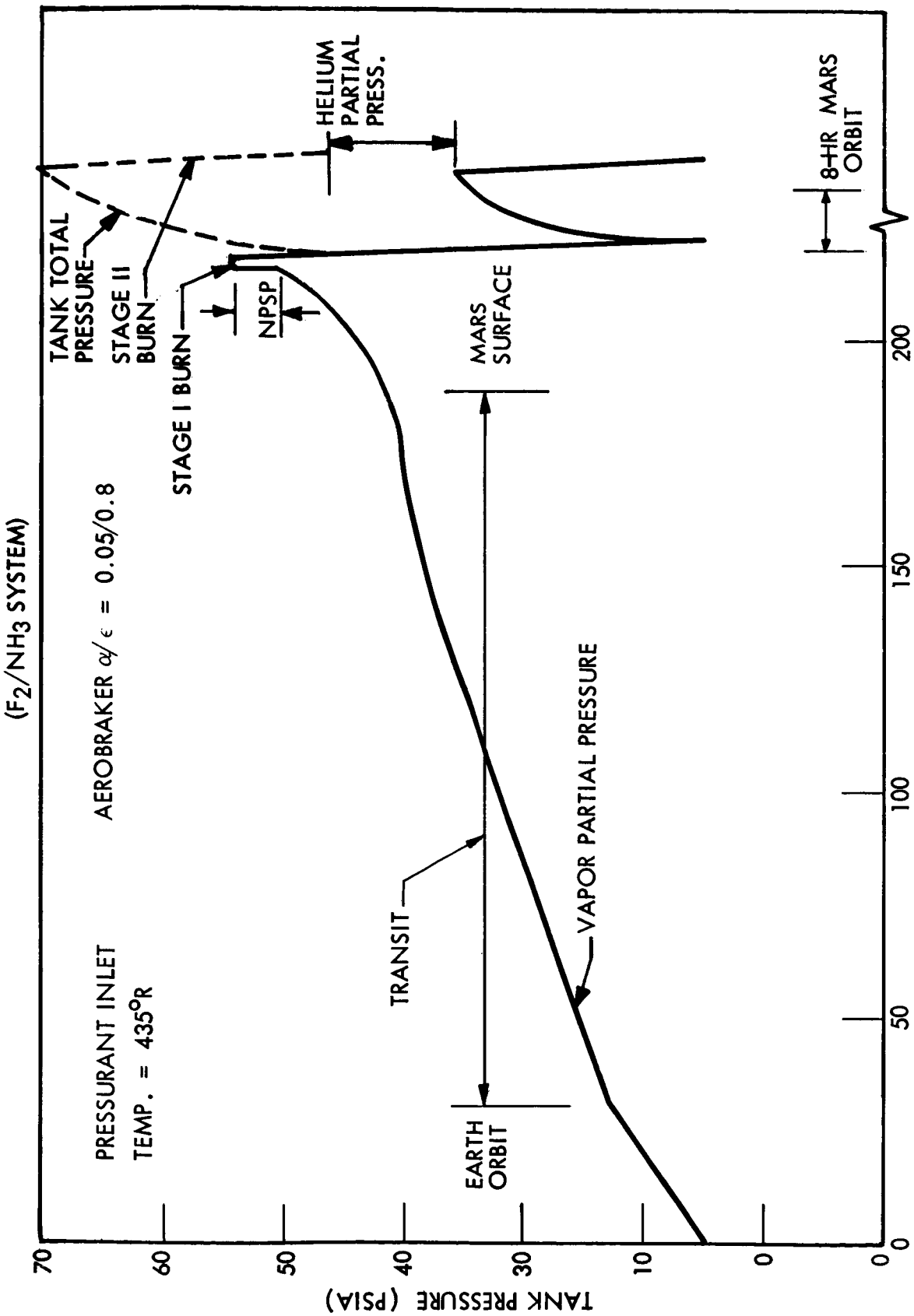

Fig. 25 MEM F_2 Tank Pressure Profile

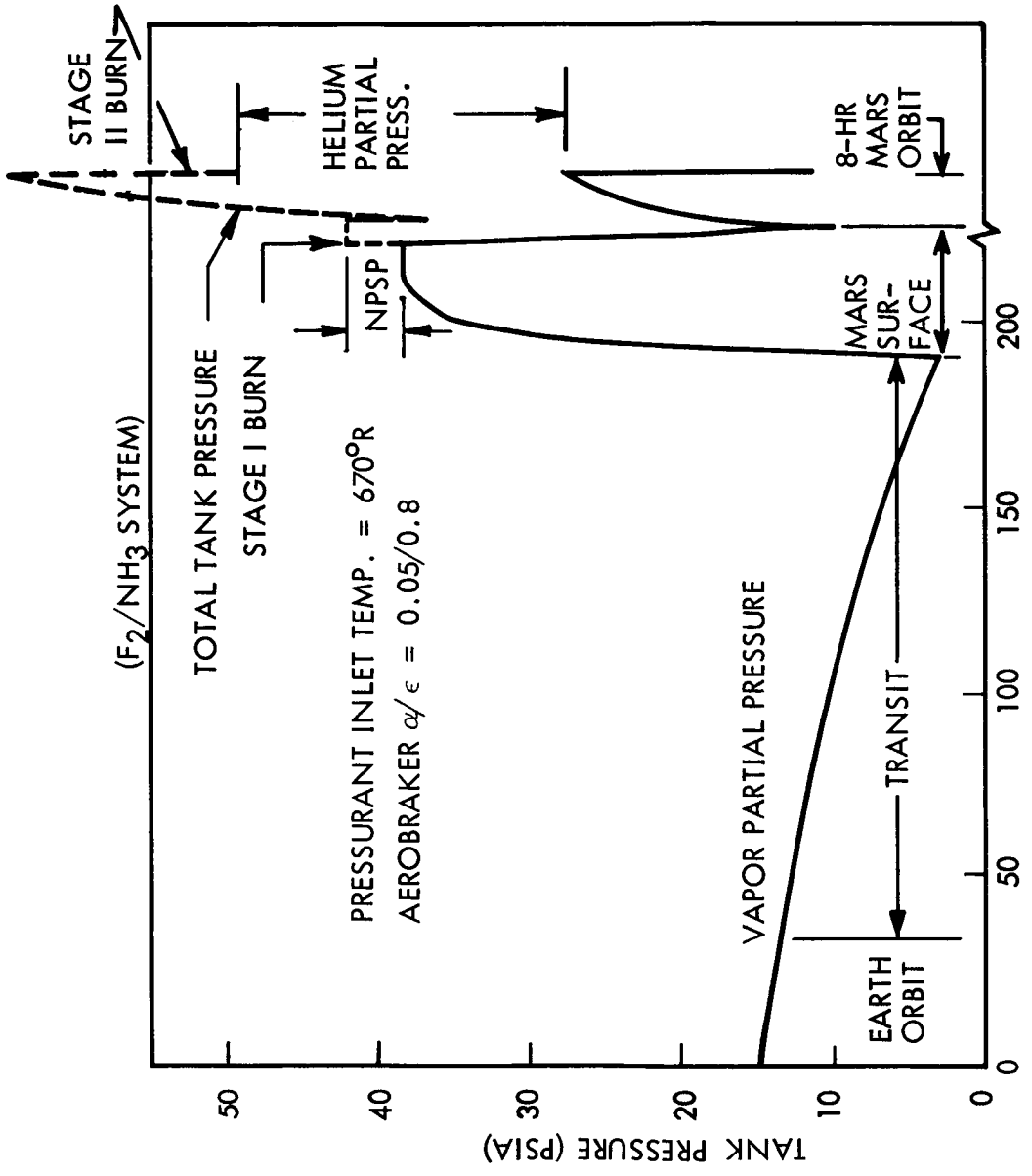

Fig. 26 MEM NH_3 Tank Pressure Profile

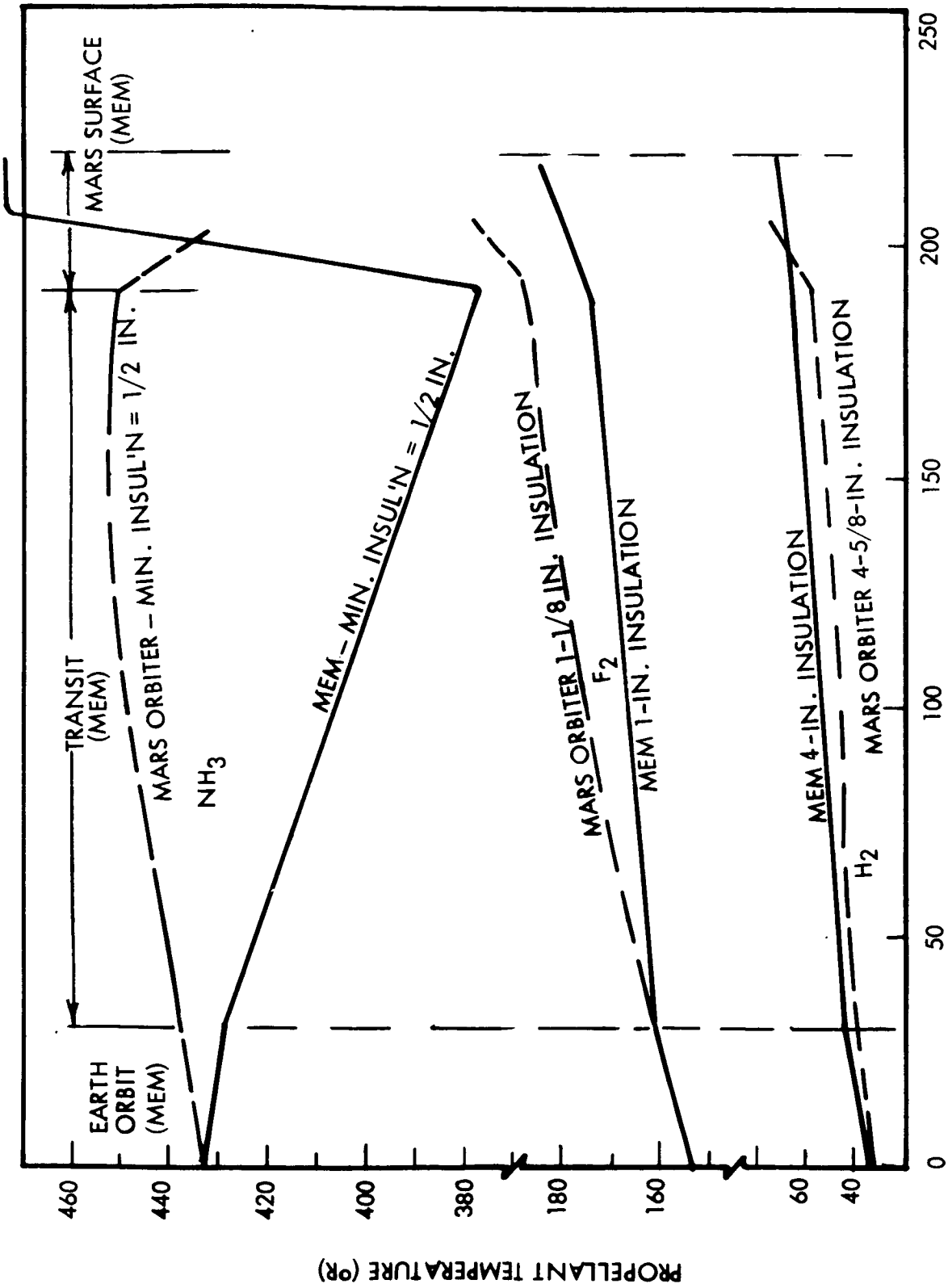

Fig. 27 Comparison of MEM and Mars Orbiter Propellant Temperature Response

Section 4

GROUND SUPPORT AND MISCELLANEOUS ANALYSES

Many studies were conducted to evaluate such items as the effect of the prelaunch and ascent phase upon the propellants and associated ground support equipment, thermal equilibrium in the tank, engine burn and heat soakback, and differential boiloff; these studies are discussed in this section.

4.1 GROUND SUPPORT ANALYSIS

Spacecraft compartments requiring thermal conditioning should be provided with an atmosphere at the minimum temperature permissible to assist in launch-pad temperature control. Propellant temperature control is required to minimize boiloff and subcooling requirements. The spacecraft equipment section temperature requirements are dominant and dictate the minimum temperature requirements, which are on the order of 40° F (500° R).

The H_2 propellant tank insulation system requires a helium atmosphere to prevent condensation of gases on the tank or within the insulation. The space storables will require either dry nitrogen or dry air to prevent condensation of water vapor on the tank or within the insulation. The earth storables will not require special measures other than those dictated by the equipment section.

To determine the operational support required for the various propellants, an analysis was conducted to evaluate the effect of the prelaunch environment on these propellants. The insulation thicknesses used for the tanks are those selected during the optimization of the Mars Orbiter pump-fed systems. The gas introduced into the shroud has been assumed to be at a temperature of 500° R. To determine the heat gains into the propellant, effective thermal resistances were determined between the propellant at its

normal boiling temperature and the environment at 500° R. The insulation conductivity was assumed to be equal to the purge gas conductivity at an average temperature between the propellant and 500° R. A convection coefficient of 1 Btu/hr-ft^2-°R was assumed over the entire outer surface of the insulation. Boiloff rates, vapor vent rates, and the amount of subcooling required as a function of the time between lift-off and end of propellant topping were determined for each propellant.

The results of the prelaunch requirements are presented on Table 20. for the cryogenic and space-storable propellants. The listed values are for all spacecraft propellant tanks. The preliminary ground support equipment requirements assumed for the various propellant combinations also are presented in the table. All fluoride propellants and B_2H_6 require closed-loop vent systems because of their reactive nature.

The analysis to determine the propellant temperature rise during the ascent phase assumed the entire outer surface of the insulation was at 600° R for this period. Since it takes approximately 200 sec to vent the insulation, a high insulation conductivity was used (about an order of magnitude lower than the gas value) for a 360-sec period to determine a conservative energy input and propellant temperature rise. Assuming that all the energy was absorbed by the propellant mass, the largest temperature rise was on the order of 0.05° F or less, which is negligible and can be accounted for by subcooling a very slight amount. Even if the ascent temperature rise were considered to occur for a 1-hr period with the same degraded conductivity and high insulation temperature, the propellant temperature increase would be 0.5° F or less, which can be compensated for by further subcooling.

4.2 INSULATION VENTING DURING ASCENT

Venting of insulation during ascent depends not only on the flow length but also upon the purge gas and any outgassing products. An analytical and experimental study of gas flow through multilayer insulations has been conducted under Contract NAS 8-11347

Table 20

PRELAUNCH TANKAGE THERMAL EFFECTS

(Mars Orbiter, Pump-Fed, 205-Day Mission)

PROPELLANT	PRELAUNCH THERMAL CONDITIONING	HEAT INPUT PER VEHICLE (BTU/HR)	VENTING		NONVENTING		
			BOILOFF (LB/HR)	VENTED VAPOR (FT^3/HR)	NONVENTED TEMP RISE ($^\circ R$/HR)	NONVENTED OPERATING PRESS. RISE (PSI/HR)	NONVENTED HOLD WEIGHT PENALTY (LB/HR)
F_2	A	3,200	43.4	416	1.6	1.5	0.75
H_2		5,150	26.7	2,900	4.6	10.0	17.5
O_2	A	6,800	73.6	410	3.1	3.2	0.96
H_2		8,160	42.3	4,600	3.7	8.0	27.6
FLOX	B	2,500	31.0	328	1.2	1.0	0.48
CH_4		3,000	13.6	310	3.4	2.3	0.39
OF_2	B	2,500	30.8	208	1.6	1.1	0.46
CH_4		3,100	14.0	318	3.3	2.1	0.37
F_2	B	1,726	23.4	224	0.9	0.9	0.43
NH_3		156	0.2	5.2	0.1	0.03	NEGLIGIBLE
N_2O_4	C	NEGLIGIBLE	NEGLIGIBLE		NEGLIGIBLE		
A-50							
ClF_5	C	NEGLIGIBLE	NEGLIGIBLE		NEGLIGIBLE		
MHF-5							

A. DRY N_2 INTO SHROUD AT 40°F AND 10 TO 50 LB/MIN, PLUS HELIUM PURGE BAG FOR H_2 TANK.
B. DRY N_2 OR AIR INTO SHROUD AT 40°F AND 10 TO 50 LB/MIN.
C. REQUIREMENTS COMPATIBLE WITH THE EQUIPMENT SECTION (40° TO 70°F)

(Ref. 13), and further investigations (including out-gassing) and tests currently are being performed under Contract NAS 8-20758 (Ref. 14).

To assess the effect of evacuation time upon propellant heating, the insulation conductivity with flight time must be determined. From the above studies, the insulation conductivity as a function of the gas pressure (both helium and nitrogen) and the insulation pressure as a function of flight time were obtained (Figs. 28 and 29). The insulation conductivity data were obtained experimentally at LMSC with an NBS-type cryostat (Refs. 13 and 14). A gas flow model was developed (Ref. 13) and correlated with experimental data to determine insulation pressure as a function of time for several flow lengths and both helium and nitrogen purge gases.

The data shown in Figs. 28 and 29 have been replotted to present the insulation thermal conductivity as a function of the flight time (Fig. 30) for pumpdown of both pure purge gases (helium and nitrogen) and both 2- and 5-ft flow lengths. The hydrogen tanks will be purged with helium. These tanks would rapidly (200 sec) vent during ascent with a reasonable flight installation flow length of 2 ft. Flow lengths of 5 ft would increase the vent time to 500 sec; however, these long flow paths can be avoided by careful design and installation. Thick insulation, required on some hydrogen tank designs, normally is installed in blankets 1-in. thick or less with a maximum width of 4 ft. Although the butt joints of these blanket gores are lapped with successive layers, the butt joints act as pumping paths or plenum chambers. The labyrinth of successively overlapped blanket butt joints does not significantly increase the pumping path length because the critical pumpdown time constant is dictated by the narrowest passages between insulation layers within the blankets. The space-storable propellants will be purged with either nitrogen or dry air, which takes about 300 sec to vent 2-ft flow lengths during ascent. Five-ft flow lengths would take considerably longer to vent; however, 5-ft flow lengths are highly unlikely for tank diameters on the order of 4-ft and insulation widths of 4 ft.

Outgassing of the multilayer insulation materials could influence thermal performance. The following conclusions were reached during investigations (Ref. 14) on crinkled

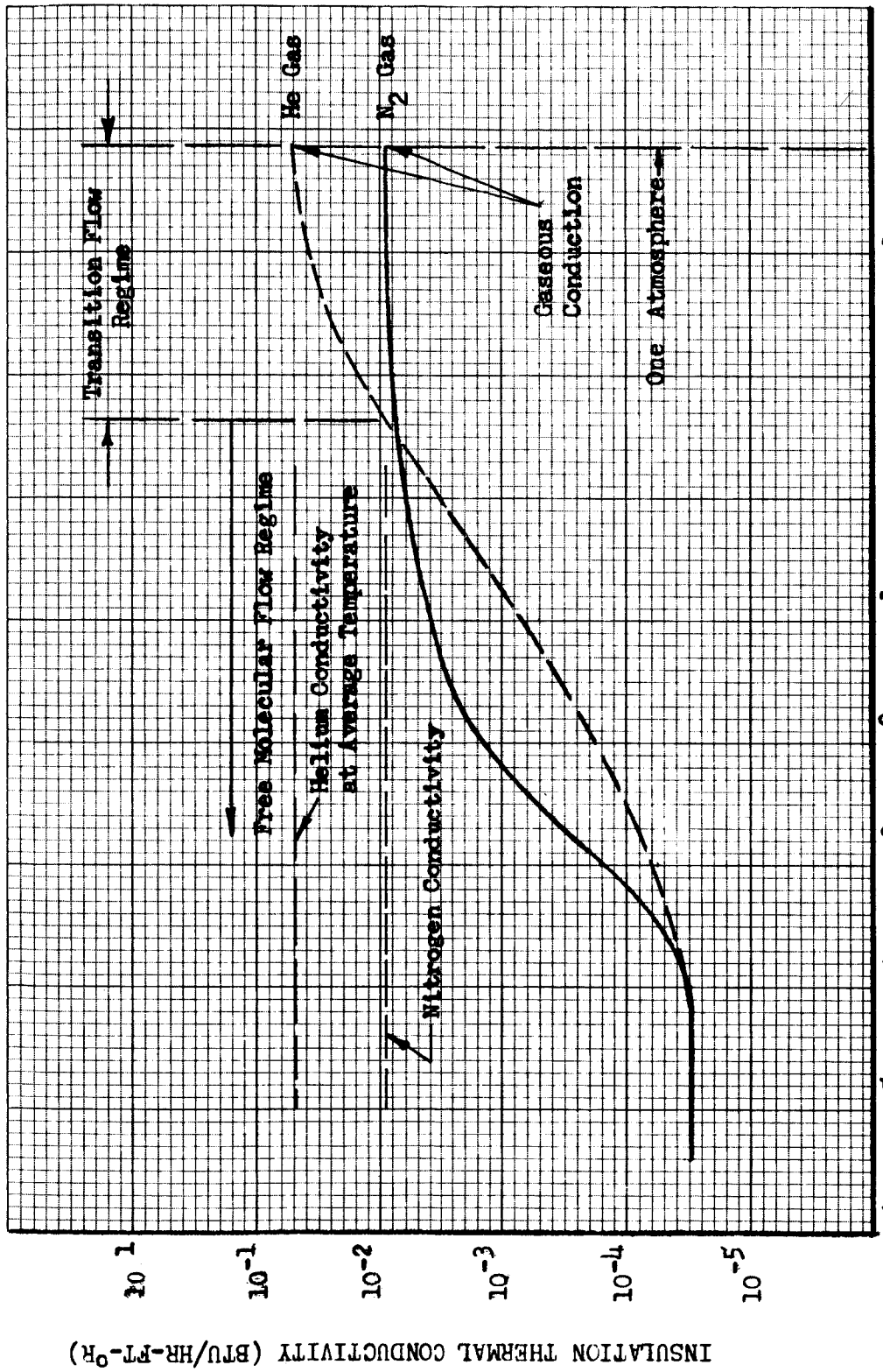

Fig. 28 Thermal Conductivity of Multilayer Composite Insulation as a Function of Gas Pressure

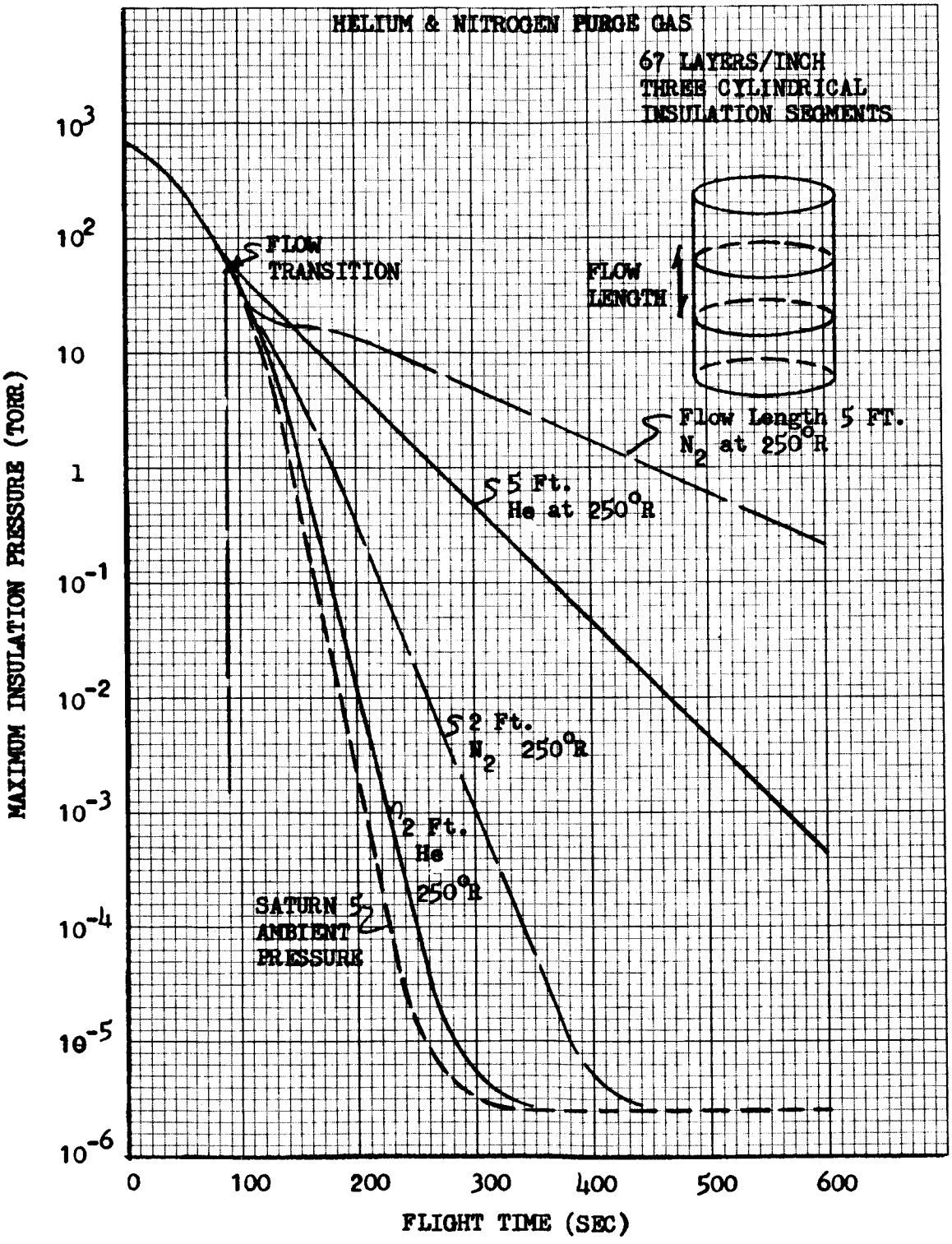

Fig. 29 Insulation Pressure/Flight-Time Histories for Flight-Type Cryogenic Tanks

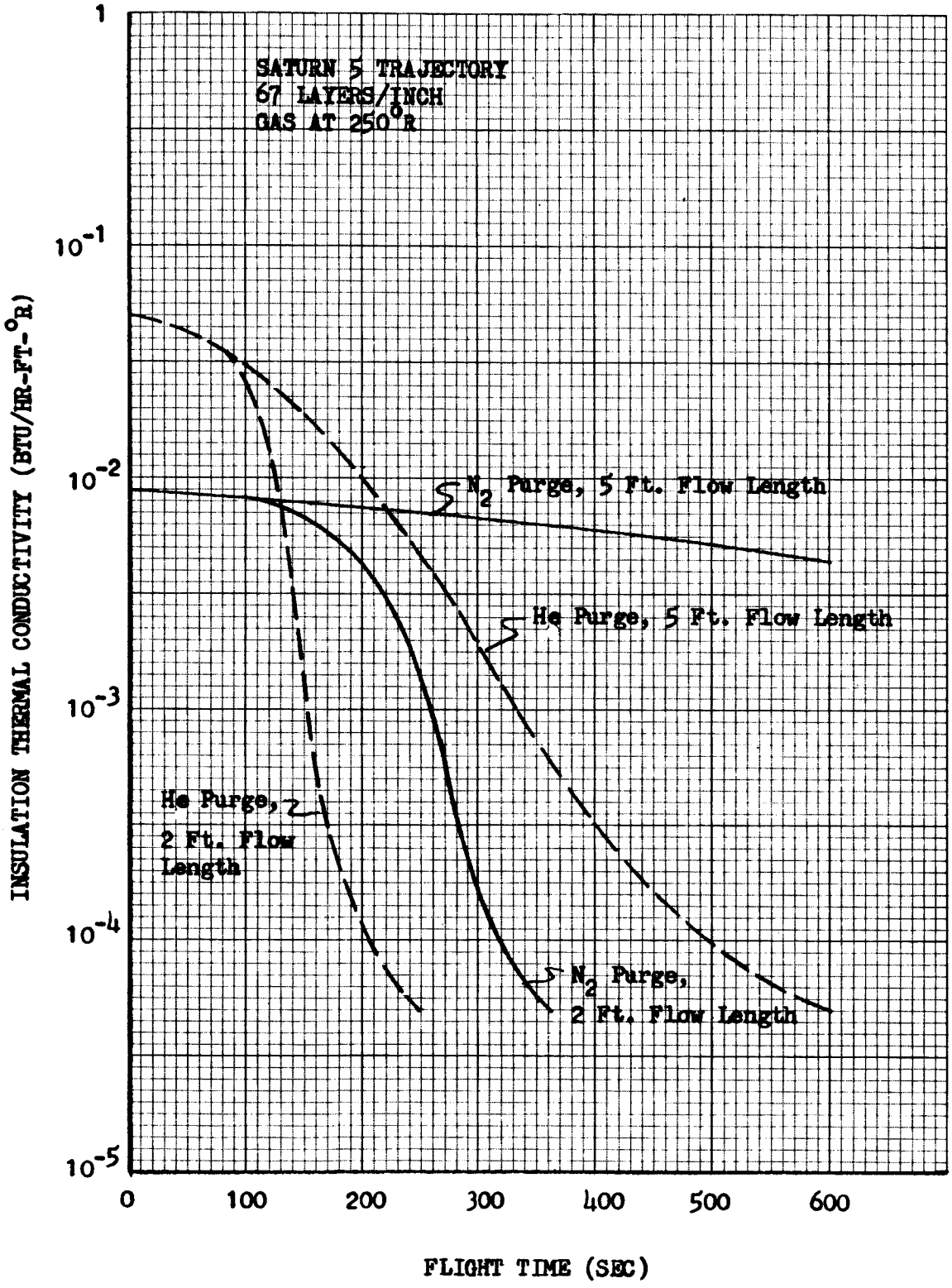

Fig. 30 Insulation Conductivity/Flight-Time Histories for Cryogenic Tanks

double-aluminized Mylar-Tissuglas and NRC-2:

- Water vapor is the major outgassing constituent for all insulation specimens tested.
- Outgassing of insulation specimens was virtually eliminated at 430° R without resorting to preconditioning techniques.
- Purging of the insulation specimens initially with either hot (672° R) helium or nitrogen removes sorbed water molecules and markedly reduces insulation outgassing rates for tests conducted at room temperature (540° R).
- Sorption of water vapor on aluminized Mylar can be significantly reduced by making minor modifications to the metalizing process (heating prior to metalizing).

The venting of insulation during ascent can be achieved within 300 sec by providing vent flow paths of 2 ft or less. Outgassing of the insulation materials is negligible, whereas water vapor is the major outgassing constituent. Insulation systems that operate above 430° R can eliminate outgassing by preconditioning techniques such as purges.

4.3 ASCENT HEATING

Ullage heating of a cryogenic propellant during ascent was analyzed to determine tank pressure rise. This potential problem required analysis because the heating rates through the multilayer are relatively high before venting is accomplished and because of the low thermal inertia of the ullage gas. Steady-state analyses indicate that a well-mixed isothermal ullage is a good assumption after 2 hr in a low-g environment; however, the ascent transients require a more sophisticated analysis.

The time-temperature history was computed for the nodal model shown in Fig. 31 with the following conditions:

- Liquid H_2 at 38° R as a sink
- Four in. of multilayer insulation

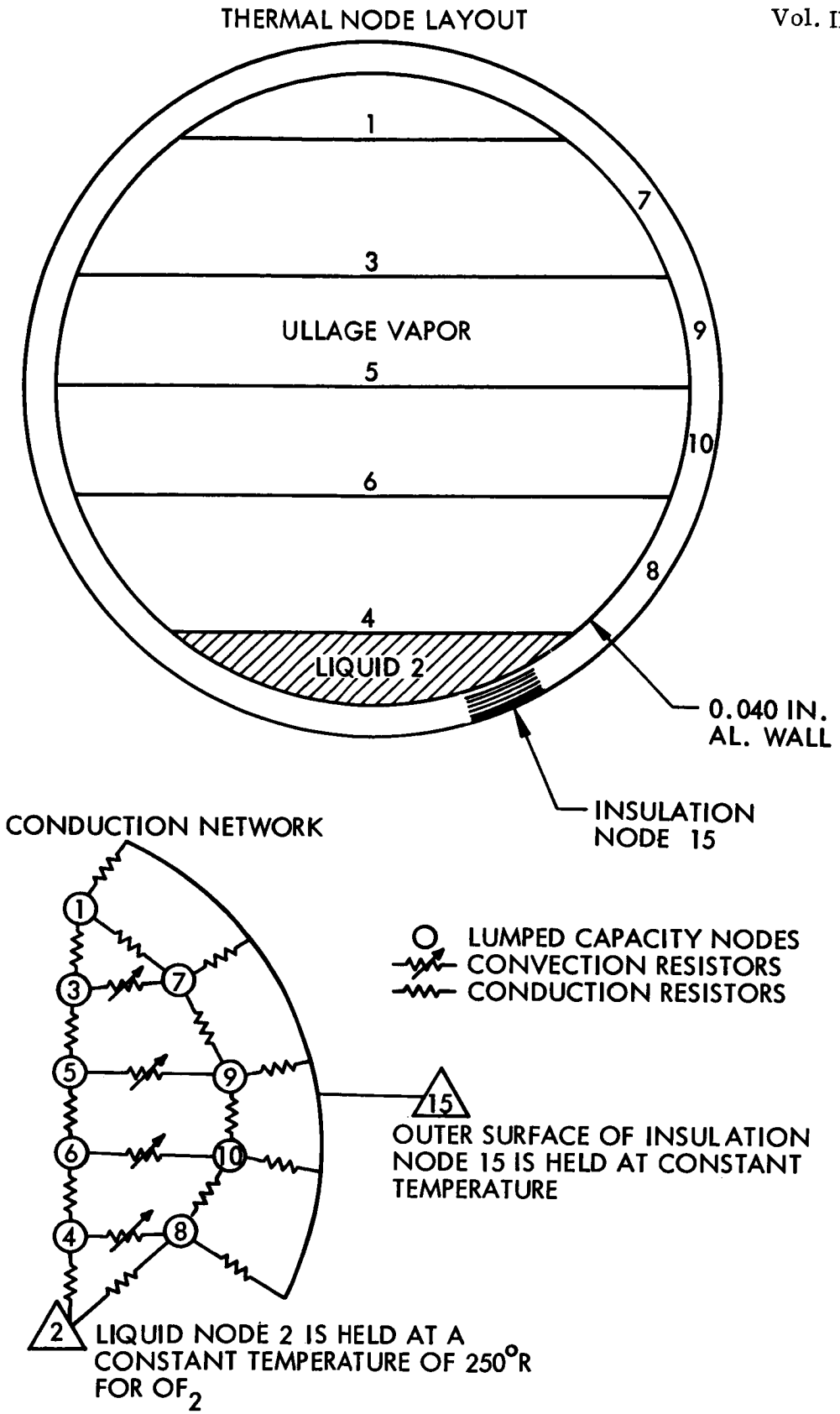

Fig. 31 Ullage-Liquid Conduction Thermal Model

- Multilayer conductivity varied with time per Fig. 30 (He purge, 5-ft flow length)
- Twenty-percent ullage volume
- Aluminum wall and H_2 ullage gas initially at 38° R
- Insulation initially at 300° R
- Insulation surface temperature at 650° R for a period of 600 sec, and then at 500° R
- Convection coefficient equal to 7.5 Btu/ft^2-hr-° R between tank wall and ullage for 600 sec, then replaced with gas conduction resistors
- Only conduction vertically between ullage gas nodes

The ullage temperature response obtained is shown in Fig. 32 for selected times. An average ullage temperature was computed and the new ullage pressure obtained assuming a constant volume process. The pressure-time response shown in Fig. 33 was obtained and the peak pressure was 22 psia. Although this analysis was for only one case, the small pressure rise obtained indicates ullage heating during ascent is not likely to be a problem.

4.4 TANK THERMAL EQUILIBRIUM

The thermal pressurization analyses described in Section 1.4 assumed thermal equilibrium within the tank between the liquid and ullage as an initial condition for determining the expulsion pressurant required. This condition was assumed to occur between burns to permit accounting for all of the enthalpy from the burn pressurant and allow computation of a total tank pressure made up of pressurant and vaporized propellant partial pressures. The pressurant requirement and maximum tank pressure are both critical weight factors in the system optimized; therefore, the tank thermal equilibrium condition required further investigation.

Propellant tank thermal equilibrium was assumed because heat transfer rates into and within the tanks are low and do not result in significant temperature gradients.

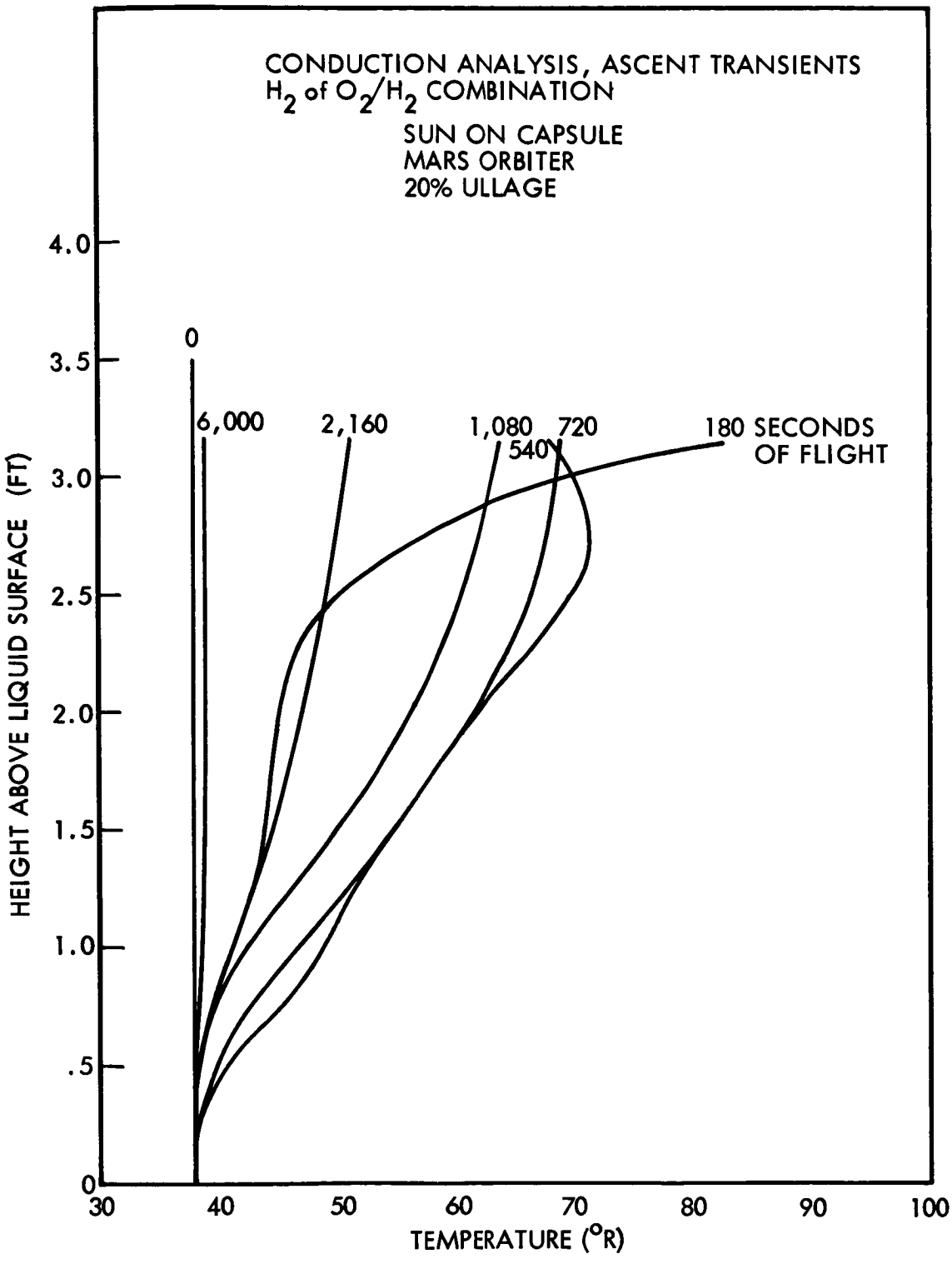

Fig. 32 H_2 Ullage Temperature Profiles During Ascent

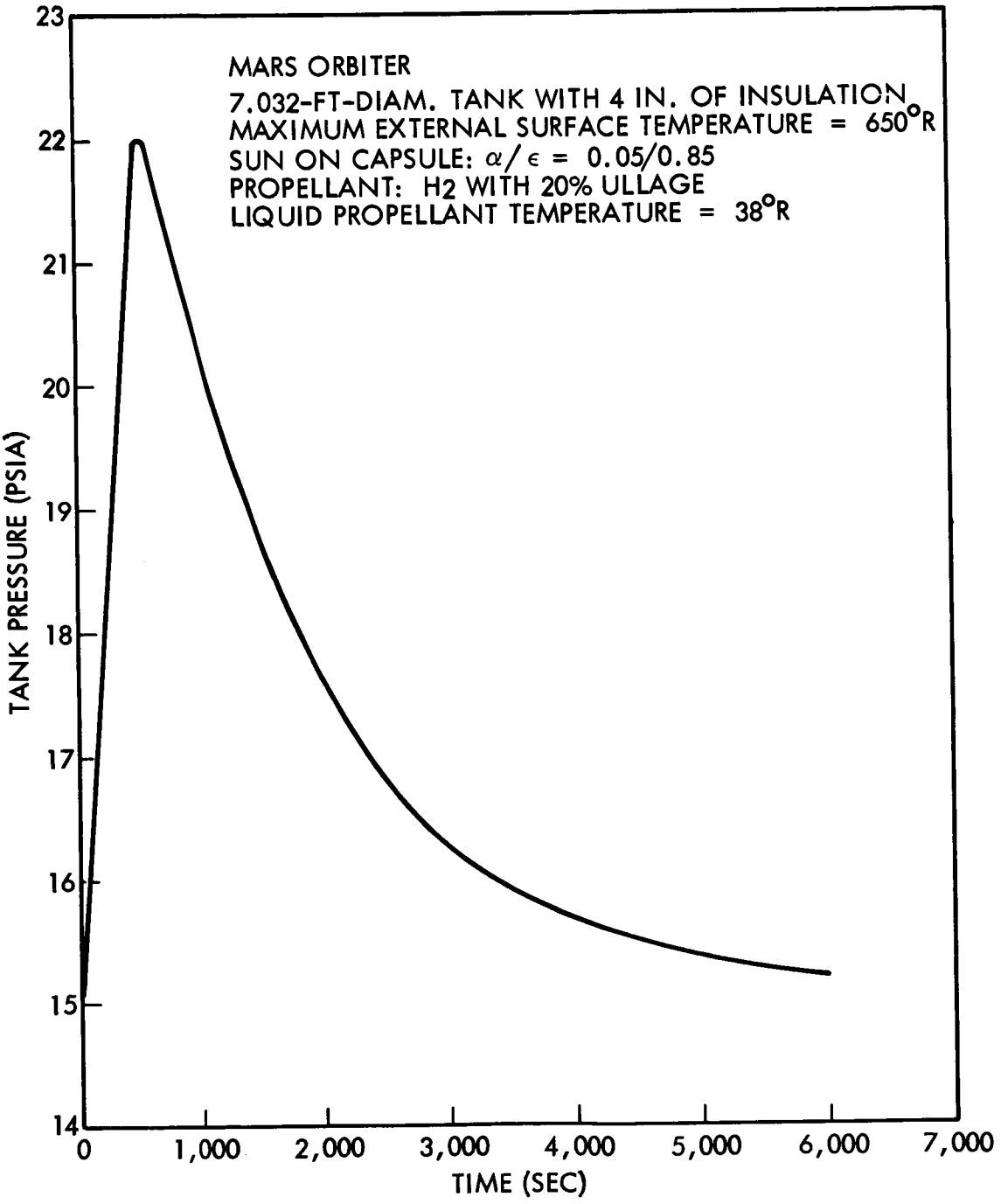

Fig. 33 H_2 Ullage Pressure History From Liftoff

A brief investigation of heat transfer and temperature gradients within a tank was conducted to substantiate the validity of this assumption. A conservative low-gravity condition was analyzed in which conduction was the only mode of heat transfer.

Assuming that conduction is the only heat transfer mode within the ullage, the time to reach thermal equilibrium would be a maximum. Diffusion would always be present and pressurant convection eddies and residual liquid motion are also likely to be present, all of which will expedite reaching thermal equilibrium. A conduction heat transfer model was constructed as shown in Fig. 31 for a typical space-storable propellant tank (OF_2). This conduction model will predict the worst temperature gradients and, therefore, the greatest tank pressure rise. The OF_2 was selected as a typical space-storable propellant because thermal conductivity values for all the space storables are nearly equal and the OF_2 operating temperature is about average. A hydrogen tank conduction model was also analyzed as a special case.

The propellant contact angles are not readily available and would require a detailed review of the literature and, probably, experimental evaluation beyond the scope of this study. A zero contact angle is a good assumption, and a liquid interface depression by capillary forces induced by the temperature gradients between the warm ullage wall and the cool, liquid wetted wall will be slight for any propellant with near-zero contact angle.

The time constant for the GF_2 tank nodal network is on the order of 2 hr for both the aluminum wall and the ullage gas, while the liquid time constant was about two orders of magnitude (200 hr) longer. Two hr is a short time interval for this mission, and the difference between liquid, wall, and ullage time constants shows that the liquid temperature approximates the system sink temperature. A steady-state temperature distribution will therefore give maximum ullage temperature gradients. The steady-state temperatures obtained were averaged and the resulting pressure differentials computed as listed in Table 21. This conservative analysis shows that the OF_2 tank pressure rise would be less than 3 psi over the thermal equilibrium

Table 21

ORBITAL OF_2 TANK CONDUCTION ANALYSIS – VALIDATION OF TANK THERMAL EQUILIBRIUM ASSUMPTION

Tank Insulation Surface Temperature (° R)	Insulation Thickness (in.)	Effective Ullage Temperature (° R)	Optimum Pressure (psia)	ΔT_{eff} (° R)(b)	ΔP (psi)(c)
201 (Sun on Capsule)	0.5(a)	236	<15	-14	-1.63
	0.625	238		-12	-1.40
	1	241		-9	-1.05
	1.375	243		-7	-0.81
	1.75	244		-6	-0.70
390 (O.S.R. α/ϵ = 0.05/0.8 Sun on Tank)	0.25	311		61	7.10
	0.5	291		41	4.77
	0.625	285		35	4.07
	1	274		24	2.79
	1.375	269		19	2.21
	1.75(a)	265	45	15	1.74
445 (White Paint α/ϵ = 0.3/0.95 Sun on Tank)	0.25	335		85	9.89
	0.5	305		55	6.40
	0.625	299		49	5.69
	1	284	58	34	3.96
	1.375	276		26	3.02
	1.75(a)	271		21	2.44

(a) Optimum thickness – Mars orbiter pump-fed.
(b) Maximum difference between average ullage and bulk liquid temperatures.
(c) Pressure differential due to ΔT eff.

pressure for the optimum insulation thickness. This will not cause a significant change in system weight, and thermal equilibrium therefore can be considered a valid assumption for all space storables.

The hydrogen propellant tank conduction model was developed and analyzed using similar assumptions, except the sink temperature was held at 50° R. The results of this analysis are presented in Table 22. The tank pressure rise over the thermal equilibrium pressure for the optimum insulation thickness was, again, on the order of 3 psi, which would not cause a significant change in system weight.

4.5 ENGINE BURN AND HEAT SOAKBACK

The effects of engine burn and the resultant heat soakback were neglected because the energy soakback due to postflow is very small. The effect upon the propellants is about equal and thus does not affect the overall validity of the system comparisons. The total burn times for all four engine firings are approximately 500 sec. It was assumed that an engine using a regeneratively cooled nozzle and chamber has surfaces, radiating to the propellant tanks, that reach maximum temperatures of approximately 300° F during burn. Propellant postflow can be used to rapidly cool the engine after burn.

A maximum temperature rise of 0.2° F was calculated for the propellant with the minimum thermal capacity (CH_4) under the following conditions:

- Radiation constants from the computer network were used
- The propellant was assumed to absorb all the energy during burns
- A nominal post flow of 0.5 sec was assumed to cool engine to 70° F

With a minimum of postflow, so that the engine remains at 300° F for about twice the burn time, the propellant temperature could rise 0.4° F. No estimate was made of the heating potential from ablatively cooled engines.

Table 22

STEADY-STATE H_2 ULLAGE CONDUCTION ANALYSIS

Tank Insulation Surface Temp. (°R)	Insulation Thickness (in.)	Average Ullage Temp. (°R)	Optimum Pressure (psia)	ΔT_{eff} (°R)(b)	ΔP (psi)(c)
201 (Sun on Capsule)	2(a)	71	55 to 90	21	2.5
	4	62		12	1.4
	6	58		8	0.9
390 (α/ϵ = 0.05/0.8 Sun on Tank)	4	76		26	3.1
	4-5/8(a)		55 to 90		
	6	68		18	2.1
445 (α/ϵ = 0.3/0.95 Sun on Tank)	4	81		31	3.6
	4-3/4(a)		115 to 150		
	6	71		21	2.5

(a) Optimum Insulation thickness for pump-fed Mars Orbiter, nonvented tanks.
(b) Maximum difference between average ullage and liquid temperature.
(c) Pressure differential due to ΔP_{eff} which would be necessary to increase tank design pressure.

4.6 DIFFERENTIAL BOILOFF

FLOX, MHF-5, and A-50 propellants considered in the studies are physical mixtures, not chemical compounds. Because each of these mixtures have slightly different boiling points, a propellant composition change could occur if a significant amount of propellant were vaporized. In the Mars Orbiter mission, a large ullage volume is present just prior to the orbit trim burn. The maximum amount of propellant vaporization will occur at this point in the mission as the tank reaches thermal equilibrium. The fluid volume also would be at a minimum at this time, resulting in the greatest change in propellant composition.

Since the components of propellant mixture have boiling temperatures and pressures that are nearly identical, they can be treated as ideal solutions whose vapor is an ideal gas. This assumes that no heat is generated due to the combination of the components and that the vapor enthalpies are insensitive to pressure changes. Since the saturation pressure differences of the mixture components are the pressure changes considered, this assumption is reasonable for this study.

With FLOX propellant, about 30 lb of FLOX would be vaporized out of an impulse requirement of 150 lb for the orbit trim for the last propulsive maneuver. The fluorine concentration in the remaining FLOX could decrease as much as 12 percent from the original value of 83 percent because of differential boiloff. Such a change would require a small increase in the impulse propellant load to compensate for the slight reduction in specific impulse.

The A-50 and MHF-5 vapor weights predicted with the same set of conditions were small; therefore, differential boiloff is not a factor for these propellants. Differential boiloff for a MEM using FLOX will be of little significance since the percent ullage volume and exposure time are both small relative to that for the orbiter.

4.7 THERMODYNAMIC ANALYSES CONCLUSIONS AND RECOMMENDATIONS

4.7.1 Conclusions

Thermodynamic analyses conducted for both the Mars Orbiter and the MEM spacecraft system have resulted in a sufficient amount of data to permit computation of overall systems performance, point out important operational considerations, and identify areas where technology advancements should be pursued. It has been established that all propellants considered can be used for the Mars missions without venting and without providing for a preferred spacecraft orientation relative to the sun. Specific conclusions arrived at for the Mars Orbiter and the MEM and some observations with regard to operational considerations applicable to both are as follows.

Mars Orbiter

- Mars Orbiter pump-fed systems tend to optimize with tradeoffs between insulation and vapor weights.
- Mars Orbiter pressure-fed systems tend to optimize with tradeoffs between pressurant system weight and tank weight, plus insulation and vapor weights to a lesser extent.
- The cryogenic and space-storable propellants require the lowest α/ϵ ratio surface of OSR for sun-on-tank orientations, and the earth storables will require a surface finish α/ϵ of 0.3/0.95 and higher.
- With the sun-on-tank orientation, increasing the mission length results in increased weights (tank, vapor, pressurant, and insulation) for the cryogenic and space-storable propellants with the optimum surface finish. For the earth-storable propellants, there is no weight penalty due to increasing the mission length providing that the optimum surface finish is selected.

- With insulation system conductivities increased to double the nominal values, both higher operating pressures and thicker insulation are required for the cryogenic and space-storable propellants and system weight is increased.
- Venting of hydrogen during the mission would result in a net saving in system weight. No significant weight savings can be realized by venting of the space and earth-storable propellants.
- Sun shadow shielding of hydrogen tankage shows considerable potential for weight savings. Lesser weight savings are realized for shielding space storables. Earth storables, in general, require heating; therefore, sun shielding would cause a weight penalty.

MEM

- The two-stage pump-fed MEM optimized with tradeoffs of insulation and pressurant weights on the first stage (outer) tankage and with tradeoffs of insulation and vapor weights for the second stage (inner) tankage.
- Vacuum jacketing is required for cryogenic and space-storable propellants.

Operational Considerations

- A helium purge of the insulation is required during ground held for the H_2 propellant and dry nitrogen or dry air for the space-storable propellants.
- Closed-loop vent or refrigerator systems are required for the propellants of the fluorine family (F_2, FLOX, and OF_2) during ground operations.
- To compensate for ground-hold propellant temperature rise, subcooling requirements range up to a maximum of 5° F for the cryogens for each hour from topping termination to liftoff. Additional subcooling could also reduce the system weights for cryogenics and space storables.
- A typical flight-type multilayer insulation installation will vent adequately in a typical booster trajectory with proper ground-hold conditioning. Ascent heating of ullage gas will not cause unacceptable pressure rises.

4.7.2 Recommendations

Recommendations as a result of the thermodynamic analyses are as follows:

- Additional development of an efficient spacecraft coating for cryogens, such as OSR, is desirable. This study was based on properties attainable with the currently qualified type of installation consisting of flat 1.5-in. square segments. A development program is now underway at Lockheed to develop an OSR-type coating that can be applied to curved surfaces at low cost. Although not yet flight proven, the finish, which consists of a controlled thickness of alumina on an aluminum substrate, appears promising. Further development should be continued to achieve very low α/ϵ surface coatings that can be applied to flexible substrates such as Mylar.
- Flight-weight vacuum jacket systems require development for cryogenic propellants to be feasible for a MEM-type mission.
- More detailed studies of thermal-related ground-handling problem areas will be necessary. These problems include fill, drain, and ground-hold conditioning to prevent venting or provide subcooling.
- A shadow-shield design should be made and analyzed in detail.
- Engine preburn and postburn thermal conditioning propellant flow requirements should be defined.
- The thermal effects of environmental changes due to maneuvers should be evaluated.
- More detailed evaluation of the pressurant storage system pressure level, storage temperature, location, and the expansion process should be analyzed to determine the impact on the total system weight.
- Better propellant property data are needed, particularly vapor enthalpy, internal energy, and heat of vaporization as a function of pressure.
- Experimental studies will be required in conjunction with a detailed literature search to determine contact angles and surface-tension forces for many of the propellants.

Section 5
PROPULSION SYSTEMS DATA ANALYSIS

5.1 INTRODUCTION

The accumulation and analysis of propulsion system data were carried out in three phases. Each phase supplemented a particular task of the overall study plan. The three phases were as follows:

- Assembly of parametric data and information relating to the application of earth-storable, cryogenic, and space-storable propellant combinations, with emphasis on the space storables
- Definition of engine requirements for the selected missions and propellants, compatible with anticipated engine characteristics
- Determination of the sensitivity of engine performance to variation in the principal design parameters

Activity in the propulsion system study began in Task I with a request for assistance addressed to several rocket engine manufacturers. A work statement was prepared and distributed specifically requesting experimental design and performance parameters for engines employing space-storable propellant combinations.

At the conclusion of Task I, two missions with appropriate stages were selected by the NASA Management Committee for detailed investigation during Task II. This selection implied specific thrust requirements for achieving each mission. At this time, the participating engine companies were asked for additional inputs of a specific nature to substantiate the information extracted from the parametric data. The response from each contractor was assessed and a specification of engine system requirements for each propellant combination was established.

The concluding phase of the propulsion system analysis was determination of the sensitivity of engine performance to variation of the major engine design parameters. Data supplied by the engine companies were used to generate this information for support of the stage analysis of Task III.

As a supplement to the three phases, the participating engine companies provided discussions of potential problem areas and technology requirements associated with the application of the specified propellant combinations. Their comments were reviewed and the principal remarks were summarized as a part of this report.

5.2 SUPPORTING DATA

At the beginning of Task I, the support of rocket engine contractors was solicited in compiling propellant and propulsion systems data for use in the Propellant Selection Study. A work statement, prepared and issued to several companies, included a specific request for experimental design and performance parameters for engines employing space-storable propellant combinations. This information was to be used to evaluate these propellants and to facilitate their selection for spacecraft propulsion systems. The following companies responded to this request by providing data:

- Aerojet General Corporation
- Bell Aerosystems Company (Limited data supplied for Task I only)
- Pratt & Whitney Aircraft
- Rocketdyne Division of NAR

To properly evaluate space-storable propellant combinations, information concerning a variety of cryogenic and earth-storable combinations was also sought. However, subsequent to Task I, the NASA Management Committee and LMSC agreed to emphasize the following propellant combinations:

- O_2/H_2
- F_2/H_2

- FLOX/CH_4
- OF_2/CH_4
- F_2/NH_3
- OF_2/B_2H_6
- N_2O_4/A-50
- ClF_5/MHF-5

The documents submitted by the companies named above are listed in Refs. 15 through 21. Data supplied for the candidate propellants include the following:

- Performance as a function of thrust, chamber pressure, nozzle expansion ratio, mixture ratio, and cooling technique
- Engine weights and dimensions
- Information on ignition and hypergolicity
- Information on materials capability

These data were assembled and organized according to nine criteria that were considered significant by the engine companies. The nine criteria, listed below, are briefly discussed in the following paragraphs.

- Performance – I_{sp}, MR, Recombination Losses, etc.
- Storability – Liquid Range
- Handling and Safety
- Thermal Stability
- Materials Compatibility
- Ignition Characteristics – Hypergolicity
- Cooling Technique – Regenerative, Ablative, Transpiration, etc.
- Bulk Density and Impulse Density
- Cost

5.2.1 Performance

Performance – the primary measure of the attractiveness of a given propellant combination – was determined for each engine configuration evaluated during the study. Specific impulse, optimum mixture ratio, and sensitivity to recombination losses at various pressure levels are among the elements that constitute performance. Data over a wide range of thrust, nozzle expansion ratio, chamber pressure, and mixture ratio combinations, as well as engine dimensional and weight data, were received and evaluated.

5.2.2 Storability

Storability is directly related to the liquid range of the propellant as a function of both temperature and pressure. Figure 34 shows the liquid range for the fuel and oxidizer of each propellant combination at earth ambient pressure and at 50 psia pressure.

5.2.3 Handling and Safety

The handling and safety characteristics of each propellant are summarized in Table 23. The cryogenic formulations require thermal protection, such as dewars, to maintain cryogenic temperatures. All space-storable formulations containing fluorine and fluorine compounds are also highly toxic and reactive, requiring passivation of all equipment that they may contact either as liquid or vapor. The propellants B_2H_6 and NH_3 also require thermal protection during storage, and B_2H_6 is highly toxic. The earth-storable propellants (N_2O_4, ClF_5, and A-50) are all highly toxic, and the first two are also highly reactive with most materials.

5.2.4 Thermal Stability

Thermal stability characteristics are summarized in Table 24, which lists the conditions under which decomposition may occur. The propellants H_2, O_2, F_2, FLOX,

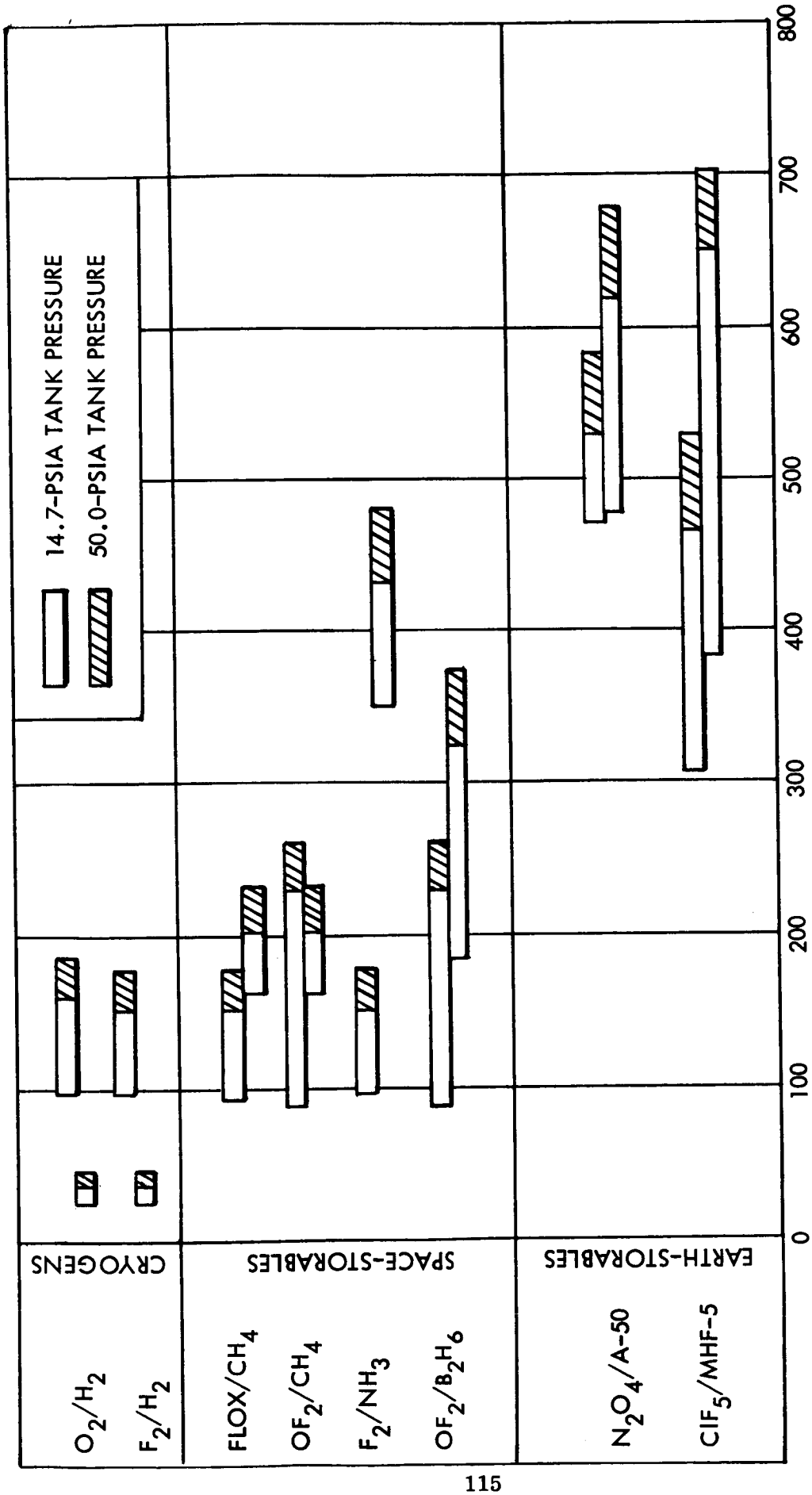

Fig. 34 Propellant Liquid Temperature Range

Table 23

PROPELLANT HANDLING SAFETY

O_2	REQUIRES DEWARS, COMPLETE SEGREGATION FROM ORGANIC SUBSTANCES; NONTOXIC AT NORMAL PARTIAL PRESSURE.
F_2, FLOX, OF_2	REQUIRES LN_2 JACKETED DEWARS, PASSIVATION OF EQUIPMENT, HIGHLY REACTIVE, HIGHLY TOXIC.
N_2O_4	NO HANDLING PROBLEMS AT ROOM TEMPERATURE; HIGHLY TOXIC.
H_2	REQUIRES DEWARS; NONTOXIC.
CH_4	REQUIRES DEWARS; NONTOXIC.
B_2H_6	PRESSURIZED, REFRIGERATED STORAGE REQUIRED; HIGHLY TOXIC.
50% N_2H_4 + 50% UDMH	REQUIRES INERT ATMOSPHERE STORAGE, SEGREGATION FROM ORGANIC MATERIALS; TOXIC.
NH_3	REFRIGERATED STORAGE REQUIRED.
ClF_5	NO HANDLING PROBLEMS AT ROOM TEMPERATURE; HIGHLY TOXIC.
MHF-5	NO HANDLING PROBLEMS AT ROOM TEMPERATURE.

Table 24

THERMAL STABILITY OF PROPELLANTS

H_2, O_2, F_2, FLOX	STABLE.
CH_4	STABLE TO BULK TEMPERATURES ABOVE 1,000°F.
B_2H_6	LONG-TERM STORAGE OF GAS SHOWS DECOMPOSITION ABOVE -4°F. DECOMPOSITION RESULTS IN RELEASE OF HYDROGEN AND FORMATION OF SOLID BORON COMPOUNDS. B_2H_6 IS UNSATISFACTORY FOR REGENERATIVE COOLING.
50% N_2H_4 / 50% UDMH	DECOMPOSES SLOWLY ABOVE 100°F. DECOMPOSES EXPLOSIVELY BETWEEN 500°F AND 716°F.
NH_3	STABLE TO 1,060°F. DECOMPOSES ENDOTHERMICALLY RAPIDLY ABOVE THIS TEMPERATURE.
N_2O_4	DECOMPOSES ENDOTHERMICALLY AT TEMPERATURES ABOVE 130°F. A STRONG PRESSURE EFFECT EXISTS.
OF_2	LONG-TERM STORAGE SHOWS SIGNIFICANT DECOMPOSITION ABOVE 160°F. ENGINE STABILITY LIMIT IS APPROXIMATELY 500°F.
ClF_5	STABLE TO +329°F.
MHF-5	STABLE.

and CH_4 are stable under most of the expected storage and operating conditions. B_2H_6 is unstable above -4° F, decomposing above that temperature into hydrogen and solid boron compounds and, therefore, limiting its applicability for regenerative cooling. NH_3 also is unstable above 1060° F, decomposing endothermically very rapidly above this temperature. Long-term storage of OF_2 shows significant decomposition above 160° F, and the engine stability limit is established at approximately 500° F.

Among the earth-storable propellants, N_2O_4 decomposes endothermically above 130° F, with a strong pressure effect. A-50 decomposes slowly above 100° F and explosively between 500° F and 716° F. ClF_5 is stable to +329° F, and MHF-5 is stable to temperatures of approximately 450° F.

5.2.5 Materials Compatibility

The problems of materials compatibility for each propellant are listed in Table 25. Liquid O_2 is reactive with some materials, but compatible with most metals, Teflon, and silicon compounds. Fluorine and FLOX are reactive with most metals, but compatible with passivated stainless steel, certain aluminum alloys, monel, copper, bronze, brass, tin, nickel, and Teflon. OF_2 is reactive with most materials, but compatible with glass, passivated stainless steel, monel, aluminum, copper, nickel, and Teflon.

Among earth-storables, A-50 and MMH are reactive with some materials, but compatible with most for short-term storage. For long-term storage, aluminum, glass, and polyethylene are compatible. ClF_5 and N_2O_4 are reactive with most materials and compatible with some aluminum alloys, passivated stainless steel, and carboxyl nitroso rubber (for seal applications only). Passivation of all equipment contacted by these propellants is necessary. Passivated aluminum alloys are recommended for long-time storage of N_2O_4 and ClF_5. Other propellant formulations used in this study pose no unusual compatibility problems.

Table 25

MATERIALS COMPATIBILITY

OXYGEN, O_2	REACTIVE WITH SOME MATERIALS. LIQUID COMPATIBLE WITH MOST METALS, TEFLON, SILICON COMPOUNDS.
FLUORINE, F_2 FLOX	REACTIVE WITH MOST METALS. LIQUID COMPATIBLE WITH PASSIVATED STAINLESS STEEL, SOME ALUMINUM ALLOYS, MONEL, COPPER, BRONZE, BRASS, TIN, NICKEL, AND TEFLON.
OXYGEN DIFLUORIDE, OF_2	REACTIVE WITH MOST MATERIALS. COMPATIBLE WITH GLASS, PASSIVATED STAINLESS STEEL, MONEL, ALUMINUM, COPPER, NICKEL, AND TEFLON.
50% N_2H_4 50% UDMH MMH	REACTIVE WITH SOME MATERIALS. COMPATIBLE WITH MOST MATERIALS FOR SHORT-TERM STORAGE. ALUMINUM, GLASS, AND POLYETHYLENE ARE SUITABLE FOR LONG-TERM STORAGE.
CHLORINE PENTAFLUORIDE, ClF_5	REACTIVE WITH MOST MATERIALS. LIQUID COMPATIBLE WITH SOME ALUMINUM ALLOYS, PASSIVATED STAINLESS STEEL, AND CARBOXYL-NITROSO RUBBER.

OTHER PROPELLANTS USED IN THIS STUDY POSE NO UNUSUAL COMPATIBILITY PROBLEMS.

5.2.6 Ignition Characteristics

As listed in Table 26, all propellant combinations except O_2/H_2 and OF_2/CH_4 are hypergolic over normal storage and usage temperature ranges.

Table 26

PROPELLANT HYPERGOLICITY

Propellant	Hypergolic
O_2/H_2	No
F_2/H_2	Yes
$FLOX/CH_4$	Yes
OF_2/CH_4	No
OF_2/B_2H_6	Yes
F_2/NH_3	Yes
N_2O_4/A-50	Yes
ClF_5/MHF-5	Yes

The O_2/H_2 formulation requires an ignition device because the propellants are completely non-hypergolic. The OF_2/CH_4 formulation is reliably hypergolic above a temperature of 130° F and erratically hypergolic (experiencing long ignition delays) at lower temperatures.

5.2.7 Cooling Technique

The major cooling methods applicable to engine system and the advantages and disadvantages of each are given in Table 27.

Table 27

ENGINE SYSTEM COOLING METHODS

Method	Remarks
Regenerative	Unlimited life No performance loss
Transpiration Cooling	Unlimited life and heat-flux capability Does not increase propellant supply pressure Small performance penalty
Dump Cooling	Lightweight Small I_{sp} penalty
Radiation	Lightweight Low heat-flux applications
Ablation	Simple Low-Pressure (low heat-flux) application Degrades performance Limited lifetime

Regenerative cooling was selected, where applicable, as the preferred method for engines of appreciable size, because it involves no performance losses and has an unlimited lifetime. It also can be adapted for autogenous pressurization systems by bleeding off hot gas or liquid propellant from the nozzle cooling jacket.

Upper limits on the chamber pressure for regenerative cooling of five of the propellant formulations are given in Fig. 35. Of the remaining combinations, OF_2/B_2H_6 was considered only in an ablative cooling mode. At low pressures, the possibility of boron compounds being deposited in regenerative cooling tubes is high. Thus, this formulation probably will be used only in a pressure-fed engine with relatively low pressure levels. The earth-storable formulations, N_2O_4/A-50 and ClF_5/MFH-5,

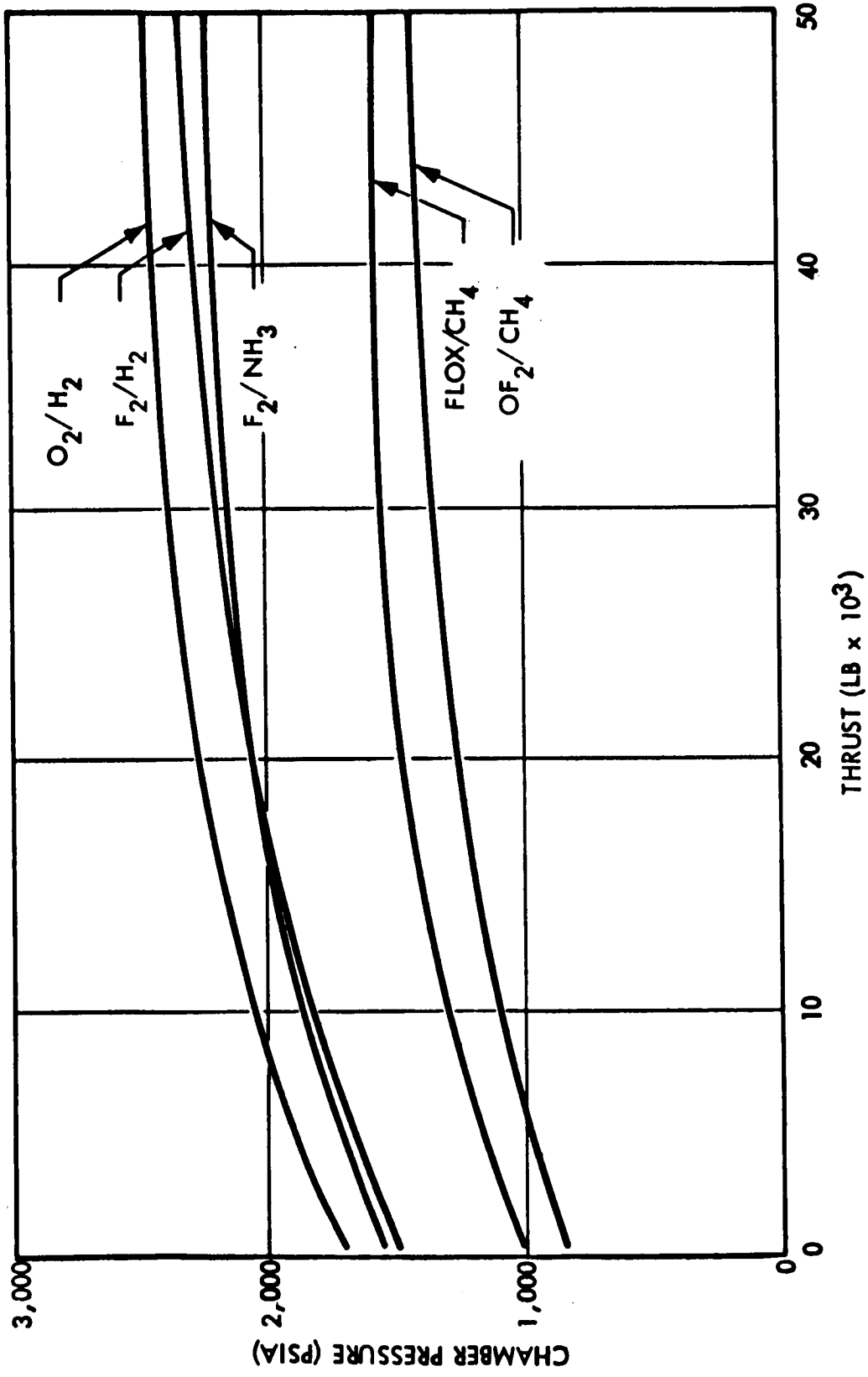

Fig. 35 Chamber Pressure Limits for Regenerative Cooling

also were considered only for ablative cooling. The decomposition of earth-storable propellants begins at temperatures that may occur in a regeneratively cooled system. Regenerative cooling has been demonstrated using these propellants, but it may not be possible at arbitrary thrust levels, especially with the inclusion of a 2:1 (or greater) throttling requirement.

5.2.8 Bulk Density and Density Impulse

The bulk densities of the various propellant combinations are shown in Fig. 36 for the mixture ratios selected for the Task II analyses. The cryogenics, especially O_2/H_2, are the least dense (density approximately one-half that of the space storables). The space storables show a marked increase in density, followed by earth storables, which are still more dense than the space storables.

Figure 37 shows the density impulse of each of the propellant combinations. The figure is based on the nominal values of mixture ratio and specific impulse that were selected for use with the Mars Orbiter in Task II.

5.2.9 Cost

Propellant costs are strongly dependent on utilization. To predict utilization, a projection of the type and number of missions must be made. Since such a projection was not a part of this study, propellant costs and their influence were not evaluated.

5.3 SENSITIVITY DATA

To support the stage sensitivity analysis of Task III, the participating engine contractors also provided information concerning the sensitivity of the performance of each propellant combination to variations in the principal engine parameters. Table 28 is a summary of these data for pump-fed engines at the 8,000-lb thrust level for propellant combinations of interest. Perturbations of the mixture ratio, nozzle expansion ratio, and chamber pressure are considered.

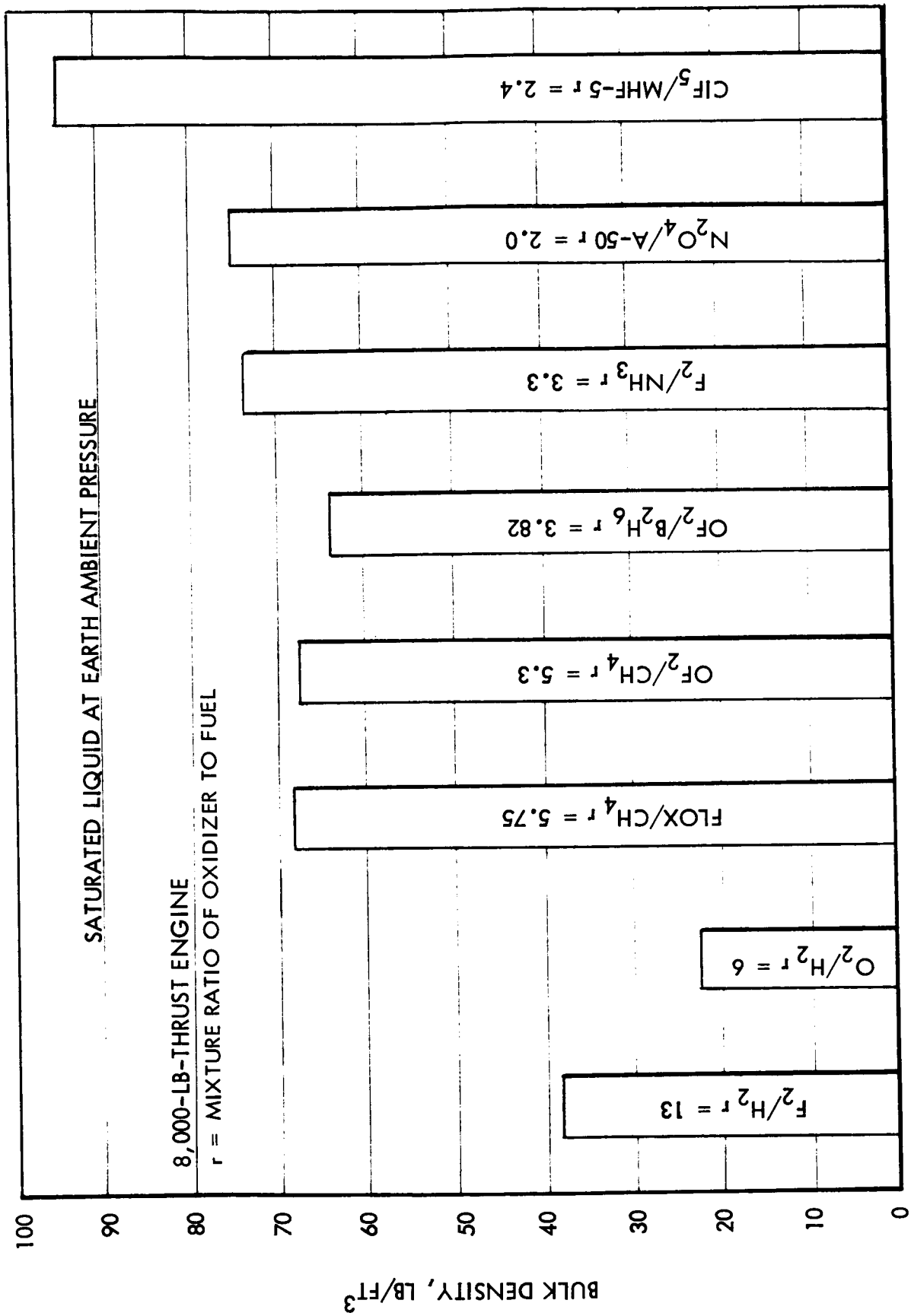

Fig. 36 Bulk Density of Propellants

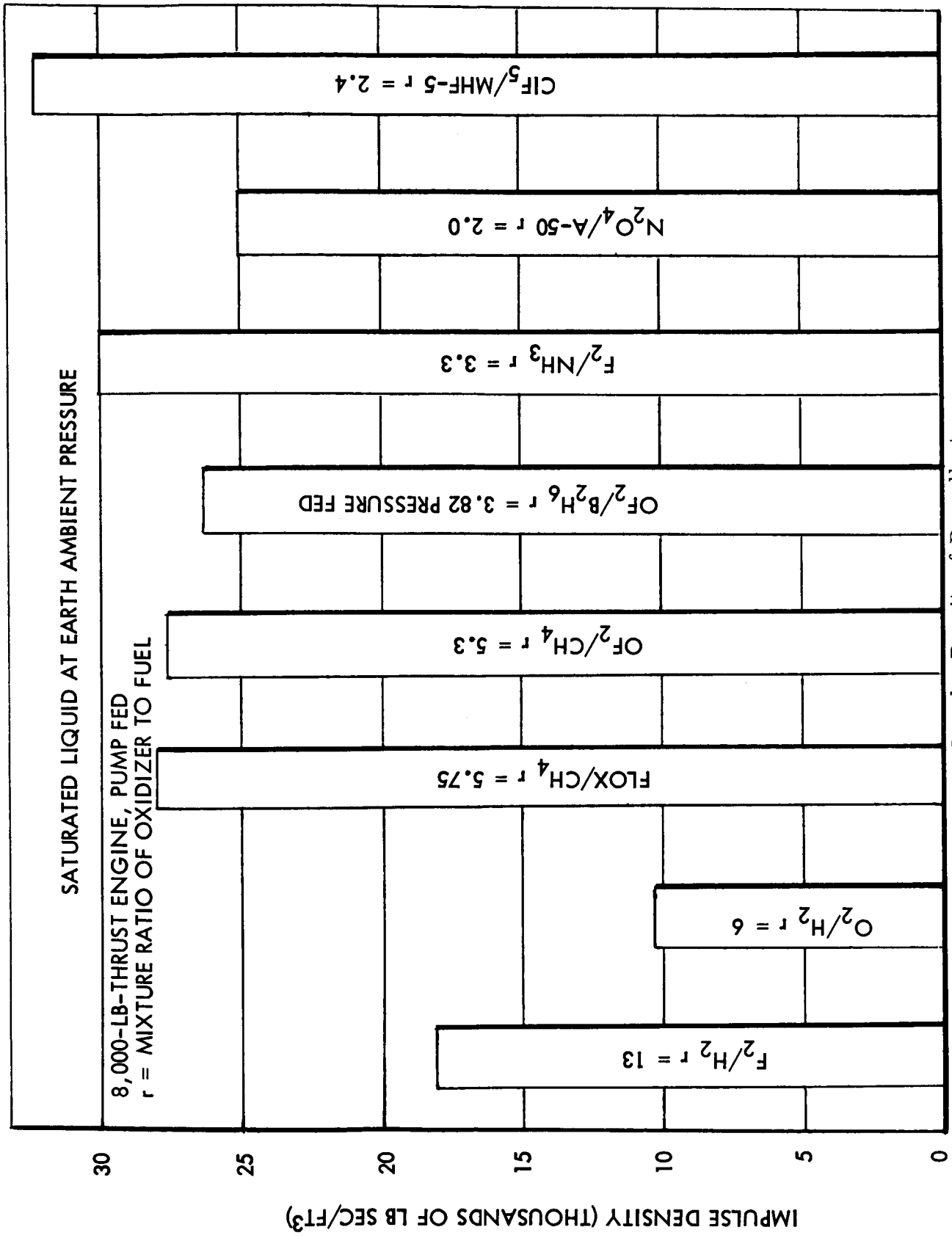

Fig. 37 Impulse Density of Propellants

Table 28

DESIGN SENSITIVITY DATA – 8,000 LB THRUST, PUMP-FED ENGINE

		Mixture Ratio Variation ϵ = 100				Expansion Ratio Variation				Chamber Pressure Variation ϵ = 100			
						ϵ = 40	ϵ = 60	ϵ = 100	ϵ = 150				
F_2/H_2	MR	11	12	13*	14	13	13	13*	13	13	13	13*	
	P_C(PSI)	900	900	900*	900	900	900	900*	900	600	750	900*	
	I_{SP}(SEC)	468.9	468.6	468.0*	467.0	456.4	462.2	468.0*	471.9	464.4	466.3	468.0*	
	WT(LB)	152	152	152*	152	152	152	152*	154	145	145	152*	
O_2/H_2	MR	5.5	5.75	6.0*	6.25	6.0	6.0	6.0*	6.0	6.0	6.0	6.0*	
	P_C	900	900	900*	900	900	900	900*	900	600	750	900*	
	I_{SP}	452.9	452.1	451.0*	449.6	439.4	443.7	451.0*	456.4	449.5	450.6	451.0*	
	WT	173+	173+	173+*	173+	152	152	173+*	182+	166+	166+	173+*	
FLOX/ CH_4	MR	5.25	5.50	5.75*	6.0	5.75	5.75	5.75*	5.75	5.75	5.75*		
	P_C	600	600	600*	600	600	600	600	600	300	600*		
	I_{SP}	408.0	409.2	410.0*	405.2	399.5	404.0	410.0*	413.7	405.4	410.0*		
	WT	152	152	152*	152	151	151	152*	156	145	152*		
OF_2/ CH_4	MR	4.7	5.0	5.3*	5.6	5.3	5.3	5.3*	5.3	5.3	5.3*		
	P_C	600	600	600*	600	600	600	600*	600	300	600*		
	I_{SP}	409.8	410.5	410.0*	409.3	396.8	402.8	410.0*	414.8	405.4	410.0*		
	WT	152	152	152*	152	151	151	152*	156	145	152*		
F_2/NH_3	M_R	2.9	3.1	3.3*	3.5	3.3	3.3	3.3*	3.3	3.3	3.3	3.3*	
	P_C	1500	1500	1500*	1500	1500	1500	1500*	1500	500	1000	1500*	
	I_{SP}	407.3	407.8	408.0*	402.3	399.0	403.3	408.0*	411.3	402.7	406.6	408.0*	
	WT	192	192	192*	192	191	191	192*	194	152	152	192*	
N_2O_4 A-50	MR	1.6	1.8	2.0*	2.2	2.0	2.0	2.0*	2.0	2.0	2.0	2.0*	2.0
	P_C	750	750	750*	750	750	750	750	750	350	550	750*	950
	I_{SP}	325.1	332.2	335.0*	333.5	325.3	330.1	335.0*	338.2	333.1	334.5	335.0*	335.2
	WT	158	158	158*	158	158	158	158*	162	152	158	158*	165

* Baseline system.
+ Two position nozzle.

In all cases, performance is most sensitive to the nozzle expansion ratio. This indicates that the largest practical value of this parameter should be employed, subject to the limitations imposed by the available envelope. The parameters of mixture ratio and chamber pressure also are available for tradeoffs. The data of Table 28 were necessary during Task III to assess the impact of perturbations in the basic engine parameters on the stage designs for the selected missions.

Section 6
ENGINE DESIGN CRITERIA

6.1 ENGINE SYSTEMS

Task I of the Propellant Selection study resulted in the selection of the following two thrust levels for use in the Task II stage analyses:

- 8,000 lbf, throttleable to 1,000 lbf, for the Mars Orbiter
- 30,000 lbf, throttleable to 15,000 lbf, for the MEM Ascent Stage

These propulsion requirements were supplied to the participating engine companies with a request for additional inputs of a specific nature in order to substantiate the selection of data from the parametric information. The performance, weight, and operational characteristics of all the engine systems from each contractor were evaluated to arrive at definitive engine systems satisfying the study criteria.

Data were compiled for engines having various nozzle configurations and feed systems. In the process of selecting an engine for a stage based on each propellant combination, the following procedure was adhered to.

Mars Orbiter – 8,000 lbf Thrust Engine:

- The bell nozzle engine configuration was used for both pump-fed and pressure-fed systems if the length could be accommodated within the TRW Voyager envelope.
- The extendable bell nozzle configuration was selected if the envelope was exceeded by the length of a fixed bell nozzle engine configuration.

MEM Ascent Stage – 30,000 lbf Thrust Engine:

- The Aerospike engine configuration was selected as the only single-engine configuration that could meet the performance requirements and the available envelope limitations within a MEM vehicle with a maximum diameter of 31.5 ft.
- Only pump-fed engines were used. (A pressure-fed OF_2/B_2H_6 engine was examined as a special case and rejected because available envelope limits were exceeded.)

Figure 38 defines the envelopes of the fixed bell nozzle, extendable bell nozzle, and Aerospike engine configurations.

6.1.1 Mars Orbiter Engine

The propulsion system parameters for the Mars Orbiter engine, as derived and refined from engine company data, are listed in Table 29. Information for both pump-fed and pressure-fed engines is presented. All of the data submitted were examined in depth to determine a consistent set of data for each engine and propellant combination.

Table 29 reflects the nominal values of the parameters employed for each engine/propellant combination, including propellant parameters, nozzle configuration, and engine size and weight. Regenerative cooling is used for all propellant combinations except OF_2/B_2H_6, N_2O_4/A-50, and ClF_5/MHF-5, which use ablative cooling. Table 30 expands the data of the previous table to include additional physical design characteristics and requirements. Figure 39 is an example of a conventional fixed bell nozzle engine configuration as sized for the Mars Orbiter stage. A typical engine with an extendable nozzle section is shown in Fig. 40.

6.1.2 Nozzle Configuration

The choice of the nozzle shape was based on envelope limitations. The fixed bell nozzle engine configuration was used whenever possible because of its light weight, high performance, simplicity, and production economy. Among pump-fed

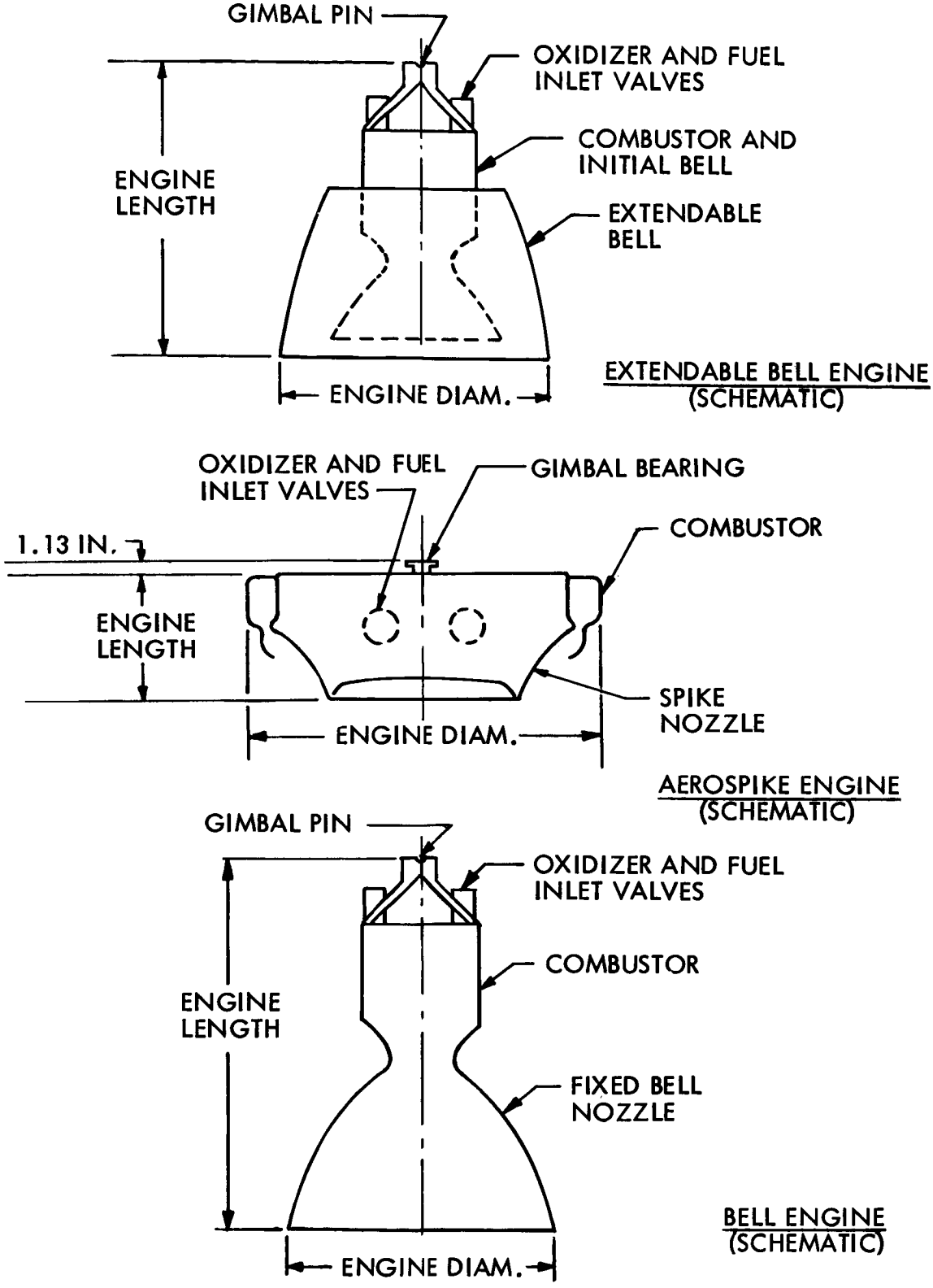

Fig. 38 Engine Designs for Propellant Selection Study

FOLDOUT FRAME 1

FOLDOUT FRAME 2

Table 29

PROPULSION SYSTEM PARAMETERS FOR 8,000 LB THRUST ENGINE

Parameter \ Propellants	O_2/H_2			F_2/H_2			FLOX/CH_4			OF_2/CH_4			OF_2/B_2H_6			F_2/NH_3			N_2O_4/A-50			ClF_5/MHF-5		
	Oxidizer	Fuel		Oxidizer	Fuel		Oxidizer	Fuel		Oxidizer	Fuel		Oxidizer	Fuel		Oxidizer	Fuel		Oxidizer	Fuel		Oxidizer	Fuel	
Heat of Vaporization at Normal Boiling Point (Btu/lb)	91.62	195.3		74.10	195.3		77.0	219.2		81.9	219.2		81.9	224.3		74.10	596.3		178.1	425.8		128.0	208.0	
Boiling Point (°R)	162.3	36.5		153.04	36.5		154.0	201.0		231.4	201.1		231.4	183.8		153.1	432.0		471.5	478.7		466.8	652.1	
Freezing Point (°R)	97.9	24.9		96.4	24.9		96.7	163.2		88.7	163.2		88.7	325.2		96.4	351.8		529.8	619.0		306.6	388.1	
Density (lb/ft^3)	71.29	4.42		94.3	4.42		91.2	26.46		95.7	26.46		95.7	28.1		94.3	42.57		89.3	56.2		118.5	63.0	
Expansion Ratio (ϵ)	100/1			100/1			100/1			100/1			100/1			100/1			100/1				100/1	
Engine Type	Bell	Extend. Bell		Bell	Extend. Bell		Bell	Extend. Bell		Bell	Extend. Bell		Bell	Extend. Bell		Bell	Extend. Bell		Bell	Extend. Bell		Bell	Extend. Pell	
Feed Type	Pump	Pump	Press.	Pump	Pump	Press.	Pump	Pump	Press.	Pump	Pump	Press.	Pump	Pump	Press.	Pump	Pump	Press.	Pump	Pump	Press.	Pump	Pump	Press.
Chamber Pressure (psia)	900	900	100	900	900	100	600	600	100	600	600	100			100	1500	1500	100	750	750	100	750	750	100
Mixture Ratio (O/F)	6	6	6	13	13	13	5.75	5.75	5.75	5.3	5.3	5.3			3.82	3.3	3.3	3.3	2.0	2.0	2.0	2.4	2.4	2.4
Isp Delivered (lb-sec/lb)	451	451	445	468	468	442	410	410	387	410	410	396			414	408	408	386	335	335	328	342	342	330
Engine Diameter (in.)	25	25	74	25	25	74	31	31	74	31	31	74			74	20	24	74	27	27	74	27	27	74
Engine Length (in.)	53	40	83	54	40	83	61	43	83	61	43	83			83	48	36	84	56	42	83	56	42	83
Engine Weight (lb)	152	173	380	152	173	375	152	174	375	152	174	380			384	192	214	375	158	188	330	167	197	384
Density of Mixture (lb/ft^3)	22.6			38.5			68.7			67.7			63.8			73.7			74.7			94.3		
Impulse Density (Pump-Fed Bell) (lb-sec/ft^3)	10,180			18,020			28,170			27,760			26,410 (Press.-Fed)			30,070			25,020			32,250		

NOTES:
1. Lengths given for extended bell engines are stowed lengths.
2. All propellant combinations will employ regenerative cooling, except for OF_2/B_2H_6, N_2O_4/A-50 and ClF_5/MHF-5 which will use ablative cooling.

Table 30

PROPULSION SYSTEM CHARACTERITICS AND REQUIREMENTS FOR 8,000-LB-THRUST ENGINE

Propellant Combination	Feed	Mixture Ratio (Optimum) (Oxid/Fuel)	Chamber Pressure (Optimum) (psia)	I_{sp} Delivered (sec)	Nozzle Expansion Ratio	Storage Temperature Range (°R)	Start Temperature Range (°R)	Pre-Heat or Pre-Chill Required	Post-Fired Purge Required	NPSP(3) Ox.	NPSP(3) Fuel	Pressurizing System (Single or Dual)	Total Engine Weight (Bell) (lb)	Total Engine Weight (Extended Bell) (lb)
F_2/H_2	Pump	13	900	468	100	Less than 620 (1)	Max 620 Min(2)	No	No	4	4	Dual	152	173
	Pressure	13	100	442	100	Less than 620(1)	Max 620 Min(2)	No	No	–	–	Single	–	375
N_2O_4/A-50	Pump	2	750	335	100	364 to 497	540 to 580	No	O and F Yes	4	4	Single	158	188
	Pressure	2	100	328	100	364 to 497	540 to 580	No	O and F Yes	–	–	Single	–	330
O_2/H_2	Pump	6	900	451	100	Less than 620 (1)	Max 620 Min(2)	No	No	4	4	Dual	152	173
	Pressure	6	100	445	100	Less than 620 (1)	Max 620 Min(2)	No	No	–	–	Single	–	380
FLOX/CH_4	Pump	5.75	600	410	100	Less than 620 (1)	Max 620 Min(2)	No	No	4	4	Single	152	174
	Pressure	5.75	100	387	100	Less than 620 (1)	Max 620 Min(2)	No	No	–	–	Single	–	375
OF_2/CH_4	Pump	5.3	600	410	100	Less than 620 (1)	Max 620 Min(2)	No	No	4	4	Single	152	174
	Pressure	5.3	100	396	100	Less than 620 (1)	Max 620 Min(2)	No	No	–	–	Single	–	380
OF_2/B_2H_6	Pump	–	–	–	–	–	–	–	–	–	–	–	–	–
	Pressure	3.82	100	423	100	Less than 620 (1)	Max 620 Min(2)	No	No	–	–	Single	–	384
F_2/NH_3	Pump	3.3	1,500	408	100	Less than 620 (1)	Max 620 Min(2)	No	No	4	4	Single	192	214
	Pressure	3.3	100	386	100	Less than 620 (1)	Max 620 Min(2)	No	No	–	–	Single	–	375
ClF_5/ MHF-5	Pump	2.4	750	342	100	405 to 510	410 to 580	No	O Yes	4	4	Single	167	197
	Pressure	2.4	100	330	100	405 to 510	410 to 580	No	Yes	–	–	Single	–	384

(1) No lower limit. The storage temperature range is a materials limit and could be adjusted during the engine development to meet mission requirements.
(2) The minimum operating temperature limit which need be considered is the propellant solidification temperature. The maximum operating temperature limit could be modified during development to meet mission requirements.
(3) NPSP = Net positive suction pressure.

PRECEDING PAGE BLANK NOT FILMED.

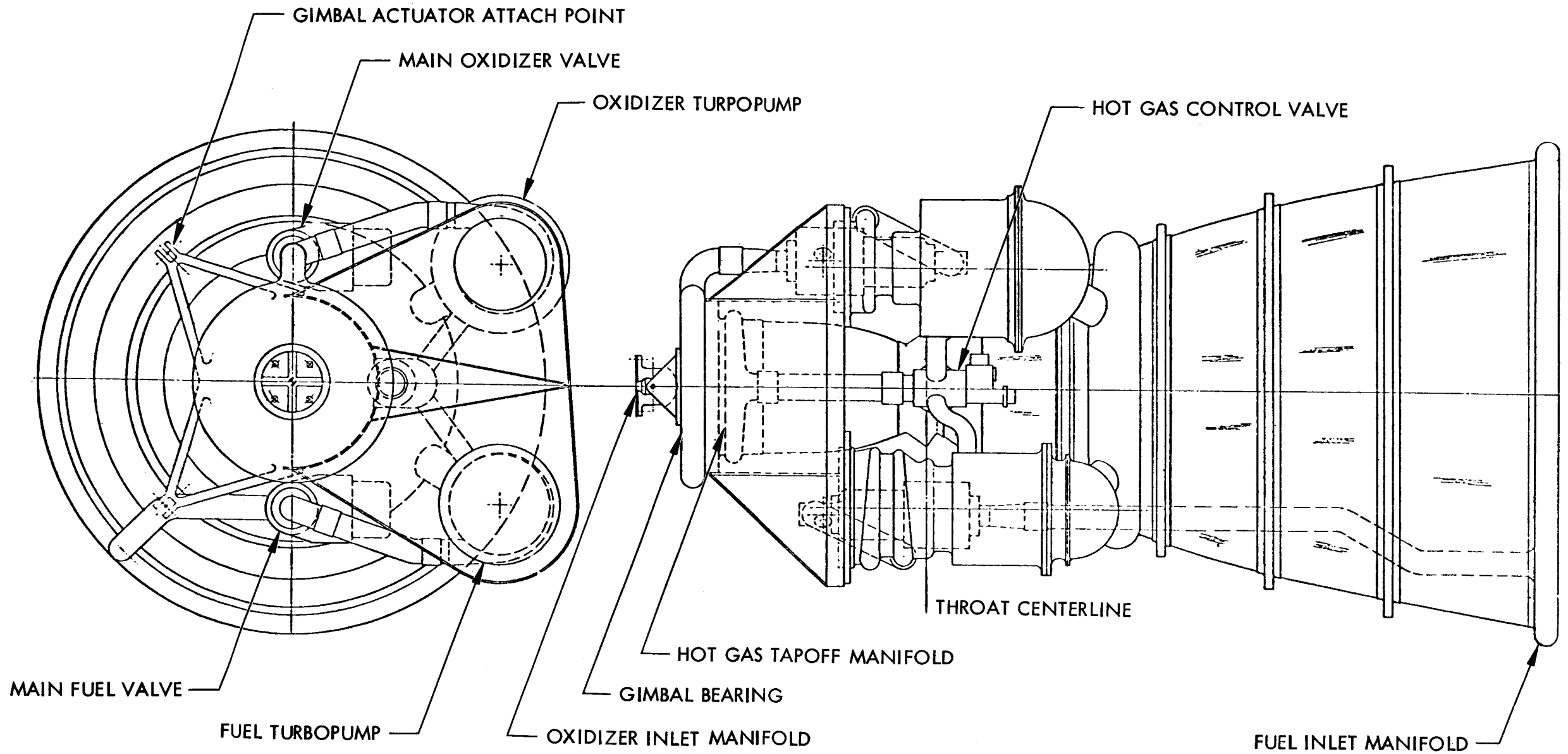

Fig. 39 Example of Conventional Bell Nozzle Engine Configuration

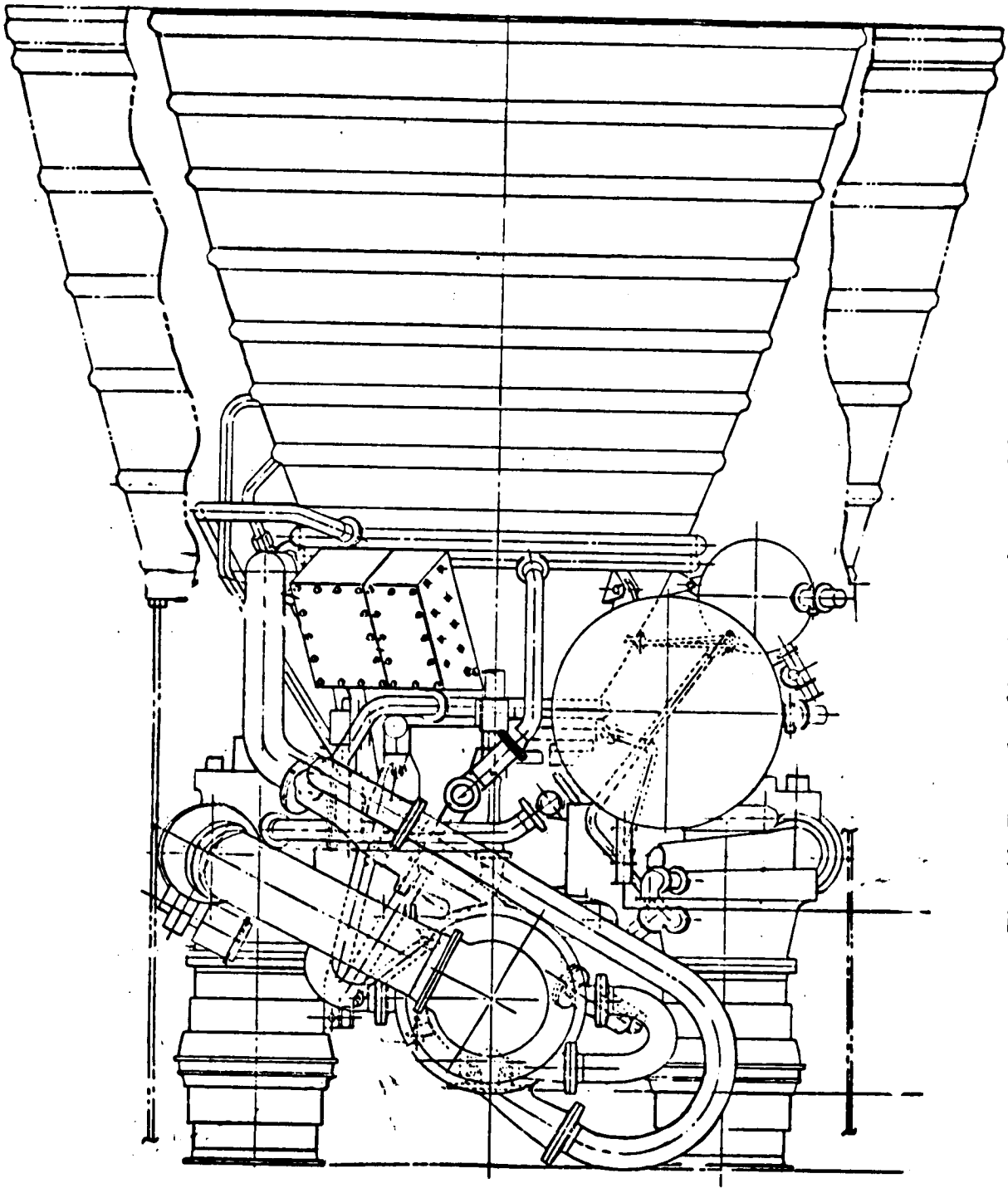

Fig. 40 Example of Engine With Extendable Nozzle Section

systems, the extendable nozzle configuration was assumed for both deep cryogenic combinations, O_2/H_2 and F_2/H_2. Also, the extendable nozzle configuration was assumed for all propellant combinations when used in pressure-fed systems, and the Voyager dynamic envelope limits were still exceeded for most.

6.1.3 Injector

It was assumed that the injector used for the Mars Orbiter engine has the capability to perform satisfactorily when throttled to 10 percent of its rated thrust. An alternative Rocketdyne concept incorporates a device that may act as an ignition stage for the full-sized engine or as a minimum impulse-bit motor. Independent of any particular concept, the capability to operate at about 10 percent of its rated thrust ensures that the engine can perform vernier corrections for such maneuvers as midcourse correction and orbit trim.

6.1.4 Secondary Engine Study

A tradeoff study was conducted to evaluate the performance of the main engine versus a secondary engine for midcourse correction and orbit trim. It was assumed that the main engine would operate in a throttled mode and that the secondary engine would employ either main tank propellants or a separate supply of earth-storable propellants. The factors considered for each of the three methods were relative propellant and inert weights required for each design, distortion of envelope dimensions, startup requirements, chilldown and soakback requirements, pressurization requirements, tank sizes, propellant settling and orientation methods, required complexity of designs, reliability of components, capability for vernier corrections, and ignition delays. The results of the portion of the study dealing with weights are presented in Table 31. On the basis of significantly lighter weight, a decision was made to consider the main-engine-throttled mode for midcourse correction and orbit trim as the preferred method.

Table 31

SECONDARY ENGINE EVALUATION – MARS ORBITER PUMP-FED SYSTEM

1ST MIDCOURSE CORRECTION → 2ND MIDCOURSE CORRECTION → ORBIT INSERTION → ORBIT TRIM

ΔV = 164 FT/SEC | ΔV = 164 FT/SEC | ΔV = 6,294 FT/SEC | ΔV = 328 FT/SEC

Propellant Combination	Mode of Operation	Weight of Propellant Used, W_p (lb)										W_p Difference Sec. Minus Main (lb)	Weight Additional Hardware and Sec. Engine (lb)
		1st Midcourse(a, b)		2nd Midcourse(a, b)		Orbit Insertion(a, b)		Orbit Trim(c)		Total			
		Main	Sec.	Main	Sec.	Main	Main	Main	Sec.	Main	Sec.		
F_2/H_2	Throttled	192	–	190	–	–		250	–	6,062	6,392	330	26
	Full Thrust	–	332	–	320	5,430	5,340	–	400				
O_2/H_2	Throttled	176	–	170	–	–	–	230	–	6,446	6,846	400	30
	Full Thrust	–	346	–	320	5,870	5,780	–	400				
FLOX/CH_4	Throttled	209	–	200	–	–	–	250	–	6,909	7,169	260	20
	Full Thrust	–	329	–	310	6,250	6,160	–	370				
OF_2/CH_4	Throttled	220	–	200	–	–	–	250	–	6,890	7,180	290	24
	Full Thrust	–	320	–	320	6,220	6,150	–	390				
F_2/NH_3	Throttled	231	–	210	–	–	–	270	–	6,961	7,221	260	20
	Full Thrust	–	341	–	320	6,250	6,180	–	380				
OF_2/B_2H_6 (Press. Fed)	Throttled	193	–	230	–	–	–	220	–	6,713	7,043	300	24
	Full Thrust	–	343	–	300	6,100	6,010	–	390				
ClF_5/MHF-5	Throttled	300	–	280	–	–	–	330	–	9,280	9,480	200	18
	Full Thrust	–	400	–	400	8,370	8,280	–	400				
N_2O_4/A-50	Throttled	313	–	310	–	–	–	340	–	9,503	–	–	–
	Full Thrust	–	–	–	–	8,540	–	–	–				

(a) All Main Engine maneuvers performed with main tank propellants.
(b) All Secondary Engine maneuvers performed with N_2O_4/A-50 contained in separate tankage. Secondary Engine is 100-lb-thrust size.
(c) Orbit insertion performed with Main Engine/Main Propellant for both cases (Main Engine only, and Main Engine with Secondary).

6.1.5 MEM Ascent Engine

The propulsion system parameters for the Mars Ascent engine, as derived and refined from engine company data, are listed in Table 32. Data provided by Rocketdyne was used to prepare this table, inasmuch as the envelope limitations within the MEM led to selection of the Aerospike engine configuration, as discussed below. This table reflects the nominal parameters that were employed for each engine/propellant combination, including propellant parameters and engine size and weight.

The selection of the engine configuration was based on the dimensional constraints imposed by the available envelope within the MEM. An Aerospike configuration was selected to meet these constraints. Table 33 presents a sample comparison of engine diameter and length for pump-fed versions of the bell nozzle, extendable bell nozzle, and Aerospike engine configurations. The Aerospike engine configuration produces approximately 1.5 percent less delivered specific impulse compared to conventional bell or 15-deg half-angle conical nozzles of the same area ratio. This minor loss is tolerable in view of envelope limitations, which render the use of more conventional designs more difficult.

The installation of multiple engines is an alternative method to meet the envelope limitations. However, data supplied to this study indicated that an 8,000-lbf-thrust engine for a given propellant combination exceeded the length limitation even if the area ratio were reduced to 50:1. The effect of the performance loss accepted by reducing the thrust level and area ratio to meet the length limitation was not examined. The desirability of a multiple engine installation relative to a single engine also was not examined.

At the 30,000-lbf-thrust level, only the pump-fed mode was considered. The use of pressure-fed systems would require substantially larger dimensions for the conventional nozzle designs and large increases in engine and propellant tankage weight when compared to pump-fed systems. In particular, the special consideration of a pressure-fed OF_2/B_2H_6 bell nozzle engine showed that such an engine exceeded the space available. Furthermore, a turbopump feed system is an integral part of the Aerospike engine design which meets the length limitation. Exhaust from the turbines is injected at the base of the truncated aerodynamic nozzle to improve performance.

Table 32

PROPULSION SYSTEM PARAMETERS FOR 30,000-LB-THRUST ENGINE

Parameter \ Propellants[a]	O_2/H_2		F_2/H_2		FLOX/CH_4		OF_2/CH_4		F_2/NH_3		ClF_5/MHF-5	
	Oxygen	Fuel	Oxygen	Fuel	Oxygen	Fuel	Oxygen	Fuel	Oxygen	Fuel	Oxygen	Fuel
Heat of Vaporization at Normal Boiling Point (Btu/lb)	91.62	195.3	74.10	195.3	77.0	219.2	81.9	219.2	74.10	596.3	128.0	208.0
Boiling Point (°R)	162.3	36.5	153.04	36.5	154.0	201.0	231.4	201.1	153.1	432.0	466.8	652.1
Freezing Point (°R)	97.9	24.9	96.4	24.9	96.7	163.2	88.7	163.2	96.4	351.8	306.3	388.1
Density (lb/ft^3)	71.29	4.42	94.3	4.42	91.2	26.46	95.7	26.46	94.3	42.57	118.5	63.0
Nozzle Expansion Ratio (ϵ)	100/1		75/1		75/1		75/1		75/1		100/1	
Engine Type	Aerospike		Aerospike		Aerospike		Aerospike		Aerospike		Aerospike	
Feed Type	Pump		Pump		Pump		Pump		Pump		Pump	
Chamber Pressure (psia	750		750		750		750		750		750	
Mixture Ratio (O/F)	6		13		5.7		5.3		3.3		2.4	
Delivered Specific Impulse (sec)	449		463		400		406		397		336	
Engine Diameter (in.)	58		51		51		51		51		58	
Engine Length (in.)	26		24		24		24		24		26	
Engine Weight (lb)	520		440		440		460		440		475	
Density of Mixture (lb/ft^3)	22.6		38.5		66.8		67.7		73.7		94.3	
Impulse Density ($lb\text{-}sec/ft^3$)	10,150		17,850		26,700		27,490		29,250		31,700	

(a) All propellant combinations will employ regnerative cooling except for ClF_5/MHF-5, which will use ablative cooling.

Table 33

ENGINE LENGTH COMPARISON – SAMPLE[(a)]

Type	Diameter (in.)	Length (in.)
Bell Nozzle	64	140
Extendable Bell	64	64
Aerospike	51	24

(a) FLOX/CH_4, ϵ = 100

Table 34 expands the material of the previous table to include additional physical design characteristics and requirements for each engine. Figure 41 shows a typical Aerospike engine configuration – in this case for a FLOX/methane engine.

6.2 PROPULSION SYSTEM TECHNOLOGY CONSIDERATIONS

As part of their contributions to the propellant selection study, the participating engine companies provided discussions of potential problem areas and technology improvement areas associated with the application of the various propellant combinations to propulsive stages. The present level of experience with each of the space-storable propellant combinations is low when compared with earth-storable and cryogenic propellants. A large portion of the data, design techniques, and other experience acquired in the development of current engines will be applicable to engines utilizing space-storable propellants. However, it is likely that design considerations peculiar to space-storable propellants will be encountered. The comments solicited as a part of this study were reviewed, and the principal remarks are summarized in the following paragraphs.

The use of fluorine or a fluorinated oxidizer with the high-energy space-storable propellant combinations presents the most difficult problem. Extreme care must be taken

Table 34

PROPULSION SYSTEM REQUIREMENTS FOR 30,000-LB-THRUST ENGINE

Propellant Combination	Mixture Ratio (Optimum)	Chamber Pressure (Optimum) (psia)	I_{sp} Delivered (sec)	Nozzle Expansion Ratio, (ϵ)	Storage Temp. Range, (^{o}R)	Operating Temp. Range, (^{o}R)	Pre-Heat or Pre-Chill Reqd.	Post-Fired Purge Reqd.	NPSH[a]/NPSP[b]		Pressure System	Total Engine Weight, Toroidal Chamb
									Ox.	Fuel		
F_2/H_2	13	750	463	75	112–165	40–46	No	Ox. Yes	38/25	52/1.6	Dual H_e/GH_2	440
CIF_5/MHF-5	2.4	750	336	100	322–492	395–678	No	Ox.& Fuel Yes	35/27	88/38	Single H_e	445
O_2/H_2	6	750	449	100	113–180	40–46	No	Ox. Yes	36/18	58/1.8	Dual H_e or GO_2/GH_2	520
$FLOX/CH_4$	5.7	750	400	75	113–175	178–225	No	Ox. Yes	41/25	87/17	Single H_e	440
OF_2/CH_4	5.3	750	406	75	104–250	178–225	No	Ox. Yes	38/25	90/17	Single H_e	460
F_2/NH_3	3.3	750	397	75	112–165	367–457	No	Ox. Yes	37/24	88/26	Single H_e	440

(a) NPSH = Net Positive Suction Head
(b) NPSP = Net Positive Suction Pressure

FOLDOUT FRAME 1 PRECEDING PAGE BLANK NOT FILMED.

FOLDOUT FRAME 2

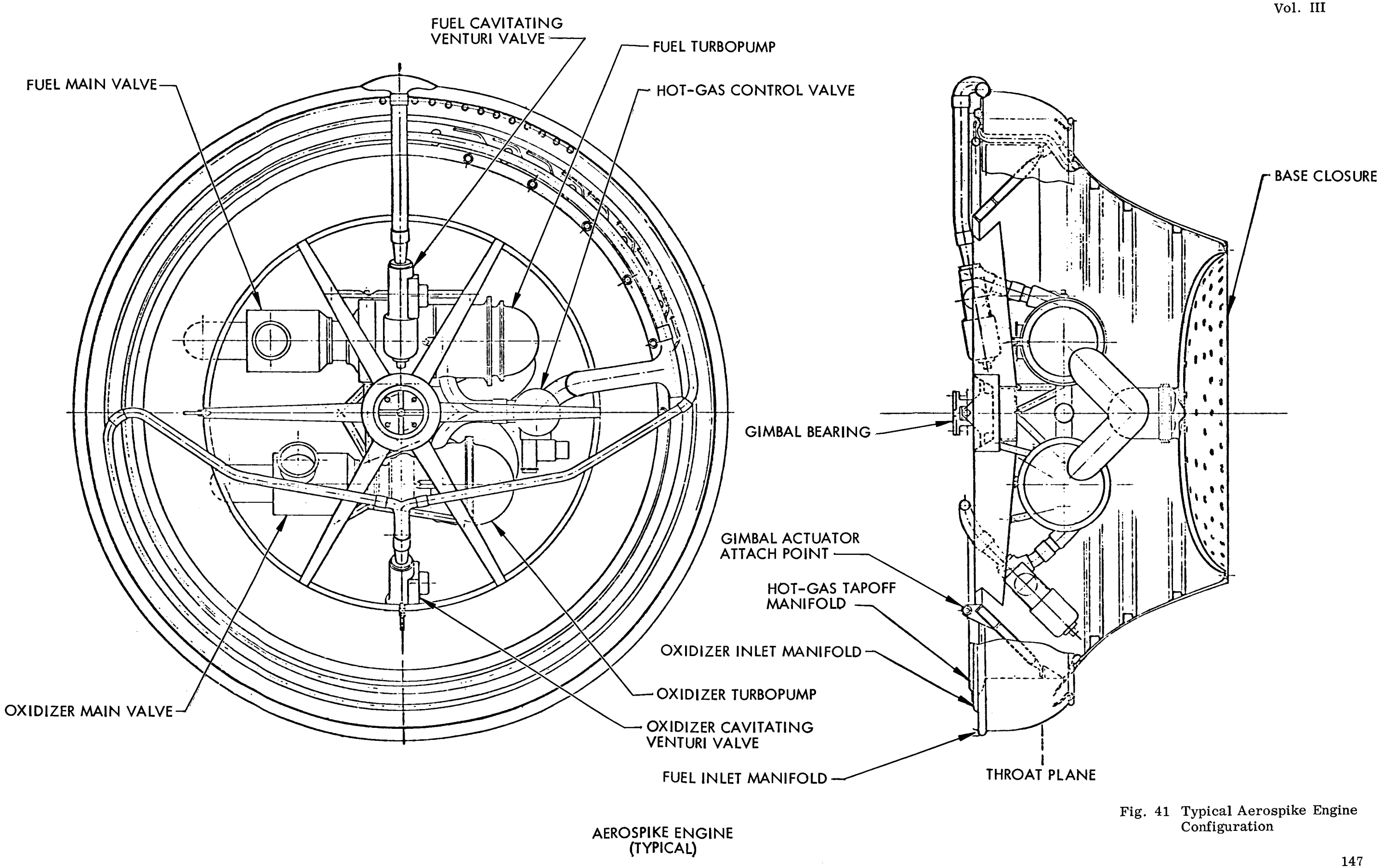

Fig. 41 Typical Aerospike Engine Configuration

in engine design, operational procedures, and cleanliness to avoid damage to hardware. Experience has shown that the combustion system and valve seals are the most vulnerable components. Rotating seals also may be a design problem, although little trouble has been experienced with pumps. Metallic surfaces in contact with fluorine or a fluorinated oxidizer must be passivated before complete exposure. Components must be designed to preserve this coating. In particular, the coating must be protected from any scrubbing action of the fluid or mechanical surfaces. One common guideline is that the fluorine flow path should be as simple as possible.

High combustion chamber pressures are desirable to attain lower engine weight, as well as the higher area ratios and consequent higher specific impulse, which can be achieved within the same packaging volume. This generalization is valid up to the pressure level at which some part of the engine system becomes critical. The characteristics of the coolant in each propellant combination, including its cooling capacity, form another upper limit on chamber pressure. Improved definition of this limit is required for alternative regenerative cooling concepts, as well as for other cooling techniques. The maximum attainable chamber pressure also is limited by the particular engine cycle selected, each cycle having a chamber pressure that maximizes performance for a given propellant combination. Studies are needed to optimize performance and weight and to assess the reliability of the various engine cycles. Furthermore, development is required to improve the pump efficiency at low flow, high-pressure-rise pumping conditions.

In spite of the considerable amount of experimental work conducted on several of the propellant combinations, the practically attainable performance with many remains uncertain; e.g., propellant performance comparisons made on the basis of delivered specific impulse reflect the current knowledge of losses for the several propellants recombination losses. However, the investigation of recombination losses for all propellants is incomplete, and additional effort in this area is needed.

Non-hypergolic propellant combinations require specific provision for ignition, such as a spark or a catalytic igniter. The system complexity is increased when there is a

multiple-start requirement. Cryogenic propellants normally require coolant flow before ignition to gradually reduce the engine temperature and therefore minimize the thermal shock during the start sequence. The impact of this requirement on the engine system can be minimized by careful design. The impact is made more severe if there is a requirement for a fast start. These ignition and prechill requirements impose an additional complexity on the engine system but, in general, are not beyond the state of the art. Only normal development will be necessary to meet these requirements.

Additional knowledge and experience in the areas previously discussed would be beneficial for the development of space-storable propulsion systems. It is also highly desirable to conduct an integrated vehicle/propulsion systems analysis to select those engine design features, such as fast engine response, that best satisfy any vehicle requirements. The experience gained in the development of existing rocket engines will be useful, but design challenges unique to space-storable propulsion systems are to be expected.

6.3 PROPULSION SUMMARY

The type of propulsion system data most useful for the Propellant Selection study varied during each of the three study phases. Initially, general information and parametric performance data over a broad range of engine design parameters permitted the comparative evaluation of many propellant combinations. When particular missions and stages were chosen for further investigation, specific data for selected thrust levels were sought. Finally, sensitivity data describing the effects of perturbations in the engine design parameters were necessary to undertake the stage sensitivity analyses. Thus, the level of detail became progressively greater. In all cases, however, the most valued data were either empirical results or realistic projections of first-hand experimental determinations. Actual or predicted performance based on experimental data was the single most important piece of information. The abundant theoretical data which were submitted served only to indicate the estimated performance efficiency.

Substantial inconvenience was experienced in attempting to discover common bases among the submitted data. To facilitate comparison, it is highly desirable that all

ground rules be explicitly stated. This statement should include the following:

- Combustion chamber pressure
- Nozzle expansion ratio
- Ambient temperature and pressure
- Engine cycle type
- Combination chamber cooling methods
- Data source: theoretical, experimental, or extrapolated
- Basis for selection of design point

Any other assumptions made during generation of data that have an impact on the quoted performance should be explicity outlined. For example, are nozzle recombination losses measured, analytically predicted, or extrapolated from other data ? A brief summary or outline of the manner in which the performance data were determined is necessary so that they may be used with confidence. To be comprehensive, all of the pertinent conditions should be specified, and a complete and consistent set of data provided.

Of particular interest to this type of study is a breakdown of so-called problem areas or technology improvement areas into two categories. The first contains advanced development design tasks. These involve application to other propellant combinations of the state of the art technology developed for a given combination. This refers, in fact, to the transfer of experience already acquired, as previously discussed. The second category contains all problems that require an advance in the state of the art or that are peculiar to a given propellant combination.

A comprehensive review of problem areas in this framework from the point of view of the engine contractors would be very useful. Then, from a system point of view, each propellant combination can be appraised with greater confidence relative to other combinations.

Section 7
REFERENCES

1. Lockheed Missiles & Space Company, "Heat Rate Computer Program – User's Manual," D/55-25, TXA 1954, T. S. Newby, dated 26 October 1966

2. -----, "Thermal Analyzer Control Systems for IBM 709-7090-7094 Computer Utilization Manual," LMSC 3-56-65-8, dated 1 September 1965

3. M. Epstein and R. E. Anderson, Advances in Cryogenic Engineering, Volume 13, Plenum Press, New York, New York, 1968

4. M. Epstein, H. K. Georgious, and R. E. Anderson, International Advances in Cryogenic Engineering, Volume 10, Plenum Press, New York, New York, 1965

5. TRW Systems Group, "Voyager Support Study – LM Descent Stage Applications Final Report," 04480-6005-R000, Contract JPL 95113, February 1967

6. Lockheed Missiles & Space Company, "Handbook of Thermal Design Data for Multilayer Insulation Systems," LMSC/A847882, dated 25 June 1967

7. A. H. Weiss and J. Jeffe, "Generalized Correlation of Effect of Pressure on Isobaric Heat Capacity of Gases," Ind. and Eng. Chem., 49, pp. 120-4, 1957

8. O. Redlich and J. N. S. Kwong, Chemical Engineering, Volume 44, p. 233, 1949

9. O. Redlich, A. T. Kister, and C. E. Turnquist, Chemical Engineering Symposium Series, No. 2, 49, 1952

10. Wallace R. Gambill, Chemical Engineering, December 1957, p. 261

11. North American Rockwell Corporation – Space Division, Draft of Final Report SD 67-755, Volume II Design, and Volume IV Briefing, "Definition of Experimental Tests for a Manned Mars Excursion Module," November 1967

12. North American Rockwell Corporation – Space Division, Draft of Final Report SD 67-994-2, Volume II: Technical Analysis, "Study of Technology Requirements for Atmosphere Braking to Orbit about Mars and Venus," January 1968

13. Lockheed Missiles & Space Company, "Analytical and Experimental Studies of Gas Flow Through Multilayer Insulation," LMSC/A742593-V, dated 16 August 1965

14. -----, "Investigations Regarding Development of a High Performance Insulation System," 3rd Quarterly Progress Report, K-17-68-3, dated 15 April 1968

15. "Rocket Engine Design Criteria as a Basis for Propellant Selection for Spacecraft Propulsion Systems," Aerojet-General, August 1967

16. "Space Storable Propellants," September 18, 1967, Bell Aerosystems S-159669

17. "Space Storable Propellant Rocket Engine Parametric Data," Pratt & Whitney, PDS-2686, January 19, 1968 (preliminary copy received September 1967)

18. "Oxygen/Hydrogen and Fluorine/Hydrogen Rocket Engine Parametric Data," Pratt & Whitney, PDS-2687, January 19, 1968

19. "High Performance Propulsion Systems for Space Missions," Pratt & Whitney, GP 68-31, February 7, 1968

20. "NASA Propellant Selection for Spacecraft Propulsion Systems Study," Rocketdyne 67RC 9355

21. Response to the Task II Request for Information as submitted by Aerojet-General, Bell Aerosystems, Pratt & Whitney, and Rocketdyne

Appendix

DISTRIBUTION LIST FOR FINAL REPORT

COPIES	RECIPIENT	DESIGNEE
	NASA Headquarters, Washington, D.C. 20546	
1	Contracting Officer, DHC-1	Same
1	Patent Office, UT	Same
	Technical Monitors	
1	Don Nored/Lewis Research Center	Same
1	Bob Breshears/Jet Propulsion Laboratory	Same
1	Keith Coates/Marshall Space Flight Center	Same
1	Bob Polifka/Manned Spacecraft Center	Same
4	Chief, Liquid Propulsion Technology, RPL Office of Advanced Research and Technology NASA Headquarters Washington, D.C 20546	Same
25	NASA Scientific and Technical Information Facility P.O. Box 33 College Park, Maryland 20740	Same
1	Mr. Joe Mahon Director, Launch Vehicles and Propulsion, SV Office of Space Science and Applications NASA Headquarters, Washington, D.C. 20546	Same
1	Mr. Charles Donlan Director, Advanced Manned Missions, MT Office of Manned Space Flight NASA Headquarters, Washington, D.C. 20546	Same
1	Leonard Roberts Mission Analysis Division NASA Ames Research Center Moffett Field, California 24035	Same

NASA FIELD CENTERS

COPIES	RECIPIENT	DESIGNEE
2	Ames Research Center Moffett Field, California 94035	H. J. Allen
2	Goddard Space Flight Center Greenbelt, Maryland 20771	Merland L. Moseson Code 620
2	Jet Propulsion Laboratory California Institute of Technology 4800 Oak Grove Drive Pasadena, California 91103	Henry Burlage, Jr. Propulsion Div., 38
2	Langley Research Center Langley Station Hampton, Virginia 23365	Ed Cortwright Director
2	Lewis Research Center 21000 Brookpark Road Cleveland, Ohio 44135	Dr. Abe Silverstein Director
2	Marshall Space Flight Center Huntsville, Alabama 35812	Hans G. Paul Code R-P&VED
2	Manned Spacecraft Center Houston, Texas 77001	Dr. Robert R. Gilruth Director
2	John F. Kennedy Space Center, NASA Cocoa Beach, Florida 32931	Dr. Kurt H. Debus

GOVERNMENT INSTALLATIONS

COPIES	RECIPIENT	DESIGNEE
1	Aeronautical Systems Division Air Force Systems Command Wright-Patterson Air Force Base Dayton, Ohio 45433	D. L. Schmidt Code ASRCNC-2
1	Air Force Missile Development Center Holloman Air Force Base, New Mexico	Maj. R. E. Bracken Code MDGRT
1	Air Force Missile Test Center Patrick Air Force Base, Florida	L. J. Ullian
1	Space and Missile Systems Organization Los Angeles 45, California	Col. Clark Technical Data Center
1	Arnold Engineering Development Center Arnold Air Force Station Tullahoma, Tennessee	Dr. H. K. Doetsch
1	Bureau of Naval Weapons Department of the Navy Washington, D.C.	J. Kay RTMS-41
1	Defense Documentation Center Headquarters Cameron Station, Building 5 5010 Duke Street Alexandria, Virginia 22314 ATTN: TISIA	
1	Headquarters, U.S. Air Force Washington 25, D.C.	Col. C. K. Stambaugh AFRST
1	Picatinny Arsenal Dover, New Jersey 07801	I. Forsten, Chief Liquid Propulsion Laboratory, SMUPA-DL
1	Air Force Rocket Propulsion Laboratory Research and Technology Division Air Force Systems Command Edwards, California 93523	RPRR/Mr. H. Main

GOVERNMENT INSTALLATIONS (Cont.)

COPIES	RECIPIENT	DESIGNEE
1	U.S. Army Missile Command Redstone Arsenal Alabama 35809	Dr. Walter Wharton
1	U.S. Naval Weapons Center China Lake California 93557	Code 4562 Chief, Missile Propulsion Division

C P I A

COPIES	RECIPIENT	DESIGNEE
1	Chemical Propulsion Information Agency Applied Physics Laboratory 8621 Georgia Avenue Silver Spring, Maryland 20910	Neil Safeer

INDUSTRY CONTRACTORS

COPIES	RECIPIENT	DESIGNEE
1	Aerojet-General Corporation P.O. Box 296 Azusa, California 91703	L. F. Kohrs
1	Aerojet-General Corporation P.O. Box 1947 Technical Library, Bldg 2015, Dept. 2410 Sacramento, California 95809	R. Stiff
1	Aeronautronic Philco Corporation Ford Road Newport Beach, California 92663	D. A. Garrison
1	Aerospace Corporation 2400 East El Segundo Boulevard P.O. Box 95085 Los Angeles, California 90045	John G. Wilder MS-2293 Propulsion Dept.
1	Arthur D. Little, Inc. 20 Acorn Park Cambridge, Massachusetts 02140	Library
1	Astropower Laboratory Douglas Aircraft Company 2121 Paularino Newport Beach, California 92663	Dr. George Moc Director, Research
1	Astrosystems International, Inc. 1275 Bloomfield Avenue Fairfield, New Jersey 07007	A. Mendenhall
1	Atlantic Research Corporation Edsall Road and Shirley Highway Alexandria, Virginia 22314	Dr. Ray Friedman
1	Beech Aircraft Corporation Boulder Division Box 631 Boulder, Colorado	J. H. Rodgers

INDUSTRY CONTRACTORS (Cont.)

COPIES	RECIPIENT	DESIGNEE
1	Bell Aerosystems Company P.O. Box 1 Buffalo, New York 14240	W. M. Smith
1	Bellcomm 1100 17th Street Washington, D.C.	Joseph Tuschurgi
1	Bendix Systems Division Bendix Corporation 3300 Plymouth Street Ann Arbor, Michigan	John M. Brueger
1	Boeing Company P.O. Box 3707 Seattle, Washington 98124	J. D. Alexander
1	Boeing Company 1625 K Street, N.W. Washington, D.C. 20006	Library
1	Boeing Company P.O. Box 1680 Huntsville, Alabama 35801	Library
1	Missile Division Chrysler Corporation P.O. Box 2628 Detroit, Michigan 48231	John Gates
1	Wright Aeronautical Division Curtiss-Wright Corporation Wood-Ridge, New Jersey 07075	G. Kelley
1	Missile and Space Systems Division McDonnell-Douglas Aircraft Company, Inc. 3000 Ocean Park Boulevard Santa Monica, California 90406	R. W. Hallet Chief Engineer Adv. Space Tech.
1	Aircraft Missiles Division Fairchild Hiller Corporation Hagerstown, Maryland 10	J. S. Kerr

INDUSTRY CONTRACTORS (Cont.)

COPIES	RECIPIENT	DESIGNEE
1	General Dynamics/Astronautics Library and Information Services (128-00) P.O. Box 1128 San Diego, California 92112	Frank Dore
1	Re-Entry Systems Department General Electric Company 3198 Chestnut Street Philadelphia, Pennsylvania 19101	F. E. Schultz
1	Advanced Engine and Technology Department General Electric Company Cincinnati, Ohio 45215	D. Suichu
1	Grumman Aircraft Engineering Corp. Bethpage, Long Island, New York	Joseph Gavin
1	Ling-Temco-Vought Corporation P.O. Box 5907 Dallas, Texas 75222	Warren G. Trent
1	Lockheed Missiles & Space Company Attn: Technical Information Center P.O. Box 504 Sunnyvale, California 94088	Y. C. Lee
1	Lockheed Propulsion Company P.O. Box 111 Redlands, California 92374	H. L. Thackwell
1	The Marquardt Corporation 16555 Saticoy Street Van Nuys, California 91409	Leo Bell
1	Denver Division Martin Marietta Corporation P.O. Box 179 Denver, Colorado 80201	Dr. Morganthaler
1	McDonnell Douglas Aircraft Corporation P.O. Box 516 Municipal Airport St. Louis, Missouri 63166	R. A. Herzmark

INDUSTRY CONTRACTORS (Cont.)

COPIES	RECIPIENT	DESIGNEE
1	Space and Information Systems Division North American Rockwell 12214 Lakewood Boulevard Downey, California 90241	Library
1	Rocketdyne (Library 586-306) 6633 Canoga Avenue Canoga Park, California 91304	Dr. R. J. Thompson
1	Northrop Space Laboratories 3401 West Broadway Hawthorne, California	Dr. William Howard
1	Astro-Electronics Division Radio Corporation of America Princeton, New Jersey 08540	S. Fairweather
1	Reaction Motors Division Thiokol Chemical Corporation Denville, New Jersey 07832	Dwight S. Smith
1	Space General Corporation 9200 East Flair Avenue El Monte, California 91734	C. E. Roth
1	Stanford Research Institute 333 Ravenswood Avenue Menlo Park, California 94025	Dr. Gerald Marksman
1	TRW Systems Group TRW Incorporated One Space Park Redondo Beach, California 90278	G. W. Elverum
1	TAPCO Division TRW, Incorporated 23555 Euclid Avenue Cleveland, Ohio 44117	P. T. Angell
1	Thiokol Chemical Corporation Huntsville Division Huntsville, Alabama	John Goodloe

INDUSTRY CONTRACTORS (Cont.)

COPIES	RECIPIENT	DESIGNEE
1	Research Laboratories United Aircraft Corporation 400 Main Street East Hartford, Connecticut 06108	Erle Martin
1	United Technology Center 587 Mathilda Avenue P.O. Box 358 Sunnyvale, California 94088	Dr. David Altman
1	Aerospace Operations Walter Kidde and Company, Inc. 567 Main Street Belleville, New Jersey 07109	R. J. Hanville Director of Research Engineering
1	Florida Research and Development Pratt & Whitney Aircraft United Aircraft Corporation P.O. Box 2691 West Palm Beach, Florida 33402	R. J. Coar
1	Rocket Research Corporation 520 South Portland Street Seattle, Washington 98108	Foy McCullough, Jr.